Production and Fractionation of Antioxidant Peptides from Soy Protein Isolate using Sequential Membrane Ultrafiltration and Nanofiltration

By

Sahan Ranamukhaarachchi

A thesis presented to the University of Waterloo

In fulfillment of the

thesis requirement for the degree of

Master of Applied Science

In

Chemical Engineering

Waterloo, Ontario, Canada, 2012

I hereby declare that I am the sole author of this thesis. This is a true copy of the thesis, including any required final revisions, as accepted by my examiners.

I understand that my thesis may be made electronically available to the public.

Abstract

Antioxidants are molecules capable of stabilizing and preventing oxidation. Certain peptides, protein hydrolysates, have shown antioxidant capacities, which are obtained once liberated from the native protein structure. Soy protein isolates (SPI) were enzymatically hydrolyzed by pepsin and pancreatin mixtures. The soy protein hydrolysates (SPH) were fractionated with sequential ultrafiltration (UF) and nanofiltration (NF) membrane steps. Heat pre-treatment of SPI at 95 ^{o}C for 5 min prior to enzymatic hydrolysis was investigated for its effect on peptide distribution and antioxidant capacity. SPH were subjected to UF with a 10 kDa molecular weight cut off (MWCO) polysulfone membrane. UF permeate fractions (lower molecular weight than 10 kDa) were fractionated by NF with a thin film composite membrane (2.5 kDa MWCO) at pH 4 and 8. Similar peptide content and antioxidant capacity (α=0.05) were obtained in control and pre-heated SPH when comparing the respective UF and NF permeate and retentate fractions produced. FCR antioxidant capacities of the SPH fractions were significantly lower than their ORAC antioxidant capacities, and the distribution among the UF and NF fractions was generally different. Most UF and NF fractions displayed higher antioxidant capacities when compared to the crude SPI hydrolysates, showing the importance of molecular weight on antioxidant capacity of peptides. The permeate fractions produced by NF at pH 8 displayed the highest antioxidant capacity, expressed in terms of trolox equivalents (TE) per total solids (TS): 5562 μmol TE g^{-1} TS for control SPH, and 5187 μmol TE g^{-1} TS for pre-heated SPH. Due to the improvement in antioxidant capacity of peptides by NF at pH 8, the potential for NF as a viable industrial fractionation process was demonstrated.

Principal component analysis (PCA) of fluorescence excitation-emission matrix (EEM) data for UF and NF peptide fractions, followed by multi-linear regression analysis, was assessed for its potential to monitor and identify the contributions to ORAC and FCR, two *in vitro* antioxidant capacity assays, of SPH during membrane fractionation. Two statistically significant principal components (PCs) were obtained for UF and NF peptide fractions. Multi-linear regression models (MLRM) were developed to estimate their fluorescence and PCA-captured ORAC ($ORAC_{FPCA}$) and FCR (FCR_{FPCA}) antioxidant capacities. The $ORAC_{FPCA}$ and FCR_{FPCA} antioxidant capacities for NF samples displayed strong, linear relationships at different pH conditions (R^2>0.99). Such relationships are believed to reflect the individual and relative combined

contributions of tryptophan and tyrosine residues present in the SPH fractions to ORAC and FCR antioxidant capacities. Therefore, the proposed method provides a tool for the assessment of fundamental parameters of antioxidant capacities captured by ORAC and FCR assays.

Acknowledgements

First of all, I would like to express my sincere gratitude my advisor, Christine Moresoli for accepting me as a graduate student and providing the opportunity to conduct exciting research. The attention, training, support, and advice provided by Christine have tremendously influenced my ability to conduct independent research, and have been indispensible to the completion of this thesis.

I would like to acknowledge the National Science and Engineering Research Council of Canada for providing the financial support to this research project. I am also thankful to the Department of Chemical Engineering, and the University of Waterloo for providing financial assistances in many ways during the course of this Masters program.

Ramila Peiris has been a mentor and has assisted this research in many different avenues. I am grateful for his guidance and presence for the duration of my Masters program.

Special recognitions of appreciation are expressed to Raymond Legge and the wonderful members of the Legge-Moresoli research group. Andrew Yeh, Jamie Cousineau, Katharina Hassel, Barbara Guettler, Nicholas Ignagni, Sarah Meunier, Rachel Campbell, and Nikhil Kumar have greatly influenced my life at the University of Waterloo, and I am thankful for everything.

I am thankful to the reviewers of my thesis, Xianshe Feng and Marc Aucoin for their time and valuable feedback; and to Robert Lencki (University of Guelph) for his assistance and influence in my decision to attend the University of Waterloo.

I would also like to express my immense gratitude to Chitral Angammana, Suramya Mihindukulasuriya, Nandana Jayabahu, Ishari Jayabahu, and Subodha Gunawardena for all the care and comfort provided during the past six years.

The constant presence, words of encouragement and incomparable attention from my family have propelled me to excel at my studies and to become the person I am today. I am forever in debt to Senaratne and Sandya Ranamukhaarachchi (my beautiful parents), and Himesha and Sithumini Ranamukhaarachchi (my two wonderful sisters), without whom I definitely would not be here today. I am also extremely thankful to Lal, Samanthi, and Ayumi Samarakoon.

Finally, I express my deepest appreciation to Mayumi Samarakoon for sharing every second of my life in Waterloo.

Table of Contents

List of Figures

List of Tables

List of Abbreviations

Roman Letters	
G	G-centrifugal force
J	Solvent flux (m s^{-1})
J_0	Initial mass flux (g m^{-2} s^{-1})
J_P	Mass flux (g m^{-2} s^{-1})
$J_P J_0^{-1}$	Normalized flux
J_{Per}	Permeate flux (m s^{-1})
R_a	Additional resistances (m^{-1})
R_f	Fouling resistance (m^{-1})
R_m	Membrane resistance (m^{-1})
R_{tot}	Total resistance (m^{-1})
S	Svedberg units
t	Time (min)
Greek Letters	
σ	Rejection coefficient of membrane towards a solute
η	Dynamic viscosity of permeating solution (kg m^{-1} s^{-1})
ζ	Zeta potential (mV)
Other Abbreviations	
AAPH	2,2'-azobis-2-methyl-propanimidamide dihydrochloride
AC	Antioxidant capacity (μmol trolox equivalents g^{-1} solids)
ACE	Angiotensin converting enzyme
ACN	Acetonitrile
AMVN	2,2'-azobis(2,4-dimethylvaleronitrile)
AUC	Area under the curve
CAT	Catalase
CPP	Caseinophosphopeptide
DH	Degree of hydrolysis
DNS	Dimethylaminoazobenzene-4'-sulfonyl
DPPH	2,2-diphenyl-1-picrylhydrazyl
EEM	Excitation-emission matrix
ET	Electron transfer
Ex/Em	Excitation and emission wavelengths
FCR	Folin Ciocalteau Reagent assay
FCR_{FPCA}	Fluorescence- and PCA-captured FCR
FRAP	Ferric reducing antioxidant power
GSHPx	Glutathione peroxidase
HAT	Hydrogen atom transfer
HPLC	High performance liquid chromatography
LAB	Lactic acid bacteria
MeOH	Methanol

MF	Microfiltration
MLRM	Multi-linear regression model
MW	Molecular weight
MWCO	Molecular weight cut off (kDa)
NF	Nanofiltration
NK	Natural killer cell activity
NMR	Nuclear magnetic resonance
OPA	O'pthaldialdehyde
ORAC	Oxygen Radical Absorbance Capacity assay
$ORAC_{FPCA}$	Fluorescence- and PCA-captured ORAC
PC	Principal component
PCA	Principal component analysis
Per	Permeate
pI	Isoelectric point
PITC	Phenyl-isothiocyanate
PLS	Partial least squares
PMMA	Polymethylmethacrylate
PMT	Photomultiplier tube
PTC	Phenylthiocarbamyl
Ret	Retentate
RMSE	Root mean squared error
RO	Reverse osmosis
RPHPLC	Reverse-phase HPLC
RS	Rayleigh light scattering
SOD	Superoxide dismutase
SPH	Soy protein hydrolysate
SPI	Soy protein isolate
SSE	Sum of squared errors
TE	Trolox Equivalents
TEA	Triethylamine
TMP	Transmembrane pressure (Pa, N m^{-2})
TS	Total solid content (g L^{-1})
UC	Ultracentrifugation
UF	Ultrafiltration
βME	β-mercaptoethanol

1. Introduction

1.1. Research Motivation

Biological molecules with antioxidant functionalities are invaluable to food and nutraceutical industries, due to preservative functions and numerous health benefits that antioxidants provide to animals. The term antioxidant, which refers to substances that are able to minimize or prevent undesirable oxidative reactions, is frequently used to advertise and promote food and nutraceutical products and to attract consumers. Progressively, worldwide consumers are becoming more conscious of dietary intakes and the health benefits from antioxidant-rich foods and beverages, including berries, tea, and red wine. As a result, discovery and development of novel sources of antioxidants and methods to incorporate highly antioxidant compounds to foods are paramount.

The antioxidant functions of amino acids and peptides, first reported by Marcuse (1960), have been explored in multiple protein sources, including soy proteins [1]. Characterization of antioxidant peptides derived from the hydrolysis of soy proteins has previously been performed [2-5]. Peptide structure-antioxidant capacity relationships in peptides have been investigated. The antioxidant capacity of a peptide can be determined using a large variety of *in vitro* assays, based on hydrogen atom transfer (HAT) and singlet electron transfer (ET) mechanisms. It has been widely accepted that results from one antioxidant assay are incomparable to another, however similarities in some assays have been identified [6,7].

Fractionation and purification of soy protein hydrolysates provide a potential means to discover and enhance these antioxidant functionalities to greater horizons [8,9]. Membrane filtration is a viable separation technology to remove or purify species of interest from liquid solutions based on molecular weight, charge, or a combination thereof [10]. Ultrafiltration (UF), a well-established membrane filtration process, is widely used in industrial processes ranging from milk production filtration to waste water treatment [11]. More recently, nanofiltration (NF), a relatively novel separation process based on size and charge, has been expanding its range of applications to the separation of biopolymers, including polysaccharide and peptides, at low concentrations [12-15]. Due to the differences in their separation mechanisms, UF and

NF can be utilized sequentially (i.e. UF followed by NF) to explore more diverse and effective separations of biopolymers, such as peptides [12,15]. Fractionation of peptides using membrane UF can alter and enhance the functionality of peptides, especially their antioxidant capacity [8,9,16].

1.2. Project Objectives

1.2.1. Goals

The overall goals of this project were to produce and improve the antioxidant capacity of soy protein hydrolysates (SPH) using sequential UF and NF; assess the potential for NF as a viable separation technology for bioactive compounds; and assess the potential for fluorescence spectroscopy and principal component analysis (PCA) of fluorescence excitation-emission matrices (EEMs) to monitor Oxygen Radical Absorbance Capacity (ORAC) and Folin Ciocalteau Reagent (FCR) antioxidant capacities during sequential UF and NF of SPH.

1.2.2. Hypotheses

The following hypotheses were tested in this project:

1. Application of heat pre-treatment to soy protein isolate (SPI) should yield a higher peptide content (per total solids) during enzymatic hydrolysis compared to SPI control (non-heat pre-treated), due to heat-induced denaturation of SPI protein structures, allowing enzymes to access hydrolysable peptide bonds more readily.
2. Heat pre-treated soy protein hydrolysates (referred to as pre-heated SPH hereforth) should yield a higher peptide content in the UF and NF permeates than then control SPH; since peptides present in pre-heated SPH are expected to be lower in molecular weight (MW) due to a higher degree of hydrolysis (DH) relative to control SPH. While, the antioxidant capacities (ORAC and FCR) of both pre-heated and control SPH should be higher in permeate fractions compared to the corresponding feed and retentate fractions; as molecular weight (MW) of a peptide decreases, its antioxidant capacities should increase.
3. NF at pH 8 should lead to higher peptide contents and antioxidant capacities in permeate fractions than at pH 4 in pre-heated and control SPH. Due to counter-ion membrane-peptide interactions at pH 4, a higher degree of electrostatic attractions

and protein adsorption on the membrane should be observed, causing membrane fouling and affecting peptide permeation.

4. Fluorescence spectroscopy, PCA, and multi-linear regression analysis should capture contributions of biological species in peptide fractions associated with their ORAC and FCR antioxidant capacities, based on detection and quantification of tyrosine- and tryptophan-containing peptides, which are known contributors to both ORAC and FCR values for peptides.
5. A relationship between fluorescence and PCA-captured ORAC ($ORAC_{FPCA}$) and FCR (FCR_{FPCA}) antioxidant capacities should not be observed, due to fundamental differences in the mechanisms employed by the two antioxidant assays.

1.2.3. Objectives

To test these hypotheses, the following objectives were established:

1. Investigate the effect of heat pre-treatment on SPI hydrolysis by applying thermal treatment to a SPI solution at 95 ^{o}C for 5 min; and comparing the DH as a function of time to a SPI control (no heat pre-treatment).
2. Examine the effects of UF on peptide fractionation and antioxidant capacity for pre-heated and control SPH using a hollow fibre polysulfone UF membrane module (10 kDa molecular weight cut off step).
3. Examine the effects of NF on peptide fractionation and antioxidant capacity for pre-heated and control SPH using a thin film composite NF membrane (flat sheet G10 membrane; 2.5 kDa MWCO step) at pH 4 and 8.
4. Investigate the potential of fluorescence analysis of UF and NF peptide fractions, in combination with PCA and multi-linear regression analysis to capture the contributions of biological species in peptide fractions to their ORAC and FCR antioxidant capacities.
5. Evaluate the relationship between ORAC and FCR antioxidant capacities of peptide fractions based on experimentally observed antioxidant capacities; and fluorescence and PCA-captured antioxidant capacities.

1.3. Thesis Organization

Chapter 2 provides fundamental principles and experimental knowledge related to soy proteins and antioxidant peptides, membrane UF and NF, and fluorescence spectroscopy.

Production and fractionation of antioxidant peptides from SPI using sequential UF and NF is investigated in chapter 3. The impacts of SPI heat pre-treatment, pH, and UF and NF membrane molecular weight on the fractionation of soy protein hydrolysates according to peptide distribution, antioxidant capacities, and membrane fouling are presented. This chapter was prepared as a manuscript for the Journal of Membrane Science.

Analysis of UF and NF peptide fractions using fluorescence spectroscopy and principal component analysis is presented in chapter 4. The potential to assess the contributions of biological species to ORAC and FCR antioxidant capacities of peptide fractions is investigated. This chapter was prepared as a manuscript for Biotechnology and Bioengineering.

Preliminary amino acid analyses of selected UF and NF peptide fractions with high antioxidant capacities obtained by reverse-phase HPLC and ^{1}H-NMR are provided in Chapter 5.

The most significant findings from this research and proposed future works are presented in chapter 6.

2. Theoretical Knowledge and Principles

2.1. Proteins

Proteins are biological macromolecules that are composed of chains of amino acids, linked together by peptide bonds, and folded into three-dimensional structures. Proteins are of utmost importance to cell functions and facilitate biological processes in living organisms. Proteins are also essential components in human and animal diets, since animals cannot synthesize some amino acids, called essential amino acids, which need to be obtained from food sources. Protein deficiency is a serious health issue in many developing countries, leading to detrimental medical conditions.

2.1.1. Soybeans and soy proteins

Soybeans were first discovered in Southeast Asia before 1100 BC. Since then, soybeans have been progressively spreading across the globe, mainly through British colonization. Soy-based products, including soy sauce, have become popular in Europe and America [17]. In the early 1900s, it was realized that soybeans were a valuable source of protein and oil, and that soil quality directly impacted the nutrition quality of the soybeans [17]. Soybean cultivation has since been promoted around the world due to its nutritional value. Dried soybeans possess a higher protein content (~40 %) compared to cereal crops (8-15 %) and legumes (20-30 %). Between 2000 and 2005, 225.6 million tons of soybeans were produced worldwide, with USA (41.3 %), Brazil (23.7 %), and Argentina (16.1 %) contributing to over 80 % of the global production [18]. Canada accounted for 1.3 % of the global soybean production. Nutritional composition of soybeans is provided in Table 1.

Typically, soybeans weigh 16-19 g per 100 seeds [18]. Though soybeans have high protein content (~40 %), they are primarily grown for oil production (~20 % on dry basis). During oil extraction, raw soybeans are initially subjected to a series of pre-processing steps where they are cleaned, dried, cracked, dehulled, and conditioned to a moisture content of ~10 % (dry basis) at 65-70 ^{o}C [19]. These dehulled and conditioned soybeans are then flaked, defatted (hexane extraction), steamed (to remove residual hexane), and toasted above 100 ^{o}C [19]. The defatted soybeans (after oil extraction) contain ~50 % protein (w/w) and can be further processed to obtain soy flour (56-59

% protein, w/w), soy protein concentrate (65-72 % protein, w/w), and soy protein isolate (90-92 % protein, w/w) as further described by Garcia et al. (1997) and Lusas et al. (1995) [20,21]. These soy products are becoming increasingly popular and used in food products.

Table 1: Nutritional composition of soybeans on dry basis [18].

Nutritional Characteristic	Composition (%)	Examples
Oil	18 – 21	-
Protein	36 – 40	Glycinin, β-conglycinin
Soluble sugar	10 – 11	Glucose, sucrose
Insoluble sugar	21 – 25	Cellulose, pectin
Minerals	5	Iron, phosphorus, magnesium

2.1.1.1. Soy proteins in foods

Soy proteins are considered a high quality source of proteins, since they contain all nine essential amino acids in sufficient quantities required by humans and animals for proper nutrition [22]. The quality of a protein can be determined by its amino acid score, which is calculated as the content of an essential amino acid in a food protein expressed as a percentage of the same amino acid in the same quantity in a standard protein [23]. The amino acid with the lowest percentage is the limiting amino acid in the protein source. Amino acid scoring is explained by Young et al. (1991) [23]. An amino acid score above 100 indicates a complete or a high-quality protein. Soy protein isolates have an amino acid score of 108. Many important health benefits from soy protein consumption, especially in cancer prevention, and the treatment of obesity and diabetes, have been reported [24]. Use of soy proteins in foods is economically attractive, since soybeans are inexpensive. Soy proteins are often utilized in food recipes for non-nutritional purposes, such as to modify sensory and physical attributes of a food product. Sensory attributes may include taste, texture, and mouth feel, while physical characteristics may include viscosity and homogeneity of a food product. Soy proteins elicit a number of important functions in food matrices, such as water binding and absorption, gelation, thickening, and emulsification. Therefore, various baked goods, breakfast cereals, pasta, beverages and toppings, meat and poultry products, and dairy products may contain soy proteins.

2.1.1.2. Characteristics of soy proteins

Three functions of proteins have been identified in soybeans; namely, proteins involved in metabolism, structural proteins, and storage proteins [21]. Majority of soy proteins are storage proteins, such as glycinin (~40 %), β-conglycinin (~28 %), and γ-conglycinin (~3 %), which do not elicit biological functions [21]. Another method for protein differentiation is based on the time they take to sediment during centrifugation, measured in Svedberg units (S). It is a measure of time and defined as 10^{-13} seconds. When protein mixtures are centrifuged, higher molecular weight (MW) proteins sediment faster than lower MW proteins, resulting in higher Svedberg units. Soy protein mixtures, when subjected to centrifugation, are separated into multiple protein fractions, which included 2S (α-conglycinin), 7S (β- and γ-conglycinin), 11S (glycinin), 9S, and 15S globulins [21].

The glycinin (11S) structure is composed of two identical hexamers. In each hexamer, there are three acidic subunits (MW ~37-40 kDa) and three basic subunits (MW ~19.9-20 kDa) [21]. Disulfide bonds link these acid-base subunits. The 7S proteins (β- and γ-conglycinin) are trimeric glycoproteins, which are made of α (MW ~57-76 kDa), α‘ (MW ~57-83 kDa), and β (MW ~42-53 kDa) subunits [21]. The isoelectric points (pI) of glycinin and β-conglycinin are 4.9 and 4.8, respectively [25]. The α-conglycinin (2S globulin; MW ~21 kDa) has a pI of 4.5 and is present at 13.8 % of soybean globulins [21]. β- and γ-conglycinin are composed of lower contents of tryptophan and sulfur-containing amino acids compared to glycinin. The absense of disulfide bonds between subunits of β- and γ-conglycinin leads to their functional differences compared to the glycinin. Glycinin, which denatures at 92 ^{o}C, is relatively more heat stable than β-conglycinin, which denatures at 71 ^{o}C [26].

2.2. Peptides

Peptides are the products of amino acid condensation or protein hydrolysis. Peptides are smaller in molecular weight and size than their native protein source. Resulting peptides from protein hydrolysis can be diverse in nature, as peptides of varying lengths, amino acid composition, and functionality can be obtained.

Physicochemical properties of peptides include solubility, size, surface hydrophobicity, charge, acid-base properties, and metal-binding properties [27]. These properties mostly depend on the presence of titratable groups between pH 0-14, such

as carboxyl-, amino-, and thiol-groups; hydrophobic groups, such as alkyl-groups; and neutral hydrophilic groups, such as amide-groups in side chains [28].

A peptide contains an α-carboxyl group and an α-amino group, however depending on the conformation of the peptide, these groups may be occupied (i.e. in cyclic peptides), and hence may not contribute to their physicochemical properties.

For many applications, such as gelation in food systems, solubility is one of the most important properties of peptides. Various factors affect peptide solubility, including pH, ionic strength, presence of divalent ions, amino acid composition, and temperature [29]. At its pI, a peptide assumes a net zero charge; at high pH conditions, it assumes a net negative charge, due to the deprotonation of carboxylate and amino groups; and at low pH conditions, it assumes a net positive charge, due to protonation of carboxylate and amino groups. In the presence of multiple charged peptides, electrostatic interactions occur: similarly charged peptides are electrostatically repulsed, while oppositely charged peptides are electrostatically attracted to each other. These pH conditions and interactions affect the solubility of peptides by influencing the interactions between peptides and the solvent [29].

Some transition metal ions, such as copper (Cu^{2+}) and nickel (Ni^{2+}), can form complexes with functional groups in peptides and amino acids, such as glutamate and histidine, and restrict the functionality of these groups [28]. Various enzymes such as collagenase contain zinc ions (Zn^{2+}) that bind to functional groups of amino acids. Another example of high affinity for metal ions is the thiol group in cysteine to silver (Ag^{+}) and mercury (Hg^{2+}) [28].

2.2.1. Production of peptides

Peptides can be produced by chemical synthesis and protein hydrolysis. In order to monitor the production of peptides through proteins hydrolysis, the degree of hydrolysis (DH), defined as the number of peptides and free amino acids present in a sample, can be determined using quantitative assays such as the O'phthaldialdehyde (OPA) assay. This assay is based on a single electron transfer and provides results due to a reaction between β-mercaptoethanol and OPA in the presence of an amino group from an amino acid or a peptide to form a multiple-ring structure [30]. Figure 1 provides an illustration of the reaction. The production of this ring-compound can be measured by a spectrophotometer at 340nm wavelength.

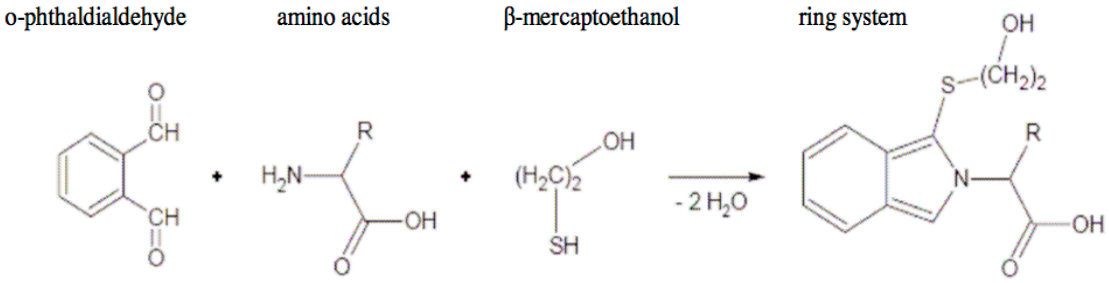

Figure 1: Mechanism of OPA assay to detect free amino acids and peptides present in a solution [31].

2.2.1.1. Enzymatic hydrolysis

Enzymatic hydrolysis of proteins is the most commonly employed technique to produce bioactive peptides *in vitro*. Unlike acid and alkali hydrolysis of proteins, enzymatic hydrolysis minimizes the production of undesirable by-products or side reactions, due to relatively mild processing conditions and the specificity of enzymes. It also allows for a controlled peptide production, in terms of final product functionality, because specific enzymes can be selected for the necessary task [32]. Gastrointestinal enzymes, such as pepsin and pancreatin mixtures, have often been used in the production of bioactive peptides, and their mechanisms will be described in the next sections [33]. Many other proteolytic enzymes and combinations thereof, such as Alcalase and Flavourzyme, can be utilized for producing peptides from proteins.

Pepsin

Among the gastrointestinal protein hydrolysis enzymes (proteases), pepsin is one of the most extensively studied. Though pepsin has a broad range of substrate specificities, its predominant cleavage sites are phenylalanine and leucine [34]. Other cleavage sites include proline, cysteine, threonine, and serine [34]. Porcine pepsin is 34.6kDa in molecular weight and consists of 324 amino acid residues [35]. Its activity ranges from pH 1.0-6.0, with maximum activity at pH 3.2. Its isoelectric point is at pH 1.0 [35,36].

Pepsin is an aspartic protease, which consists of two aspartic acids in its active site that facilitates the hydrolysis of peptides [35]. Mechanism of action of aspartic proteases is unknown. It has been proposed that the two aspartic acids collaboratively catalyze a nucleophilic attack by a water molecule on the carbonyl group of the peptide bond that is being cleaved [35].

Pepsin activity is dependent upon the size of the substrate [35]. The presence of hydrophobic residues at the cleavage site facilitates peptide hydrolysis by pepsin [35]. During the hydrolysis of a polypeptide chain, the structure and state of pepsin changes after each subsequent dissociation, which is known as an iso-mechanism [35]. After the penultimate dissociation, the state of pepsin is altered. This subsequently suggests that pepsin undergoes isomerization, such as changes in its conformation, in order to recover its substrate binding state to be functional [35].

Pancreatin

Pancreatin is a mixture of enzymes produced by the human pancreas. These enzymes include proteolytic enzymes (trypsin, chymotrypsin, carboxypeptidases and pancreatopeptidases), amylases, and lipases [37]. Their activity is best observed at pH 6.5-9.0 and 37-40 ^{o}C [37]. For proteolytic activity, trypsin and chymotrypsin enzymes are of interest.

Classified as a serine protease due to a serine residue at its active site, trypsin is a pancreatic enzyme that is well known for its proteolytic activity. The active sites of serine proteases consist of histidine (residue 57), aspartate (residue 102), and serine (residue 195) to form a catalytic triad that contributes to their specificities, such as serine nucleophilic property [35]. Trypsin mainly cleaves peptides at basic amino acids, especially lysine and arginine [35]. This cleavage usually occurs on the carboxyl ends of these amino acids. When a proline residue follows a basic amino acid, tryptic hydrolysis does not occur. This enzyme has shown proteolytic activity in the absence of these basic amino acid residues [35].

Chymotrypsin is also a serine protease. Predominant proteolysis by chymotrypsin is observed at the carboxyl ends of tyrosine, tryptophan, and phenylalanine residues, all of which are aromatic amino acids [35]. These aromatic side chains (with ring structures) can fit into the hydrophobic pocket (active site) of chymotrypsin. Another cleavage site includes the amide bond near the carboxyl end of leucine, though this catalysis is relatively gradual. Optimum hydrolysis activity conditions for chymotrypsin are 37 ^{o}C and pH 7.0 [35].

Alcalase and Flavourzyme

Subtilisin carlsberg, which is purified from Bacillus licheniformis, is the main enzyme in the alcalase enzyme mixture [38]. Due to its cost-effectiveness, it is

advantageous to use alcalase when compared to other protease enzymes, such as trypsin. Its best-known application is the production of caseinophosphopeptides (CPPs), which are milk protein-derived peptides that have shown to prevent dental cavities and tooth decay [38]. Optimum operating conditions for alcalase are 50 ^{o}C at pH 4.6, with an enzyme: substrate molar ratio of 1:50 [38]. Alcalase has a broad specificity in terms of cleavage sites on a peptide. The following have been identified to be preferential cleavage sites: glutamate, methionine, leucine, tyrosine, lysine, and glutamine [38].

Flavourzyme consists of endo- and exo-peptidases [39]. The protein hydrolysates produced by flavourzyme have shown to be less bitter compared to those produced by other proteases, therefore they are more desired for food applications. Cleavage sites and mechanisms of flavourzyme enzymes have not been widely studied. Optimum hydrolysis conditions for flavourzyme are 50 ^{o}C for 90 min with an enzyme: substrate mass ratio of 1:50 [39].

2.2.1.2. Microbial fermentation

Microbial fermentation is employed to produce peptides mainly in dairy products, such as in yoghurt and cheese production. Dairy starter cultures, such as lactic acid bacteria (LAB), are extremely proteolytic. Some of the commonly used LAB cultures include *Lactococcus* lactis, *Lactobacillus* helveticus, and *Lactobacillus* delbrueckii spp. bulgaricus [33]. LAB cultures possess proteinases in the cell walls and intracellular peptidases (i.e. endopeptidases and dipeptidases) [33]. Peptide production using microbial fermentation can be controlled to a desired extent. This is because microbial peptidase activities are dependent upon the growth conditions of the microorganism; therefore by controlling the growth conditions, it is possible to obtain microbial peptidases that provide the desired functionalities [33].

2.2.2. Peptide and amino acid analysis techniques

Peptides, including antioxidant peptides, can be analyzed for amino acid composition. Amino acid analyses can provide information on peptide functionality and behavior. For example, the presence of amino acids with phenolic (ring) structures (i.e. histidine, tyrosine, phenylalanine, tryptophan) has shown to influence the antioxidant capacities of peptides; and their concentrations in a peptide solution can be determined by conducting amino acid analysis [2]. Among many analytical tools, reverse phase high

performance liquid chromatography (RPHPLC) and nuclear magnetic resonance (NMR) spectroscopy are widely used methods for amino acid analysis.

2.2.2.1. Reverse-phase high performance liquid chromatography

Chromatography is a powerful tool to separate and quantify alike components of interest from a mixture based on their distinctive properties, such as structure, hydrophobicity and composition. Among the many chromatography methods available, RPHPLC is the most commonly used method for peptide and amino acid analysis. The main separation mechanism is based on hydrophobicity, and is applicable to neutral and charged peptides [46]. An RPHPLC column generally consists of a non-polar (hydrophobic) stationary phase. A stationary phase can range from C_1-C_{18} to cyano and phenyl functional groups [46]. The mobile phase is a mixture of water and an organic solvent, with acetonitrile (ACN) or methanol (MeOH) being the most preferred options [46]. Differences between ACN and MeOH include absorption in the UV short-wavelength range, elution strength, and viscosity. A suitable organic solvent for RPHPLC must be water-miscible, stable under operating conditions, non-viscous to obtain continuous volumetric flow in the system, inexpensive, readily available, and clear at wavelengths below 280nm for UV detection [46]. Examples of other organic solvents (also known as B-solvents) are isopropanol and tetrahydrofuran. When separating pH sensitive samples, a buffered mobile phase is required.

Retention in RPHPLC depends on the interactions of molecules with the stationary and the mobile phase. Polar molecules (hydrophilic) will interact strongly with the polar mobile phase and weakly with the stationary phase. This would lead to low retention of polar molecules by the column [46]. Therefore polar molecules will elute early as a result of the weaker interactions of the molecule with the stationary phase. Less polar molecules will interact strongly with the non-polar stationary phase, leading to their elution at longer retention times. Molecules of similar size can be eluted at different times by inducing polarity differences.

Although it is widely accepted that hydrophobicity is the main factor affecting peptide separation in RPHPLC, pH and ionic strength play important roles due to the charges on the peptides and the lability of the silica sorbents in the stationary phase [47]. pH values between 2-8 have been widely used during separations [47]. For stationary phase base on C_{18} bonded to silica, peptides can display higher retention at

acidic pH conditions than at neutral or basic pH conditions [47]. Therefore, the mobile phase has been occasionally modified by incorporating 0.1 % phosphoric acid (pH 2.2) to ACN to improve peak resolutions [47]. Similarly, 0.1 % hydrochloric acid in ethanol or ACN has also improved peak resolutions [47]. However, due to the dynamic behavior of peptides as a function of pH, separation by RPHPLC is affected in a very complex manner.

At net zero ionic strength, peptides tend to be characterized by longer retention times and lead to lower resolution [47]. As ionic strength increases, peptides interact strongly with the stationary phase and lead to peaks with improved resolution [47]. Imoto and Yamada (1983) found that effects of ionization were more dominant on shorter tryptic peptides of lysozyme or free amino acids (mostly hydrophobic peptides), and resulted in longer retention time [47]. The ionization of hydrophobic residues and side chains resulted in shorter retention time for these peptides. For charged peptides, the position of a charged group can also be a factor in the retention mechanism. Temperature dependence of peptide separation does not seem to be important for temperatures between 25 and 55^{o}C [47]. Therefore, retention times of peptides in RPHPLC are predominantly influenced by hydrophobicity, followed by the ionization state and overall charge of peptides [47].

2.2.2.2. Nuclear magnetic resonance spectroscopy

NMR spectroscopy has the ability to handle samples with complex mixtures of multiple bio-molecular species at low concentrations simultaneously [48]. NMR can provide information on the amino acid composition of proteins, along with protein structural analysis [49]. In fact, proton NMR is an alternative to conventional amino acid analysis techniques, such as HPLC, as discussed by Kellenbach, et al. (2008) [50].

Magnetic nuclei in a magnetic field can absorb and emit electromagnetic radiation at specific resonance frequencies that depend on the magnetic properties of the isotope of the atom and the magnetic field strength [50]. The predominantly studied nuclei using NMR are ^{1}H and ^{13}C, though other nuclei, such as ^{2}H and ^{10}B, have also been investigated [50]. NMR can be conducted using one- (1D), two- (2D), three- (3D) and higher-dimensional multi-frequency techniques, as explained by Kellenbach et al. (2008) [50].

The underlying mechanism of 1D-^{1}H NMR is the excitation of hydrogen atoms (protons) in samples using a strong magnetic field pulse (i.e. 400-800 MHz). Upon completion of the pulse, molecules relax from the excited states, emitting magnetic frequency that is unique to each molecule in the sample. A 1D proton spectrum can identify the 20 naturally occurring amino acids as well as unnatural amino acids (i.e. from synthetic peptides) [50]. The 1D-^{1}H NMR spectrum of a peptide is directly related to the specific amino acid residues and their concentrations in a peptide sequence [50]. Thus, the intensity of the proton signal obtained for a peptide corresponds to the relative number of protons at a given location within that peptide [50]. Other factors affecting the NMR spectrum include the solvent, pH conditions, temperature, buffer composition, and NMR acquisition and processing parameters [50]. However, as the molecular size of a peptide increases, the number of resonances increases and signals become broader, compromising the resolution of the NMR spectra. Consequently, the accuracy of amino acid quantification using NMR will decrease as the size of peptides increases [50,51].

Detailed information on principles of NMR spectroscopy, its applications, and developments can be found in Diehl et al. (2008) [52].

2.3. Antioxidants

An antioxidant is defined as a substance that can significantly decrease or retard the unfavorable effects of reactive species, such as oxidative free radicals, on normal human physiological functions, and in biological and food systems [53]. However, not all oxidizing agents in a reaction are antioxidants, as not all of them protect biological targets from oxidation [54]. There are two types of antioxidants: primary antioxidants, which terminate radical chain reactions (free radical scavengers); and secondary antioxidants, which eliminate oxidation reactions by preventing the formation of reactive oxidants (preventive antioxidants) [54].

The human body possesses enzymatic and non-enzymatic systems to counteract against oxidative damage, to protect tissues and organs, and eradicate oxygen or free radicals. Among these are superoxide dismutase (SOD), glutathione peroxidase (GSHPx), and catalase (CAT) enzymes [55]. SOD works to mutate the superoxide radical, leading to the formation of O_2 and H_2O_2 [55]. GSHPx and CAT enzymes cause the decomposition of H_2O_2 to O_2 and H_2O [55]. Other molecules found in foods that have

displayed high antioxidant capacity include vitamins C, E, and A; beta-carotene; and glutathione. These antioxidants are commonly found in high concentrations in food and beverages, such as blueberry, blackberry, black tea and red wine.

Antioxidant capacity describes the overall effectiveness and efficiency of chemical specie in performing antioxidative functions, and is influenced by various factors, such as oxidative environment and the physical state of oxidizable substrates [54].

2.3.1. *In vitro* antioxidant assays

Numerous well-established *in vitro* assays are available to measure antioxidant capacities of substances, as presented in Karadag et al. (2009) and Apak et al. (2007). These assays can be broadly categorized as hydrogen atom transfer (HAT)- and electron transfer (ET)-based assays. HAT-based assays, such as Oxygen Radical Absorbance Capacity (ORAC), involve a complex scheme of reactions whereby an antioxidant and a substrate compete for peroxyl radicals, which were thermally generated by the breakdown of azo-compounds [6]. In the ORAC assay, fluorescence decay due to oxidative degeneration of fluorescein by peroxyl radicals is monitored in the absence and presence of antioxidants. Fluorescence decay plots can be generated to obtain the net area under curve (AUC), which indicates the antioxidant capacity of a sample [6]. An antioxidant's ability to quench free radicals by donating an H-atom is therefore realized. A possible oxidation pathway for fluorescein in the presence of AAPH is provided in Figure 2.

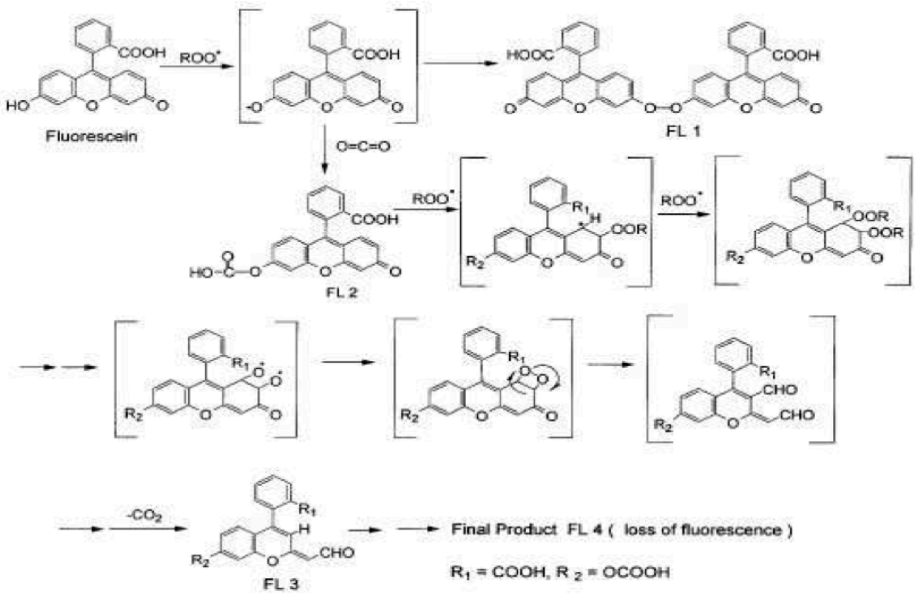

Figure 2: Possible fluorescein oxidation pathway induced by AAPH [32].

ET-based assays, such as the Folin Ciocalteau Reagent (FCR) and Ferric Reducing Antioxidant Power (FRAP) assays, employ simulated antioxidant actions where a redox-potential probe (i.e. fluorescent or colored probe) is used. Antioxidant capacity is thus measured by the reduction of an oxidant with a single electron transfer, upon which a color change in solution can be observed and quantified spectrophotometrically [6]. The mechanism employed by the FCR assay to determine the antioxidant capacity is presented in Figure 3.

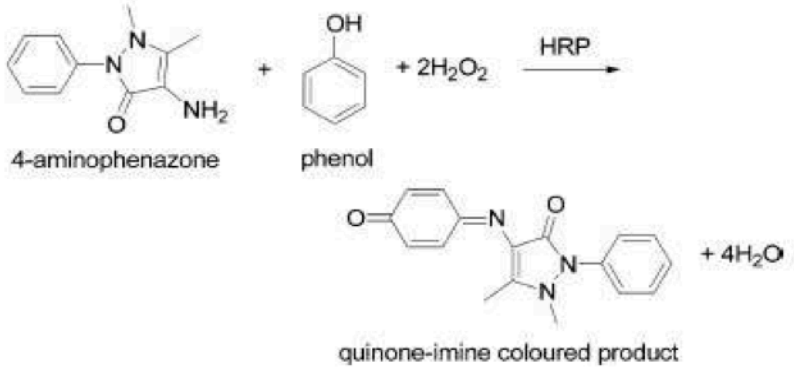

Figure 3: Mechanism of FCR assay to measure antioxidant capacity [33].

ET-based mechanisms employ non-physiological conditions (i.e. room temperature, irrelevant pH conditions, etc.) and measure the reducing capacity of a molecule in the absence of reactive free radicals, whereas ORAC measures the radical scavenging ability of a molecule, and is thus a superior method [56]. ORAC results

combine inhibition percentage and length of inhibition time of free radicals into one quantity to provide the antioxidant capacity [57].

2.3.2. Differences between *in vitro* versus *in vivo* antioxidant assays

It is important to understand the differences between *in vivo* and *in vitro* antioxidant activity determinations. *In vivo* studies involve the use of living organisms to test for antioxidant effects on physiological and metabolic functions, and to monitor health effects. Most *in vivo* studies on antioxidant activities are and have been conducted using laboratory rats, similar to drug screening tests. This is often preferred over *in vitro* studies as the observed effects can be directly related to humans. However, many disadvantages to *in vivo* studies are present, including high time consumption, lack of reproducibility, and high overall expenses. Many legal and ethical approvals are required to perform *in vivo* studies, sample preparations are extensive, a high sample population is necessary, appropriate facilities are required, and a large collection of chemicals treatments, such as anesthetics, are required.

In contrast, *in vitro* studies are conducted in controlled environments more frequently due to cost benefits, rapidity, and lack of complexity. The major drawback of *in vitro* studies, however, is the lower degree of relevance laboratory results have to human physiological functions, compared to *in vivo* studies.

The results obtained from *in vivo* studies may not directly correlate to results from *in vitro* studies [55]. However, they provide different perspectives to assess the quality of antioxidants. Using control-treatments in antioxidant assays, the extent to which antioxidant functions are displayed can be found.

2.3.3. Antioxidant soy peptides

Proteins may contain the correct amino acid and peptide sequences for bioactive functions. However, these peptides are restricted from eliciting their functions within the sequence of its native protein by peptide bonds, which occupy the N-terminus and C-terminus of peptides, and by side chain interactions between peptide chains. Upon liberation from their native protein sequence, peptides have displayed ACE inhibitory, opioid, mineral binding, immunomodulatory, antimicrobial, antithrombotic, and antioxidative functions in biological and food systems. It has been reported previously

that soy proteins have yielded bioactive peptides, including hypocholesterolemic and antioxidant peptides [2-5,41,58].

One of the highly antioxidant peptides identified in soy protein hydrolysates is leucine-leucine-proline-histidine-histidine peptide (leu-leu-pro-his-his) [2]. Based on this peptide, numerous antioxidant peptides were synthetically formulated. Chen et al. (1998) used the following antioxidant assays to verify the antioxidant capacity of synthetic peptides: (i) 2,2'-azobis-2-methyl-propanimidamide dihydrochloride (AAPH) induced oxidation, (ii) 2,2'-azobis(2,4-dimethylvaleronitrile) (AMVN) induced oxidation, (iii) 2,2-diphenyl-1-picrylhydrazyl (DPPH) radical scavenging, (iv) superoxide scavenging, and (v) chelating activity of metal-ions [2]. Results showed that pro-his-his and his-leu-his peptides demonstrated high antioxidant capacity in the AAPH-induced oxidation system (water soluble), but no activity was observed in the AMVN-induced oxidation system (oil soluble) [2]. The his-his portion of this leu-leu-pro-his-his peptide was the primary contributor to its antioxidative property. It was found that pro-his-his, as an individual peptide, displayed the highest antioxidant capacity. Furthermore, the presence of a leucine or proline residue at the N-terminus of a his-his-containing peptide enhanced the antioxidant capacity and hydrophobicity of the peptides [41]. Histidine and other aromatic amino acids contribute to antioxidant capacity, due to their ring structures [2,59]. However, the antioxidant capacity of a histidine residue is greater within a peptide, compared to when it stands alone, due to synergistic effects with other amino acid residues, like those from proline and leucine [2].

Enzymatic hydrolysis of proteins has been shown to be a viable method for the preparation of antioxidant peptides:

1. Given that the presence of a proline or a leucine residue at the N-terminus of a histidine-histidine peptide contributes to antioxidant activity [2], the ability of pepsin to cleave at these specific sites leads to a higher likelihood of obtaining antioxidant peptides. Experimental conditions employed in the production of antioxidant soy peptides using pepsin must be similar to operating conditions of pepsin in the human body (37 ^{o}C and acidic conditions).
2. Given that it has been found that positively charged lysine and arginine groups must be present at the C-terminus of a peptide for ACE-inhibitory effects, and a leucine

residue at the C-terminus for antioxidant functionality of a peptide, an enzyme system that allowed these characteristics is desired. Both trypsin and chymotrypsin can be used to achieve this type of digestion.

3. Alcalase and flavourzyme have also been investigated for the production of antioxidant peptides [32].

2.4. Membrane Filtration

Membrane filtration is a physical process of separating components by using a membrane material that allows the selective passage of components according to the membrane material properties [10]. The most common classes of filtration include microfiltration (MF), ultrafiltration (UF), nanofiltration (NF) and reverse osmosis (RO). Commercial filtration membranes are produced with many types of polymers, and used for different separation processes. Factors that differentiate between these classes of membrane filtration include the overall separation mechanism (i.e. size, charge, or both), the membrane material properties, the driving forces for separation (i.e. vacuum or pressure), the ultimate goal of filtration, and the nature of samples being separated [10]. Table 2 provides a guide to differentiate between the tangential flow membrane filtration methods according to membrane pore size, molecular weight cut off (MWCO) of compounds, pressure, and permeation.

Table 2: Properties of different tangential flow membrane filtration methods [60].

Method	Membrane pore size (nm)	MWCO (kDa)	Pressure (Pa)	Permeation
Reverse osmosis (RO)	<0.6	<0.5	435–1015	Water
Nanofiltration (NF)	0.6–5	0.3–2	145–580	Water, low molecular solutes
Ultrafiltration (UF)	5–50	2–500	7–145	Above and macromolecules
Microfiltration (MF)	50–5000	>500	7–29	Above and colloids

In membrane filtration, the feed solution is placed in contact with a membrane. A transmembrane pressure (TMP) is applied to the system to drive the feed solution through the membrane. A portion of the feed solution will diffuse through the membrane (permeate) while some will be rejected by the membrane (retentate or

concentrate). There are two modes of filtration configurations: dead-end and tangential flow. In dead-end filtration, a fluid passes through the membrane while all particles larger than its pore sizes are retained at the membrane surface, and particles smaller than its pore sizes diffuse through. Over time, a build-up of retained material collects on the membrane surface, known as a cake layer, and compromises the efficiency of the filtration process. Then, the membrane requires cleaning and backflushing to recover its functionality. In tangential flow filtration, a fluid feed runs tangential to the membrane surface, leading to a pressure difference across the membrane. Particles smaller than the membrane's pore sizes diffuse through the membrane, while particles that are larger than its pore sizes continue to flow across the membrane, minimizing the cake layer formation that occurs in dead-end filtration.

2.4.1. Membrane fouling

Membrane fouling refers to the gradual accumulation, deposition and adsorption of retained components on the membrane surface or within a porous membrane, which affects mass transfer across the membrane and reduces filtration efficiency [10]. Figure 4 depicts an early representation of the concentration profile occurring during membrane filtration, where C_b is the concentration of a solute in the bulk phase (feed) and $C_{m,2}^{ext}$ is the final solute concentration in the permeate [61]. This model assumes that an external pressure is applied adjacent to the semi-permeable membrane. Solutes present in the bulk feed solution flow towards the membrane. If solutes are rejected, partial permeation occurs, and non-permeated solutes accumulate on the boundary layer [61].

During membrane filtration, rejected solutes accumulate on the membrane to form a cake layer as depicted in Figure 4, adapted by Trimmer (2001), while only a limited concentration of solutes would permeate through the membrane (i.e. neutral, uncharged compounds). These movements would occur by convection and diffusion [61]. Due to the accumulation of solutes at the cake layer, a concentration profile is established, in a process known as concentration polarization [61]. This phenomenon, along with fouling and gel layer formation, can contribute to additional resistances (R_a), including fouling resistance (R_f). The total resistance (R_{tot}) by the membrane during and after a filtration is the sum of membrane resistance (R_m) and R_a [12].

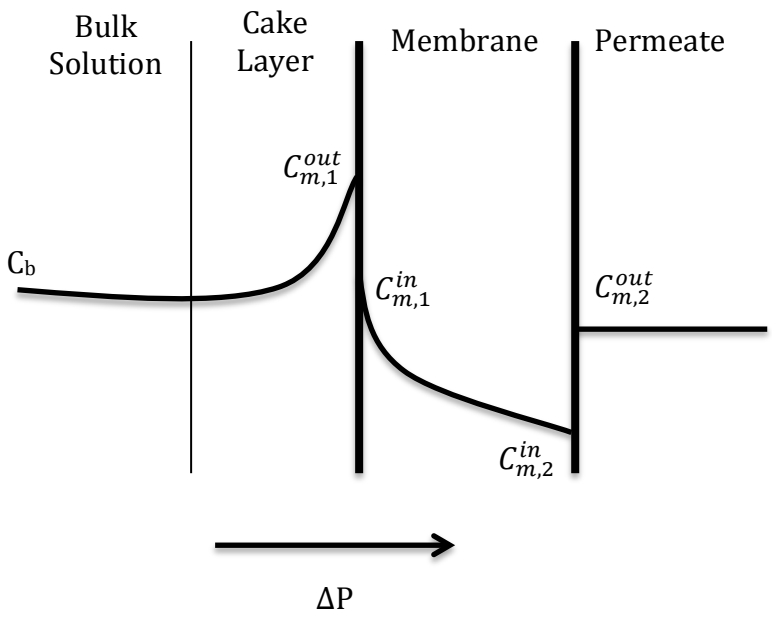

Figure 4: Model for mass transfer through a NF membrane.

Solvent flux (J, m s^{-1}) through a membrane can be explained according to Darcy's Law (equation 1):

$$J = \frac{TMP - \sigma\,\Delta\pi}{\eta\, R_{tot}} \qquad (1)$$

where σ is the rejection coefficient of the membrane towards a solute ($0<\sigma<1$), $\Delta\pi$ is the osmotic pressure difference across the membrane (N m^{-2}), and η is the dynamic viscosity of the permeating solution (kg m^{-1} s^{-1}). TMP is given in N m^{-2} and R_{tot} in m^{-1} [12,61]. The solvent flux equation (above) can be modified to express the permeate flux (J_{Per}; m s^{-1}) in terms of TMP, viscosity of the permeate (η_{Per}) and R_{tot} by equation 2:

$$J_{Per} = \frac{TMP}{\eta_{Per}\, R_{tot}} \qquad (2)$$

The TMP is expected to increase during filtration due to the increase in concentration of molecules in the retentate stream, which in turn causes an increase in η of the retentate that is being recycled. This increase in η leads to a decrease TMP and subsequently J_{Per}.

Permeate mass flux analysis can be performed to determine the normalized flux during membrane filtration, thus determining the extent to which membrane fouling has occurred at a given time. Normalized flux (J_P J_0^{-1}) is calculated by dividing the permeate mass flux (J_P) of the solution at a given time, t (m s^{-1}), by the initial permeate mass flux (J_0) of the same solution (m s^{-1}) in a filtration. Water flux measurements can

be performed before and after each filtration experiment and their cleaning protocols to determine the R_m and R_f, respectively. When water is used as the filtering solution, R_{tot} becomes R_m. When peptide solutions are used, R_{tot} is the sum of R_m and R_f.

2.4.2. Ultrafiltration

UF is one of the most popular means of membrane filtration, which removes or concentrates target components present in a solution via a molecular sieve-effect. The molecular sieve effect occurs due to size differences between a membrane's pore and components in the feed solution. Figure 5 illustrates the components and configuration of a lab-scale UF system, adapted by Skorepova (2007). UF membranes can possess a distribution of pore sizes, which depends on the membrane material and its manufacturing process. UF membranes can be identified by their nominal pore size (typically between 0.01-0.05 μm) or by MWCO values (typically between 10-500 kDa) [10].

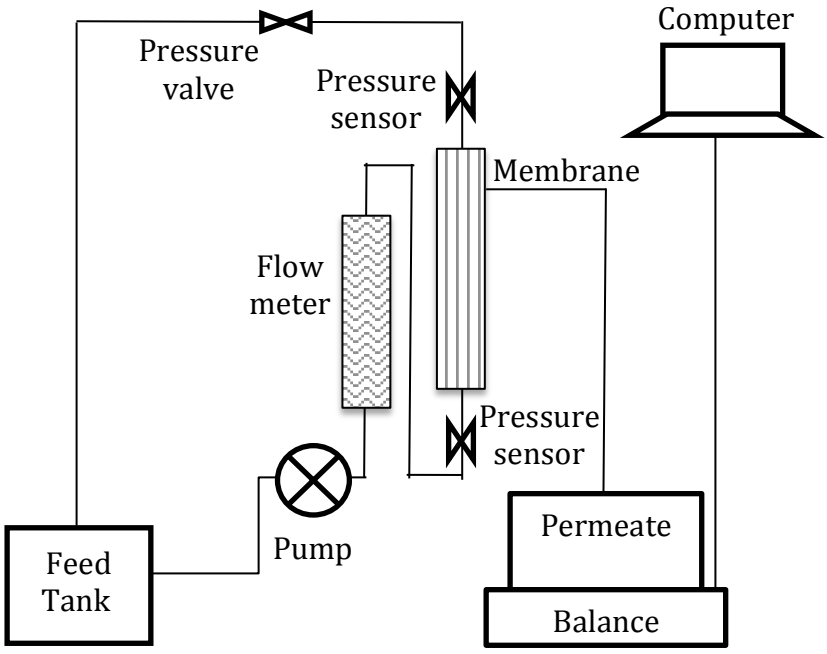

Figure 5: Components and configuration of a lab scale UF system.

2.4.3. Nanofiltration

Most NF membranes have MWCO values between 0.2 to 1 kDa, since their average pore sizes are between 0.5-2.0 nm, however membranes with MWCO values of up to 3 kDa can be considered loose-NF membranes [10,61]. NF is unique, since separation is achieved by charge and size rather than solely size. NF requires higher TMP due to lower membrane permeability and MWCO than UF and MF. However, NF

operating TMP is lower and MWCO is higher than RO [62]. The charges of ionic compounds being separated and the NF membrane play an important role in the separation. Therefore, NF systems can be efficient for demineralization, desalting, and purification of ionic compounds, including peptides. Figure 6 illustrates the configuration of a lab scale NF system.

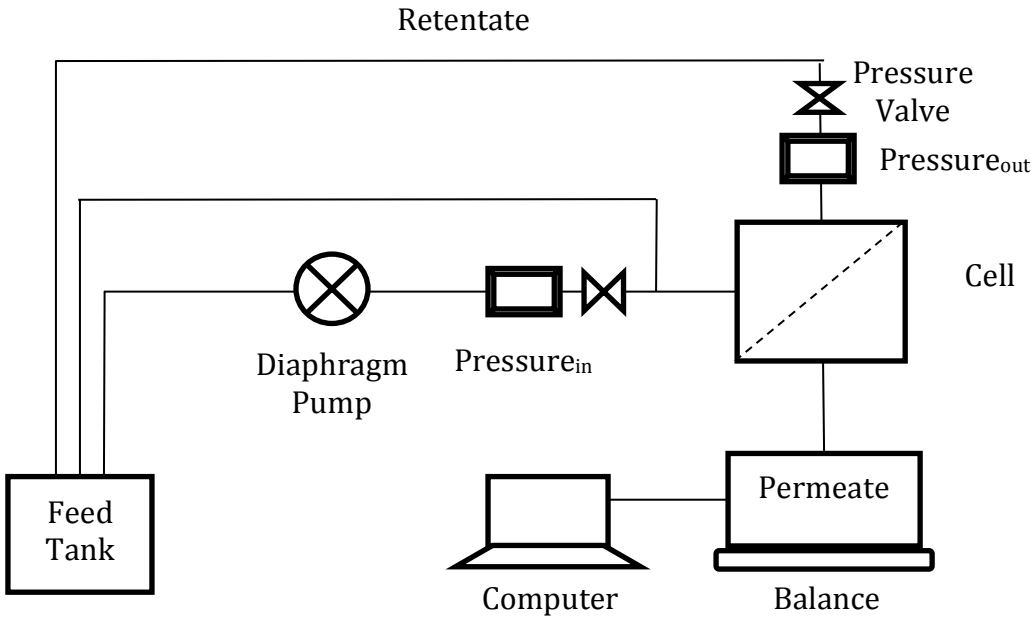

Figure 6: Components and configuration of a lab scale NF system.

The basis of separation (i.e. molecular sieve, charge, or both) in NF is particularly dependent upon the membrane used and the composition of the feed solution. Due to the charge and size interactions that occur in NF, a solute (ionic compound) may be filtered or rejected by the membrane. The solutes that are separated by NF can be categorized as co-ions and counter-ions, based on their net charge compared to the charge of the membrane surface. Co-ions refer to ions that assume the same charge as the membrane, and counter-ions to ions with the opposite charge. When mixtures of co-ions and counter-ions are present in the NF feed, the co-ion concentration at the membrane surface is lower compared to the feed solution, while the counter-ion concentration is higher at the membrane surface compared to the feed solution [12]. Due to this ion concentration difference, a potential difference is developed at the interface between the bulk feed solution and the membrane, called the Donnan Potential [12]. Due to the Donnan Potential, counter-ions are electrostatically attracted to the NF membrane, while co-ions are repulsed. This phenomenon leads to a higher permeate flux of counter-ions. By manipulating the charges on membrane and ionic

compounds of interest by adjusting the pH and ionic strength, desired separations can be enhanced. If the ion concentration in the solution is increased, while the charge on the membrane is decreased, a higher concentration of co-ions will be observed at the NF membrane surface, as co-ion exclusion is reduced [12]. As the counter-ion valence increases and co-ion valence decreases, the co-ion concentration in the membrane increases, which is an important theory to describe NF membranes in terms of their selectivity and permeability using simple electrolyte solutions [12].

When separating peptides using NF, physicochemical properties (pH and ionic strength) of peptides and concentration of amino acids in the protein hydrolysate are important factors [12]. In the presence of a charged NF membrane, membrane-peptide interactions for negatively charged peptides and positively charged peptides are likely to be different. Relative to the charge on a membrane, charged peptides can also be categorized as co-ions and counter-ions, and they follow similar behaviors as ionic compounds during fractionation by NF. Membrane-peptide relationships are established experimentally. It has been suggested that the charge of individual amino acids on a peptide sequence has a greater impact on membrane-peptide interactions than the net charge of the entire peptide [12].

Pouliot et al. (1998) performed a tryptic digestion of commercial whey protein and fractionated the hydrolysates with a SG13 NF membrane at pH 5 and 9, to investigate the effects of counter-ion and co-ion interactions on peptide fractionation, respectively [12]. Their study indicated that peptide charge affected permeability and fouling of the membrane. Fouling of NF membranes can occur via cake layer formation, and preferential adsorption of proteins to the membrane [12]. Pouliot's experiments showed that counter ion interactions between membranes and peptides, obtained by changing the pH, lead to preferential binding of peptides to the membrane, resulting in a higher extent of membrane fouling [12].

A similar experiment was performed by Butylina et al. (2006) to separate bioactive peptides from whey proteins using a sulfonated polyether sulfone NF membrane (NTR 7450; 1 kDa MWCO) at pH 3 and 9.5, to investigate the effects of counter-ions and co-ions on peptide fractionation, respectively [14]. The results of Butylina were in agreement with Pouliot.

2.4.4. Selection of operating parameters

For the fractionation of SPH, appropriate TMPs, temperatures, and volumetric flow rates for UF and NF experiments have been determined by Skorepova (2007), Bissegger (2009), and Meissner (2010). Permeate fluxes were determined as a function of time for 2 % and 8 % (w/w) SPI solutions at a TMP range of 14-170 kPa for UF. A flow rate of 2.4 L min^{-1} at 22 ^{o}C was employed [22,63,64]. During filtration, the permeate flux increases as a function of TMP to a certain extent, beyond which the permeate flux becomes independent of the TMP and the filtration does not proceed efficiently. It was found that UF conducted in concentration mode (i.e. permeate collected separately, retentate recycled) performed efficiently between a TMP range of 40-70 kPa, and hence UF of SPI solutions were conducted at a TMP of 62 kPa (9 psi) and flow rate of 2.4 L min^{-1}. Similarly, conditions for NF of SPI were identified to be efficient at 22 ^{o}C, 2 MPa (290 psi), and 1.8 L min^{-1}.

2.5. Fluorescence Spectroscopy

Fluorescence is a term used to describe cold light emission, which occurs when molecules are excited by photons, due to electron transfer in the singlet state [65]. It occurs in three stages: a fluorophore is excited to a singlet state by a photon. The excited state undergoes conformation changes and interactions with the molecular surroundings, and fluorophore returns to the ground state emitting a photon at a longer wavelength [65]. Intrinsic fluorescence refers to fluorescence that is caused due to fluorophores present in a sample, in the absence of scatterers and absorbers [66]. Intrinsic fluorescence measurements are affected by quenching, the concentration of fluorophores in a sample, and their molecular environment.

Various organic compounds, such as polyaromatic hydrocarbons, present in food and nutraceutical products are naturally occurring fluorophores and therefore fluoresce. These naturally occurring fluorophores include tyrosine, tryptophan, phenylalanine, retinol, and riboflavin. Uses of fluorescence in food analysis are explained in detail by Christensen et al. (2006) [65]. In meat and fish industries, fluorescence has been commonly used for quality control purposes, to measure collagen in connective and adipose tissues. Components in meat, including bone, cartilage and connective tissues have different fluorescent properties, which are exploited to detect adulterations. Fluorescence has also been used to detect bone in fish fillet products [65].

Other uses of fluorescence in food and agriculture research and processes include investigating protein structures, monitoring milk composition after thermal treatments [67], and ripening of tropical fruits [68].

Fluorophores have discrete spectral excitation-emission profiles to describe their distinctive fluorescence properties. At a given excitation wavelength, fluorescence intensities of a sample can be collected at a range of emission wavelengths. By collecting the fluorescence intensities at a range of excitation and emission wavelengths (Ex/Em), a fluorescence landscape or excitation-emission matrix (EEMs) can be constructed. A fluorescence EEM may contain thousands of intensity points depending on the range of Ex/Em used. Complex data obtained by fluorescence analyses can be combined with multivariate statistical methods, such as principal component analysis (PCA) and partial least squares (PLS) regression, to capture variances and extract significant systematic trends in a sample data set [65,69].

2.5.1. Principal Component Analysis

PCA is a widely used technique to extract information from a large number of variables. It extracts a smaller set of new variables, known as principal components (PCs) that are uncorrelated, mutually independent, and linearly related to the original variables in the data matrix [11]. PCs take into account a large proportion of variance present in a data matrix as explained by Eriksson et al. (2001) [70]. Hence, PCs can provide information on patterns and changes that occur in the original spectral data matrices. The process of data decomposition in a matrix *X* by PCA can be explained by equation 3;

$$X = \sum_{i=1}^{n} t_i \cdot p_i + E \qquad (3)$$

where n represents the number of samples in the X data set, t_i represents scores, p_i represents loading values, and E is the residual matrix [71]. A detailed description of data decomposition by PCA can be found in Peiris et al. (2010) [11]. PCA has been used to project fluorescence intensities to new planes with PCs, where the scores (t_i) become the new coordinates. PCs are related to the original data set X by the loadings, which upon examination can be used to identify spectral variables in the X data set that are represented by each PC [11]. Detailed descriptions of PCA can be found in Eriksson et al. (2001) [70].

3. Production and Fractionation of Antioxidant Peptide Fractions from Soy Protein Isolate using Ultrafiltration and Nanofiltration

S. Ranamukhaarachchi, L. Meissner, C. Moresoli

Prepared for the Journal of Membrane Science

This manuscript was prepared under the supervision of Dr. Christine Moresoli. Ms. Lena Meissner conducted preliminary studies of fractionating antioxidant soy protein hydrolysates using multiple nanofiltration membrane materials. All of the experiments, results, and data analyses included in this manuscript were performed by Mr. Sahan Ranamukhaarachchi.

3.2. Abstract

Antioxidants are molecules capable of stabilizing and preventing oxidation. Certain peptides, protein hydrolysates, have shown antioxidant capacities, which are obtained once liberated from the native protein structure. Soy protein isolate (SPI) was enzymatically hydrolyzed by pepsin and pancreatin mixtures. The soy protein hydrolysates (SPH) were fractionated with sequential ultrafiltration (UF) and nanofiltration (NF) membrane steps. Heat pre-treatment of SPI at 95 ^{o}C for 5 min prior to enzymatic hydrolysis was investigated for its effect on peptide distribution and antioxidant capacity estimated by ORAC and FCR. The ORAC and FCR are fundamentally different antioxidant assays, which employ hydrogen atom transfer (HAT) and electron transfer (ET) based mechanisms, respectively. SPH were subjected to UF with a 10 kDa molecular weight cut-off (MWCO) polysulfone membrane. UF permeate fractions (lower MW than 10 kDa) were fractionated by NF with a thin film composite membrane (2.5 kDa MWCO) at pH 4 and 8. Similar peptide content and antioxidant capacity (α=0.05) were obtained in control and pre-heated SPH when comparing the respective UF and NF permeate and retentate fractions produced. FCR antioxidant capacities of the SPH fractions were significantly lower than their ORAC antioxidant capacities; and the distribution among the UF and NF fractions was generally different. Most UF and NF fractions displayed higher antioxidant capacities when compared to the crude SPI hydrolysates, showing the importance of molecular weight on antioxidant capacity of peptides. The permeate fractions produced by NF at pH 8 displayed the highest antioxidant capacity, expressed in terms of trolox equivalents (TE) per total solids (TS): 5562 μmol TE g^{-1} TS for control SPH, and 5187 μmol TE g^{-1} TS for pre-heated SPH. Due to the improvement in antioxidant capacity of peptides by NF at pH 8, the potential for NF as a viable industrial fractionation process was demonstrated.

3.3. Introduction

A variety of peptides obtained from plant and animal proteins have shown bioactive functions when liberated by hydrolysis from their native protein. It has been reported previously that soy proteins, which are plant-based, are abundant, inexpensive, and yield bioactive peptides that are hypocholesterolemic and antioxidant [2-5,41,58]. To fractionate bioactive peptides, membrane filtration technologies can be used [8,12,16]. Membrane filtration, such as microfiltration (MF), ultrafiltration (UF) and nanofiltration (NF), is a separation process based on the properties of a membrane material. The separation mechanism employed by MF and UF is a molecular sieve effect. NF is unique in comparison to MF and UF, since separation is achieved by charge and size rather than solely size. NF requires higher transmembrane pressure due to the lower membrane permeability and associated molecular weight cut off (MWCO) than UF. NF operating transmembrane pressure is lower and the membrane MWCO is higher than reverse osmosis (RO) [62]. Most NF membranes have MWCO between 0.3-1 kDa, since their average pore sizes are between 0.5-2.0 nm [61]. However, loose NF membranes have MWCO around 2-3 kDa. The charge of NF membranes plays an important role in separation. As a result, NF systems are efficient for demineralization, desalting, and purification of ionic compounds, including peptides [62].

When separating peptides by NF, pH and ionic strength of the protein hydrolysate solutions and characteristics of amino acids in the protein hydrolysate are important factors [12]. Membrane-peptide interactions will differ according to the charge of the membrane. Therefore according to their respective charge, peptides can be categorized as co-ions (same charge as membrane) or counter-ions (opposite charge as membrane). In an aqueous solution at pH conditions where electrostatic interactions exist between a membrane and ions in solution, the co-ion concentration will be lower at the membrane compared to the bulk phase, but the counter-ion concentration will be higher at the membrane surface [12]. This ion concentration gradient will lead to a potential difference, known as the Donnan Potential, at the bulk-membrane interface [12,62]. As a result, co-ions are subjected to repulsion by the membrane, while counter-ions are attracted, leading to higher membrane fouling by counter-ions. For peptides, it is suggested that charges of individual amino acids have greater impacts on membrane-peptide interactions than the net charge of the entire peptide [12].

Pouliot et al. performed a tryptic digestion of commercial whey protein and fractionated the hydrolysates with a SG13 NF membrane at pH 5 and 9 [12]. Their study indicated that peptide charge affected permeability and fouling of the membrane. Counter ion interactions between the membrane and the peptides, obtained by changing the pH, lead to preferential binding of peptides to the membrane, resulting in a higher extent of membrane fouling [12].

An important functionality of peptides produced by hydrolysis of proteins is antioxidant capacity [72]. Proteins extracted from soybeans, fish, milk, and wheat can generate antioxidant peptides upon hydrolysis [41]. In fact, amino acid and peptide sequences with antioxidant functionality may be present in many proteins. However, these peptides are restricted from eliciting their function within the sequence of their native protein because of peptide bonds, which occupy amino (N) and carboxyl (C) termini of amino acid residues and peptides; and side chain interactions between peptide chains. Therefore, upon liberation from their native protein sequence, antioxidant functions can be displayed by peptides. Protein hydrolysis can be achieved by microbial fermentation, gastrointestinal digestion, enzymatic hydrolysis of proteins, and acid hydrolysis [34]. Heat pre-treatment of proteins prior to enzymatic hydrolysis can be performed to yield a higher number of peptides. Heat denaturation of proteins allows enzymes to readily access peptide bonds in polypeptide chains leading to a higher number of cleavages of peptide bonds.

The objectives of this work were to obtain antioxidant hydrolysates from soy protein isolates by enzymatic hydrolysis and explore the potential of a loose NF membrane as a viable fractionation process for the improvement of the antioxidant capacity of soy protein hydrolysates. Soy protein hydrolysates (SPH) were first treated by UF with a 10 kDa MWCO hollow fiber membrane system for the removal of large fragments. UF permeates were fractionated with a thin film composite NF membrane with a MWCO of 2.5 kDa. The role of the pH during NF on the peptide content and antioxidant capacity of the fractions was also investigated.

3.4. Materials and Methods

3.4.1. Preparation of soy protein hydrolysates

3.4.1.1. SPI solution

Soy protein isolate (SPI) PRO-FAM 974 powder (Archer Daniels Midland Company, Decatur, IL, USA) was dissolved in Millipore water to obtain a 3.12 % (w/v) solution. The SPI solution was heated to 95 ^{o}C (Isotemp ceramic stirring hot plate, Fisher Scientific, Ottawa, ON, Canada) for 5 min to produce pre-heated SPI. The control SPI solution was not subjected to heat treatment.

3.4.1.2. Enzymatic hydrolysis of SPI solutions

Enzymatic hydrolysis procedure for SPI was developed from the work of Vilela, et al. (2006) [74]. Pepsin (Sigma-Aldrich, St. Louise, MO, USA) from porcine stomach mucosa, and Pancreatin (Sigma-Aldrich, St. Louise, MO, USA) from porcine pancreas were used for SPI hydrolysis, conducted in a temperature-controlled G-76 water bath shaker (New Brunswick Scientific, Edison, NJ, USA). SPI solutions were adjusted to pH 1.5 with 1.0 M hydrochloric acid, and placed in the water bath shaker, at 37 ^{o}C [37]. At time, t=0 min, 25 mL of 0.5 % (w/v) pepsin solution was added to 500 mL of SPI solution in the water bath shaker and with continuous agitation, to begin the hydrolysis. At time, t=30 min, hydrolysis by pepsin was terminated by adjusting the pH of the solutions to 7.8 with 1.0 M sodium hydroxide. The temperature was increased to 40 ^{o}C and 100 mL of 0.5 % (w/v) pancreatin solution was added to the previous SPI solution [75]. At time, t=90 min, pancreatin activity was terminated by adding 3.5 mL of 0.15 M sodium carbonate to the solution. During the hydrolysis procedure, samples were taken at 15 min intervals to determine the degree of hydrolysis using the O'pthaldialdehyde (OPA) spectrophotometric assay [75]. Heat pre-treatment and hydrolysis were performed in 500 mL batches, until 2 L of SPH were obtained for each treatment. SPH were frozen at -20 ^{o}C until use.

3.4.1.3. Ultracentrifugation

Frozen SPH were thawed overnight, and ultracentrifuged (Sorvall WX Ultra 100 (Thermo Scientific, Asheville, NC, USA) with a A-621 rotor (31,901 *G* and 22 ^{o}C for 30 min) to remove non-dissolved solids and to prepare the UF feed.

3.4.2. Filtration experiments

3.4.2.1. Ultrafiltration experiments

Ultrafiltration was performed with a hollow fibre polysulfone UF membrane module (UFP-10-E-4MA; 10 kDa MWCO, active area of 4.2 x 10^{-2} m^2; Amersham Biosciences; Westborough, MA, USA). The membrane area was soaked in 30 % (v/v) ethanol overnight prior to each filtration. UF was operated at a transmembrane pressure (TMP) of 62 kPa, feed flow rate of 2.4 L min^{-1}, and at room temperature (22 ^oC). UF experiments were performed in duplicates for each SPH treatment, with a feed volume of 1100 mL, and until 650 mL of permeate was collected. Mass of permeate collected was recorded as a function of time during UF using LabView 7.1 software (National Instruments, Austin, TX, USA). Permeate flux analyses were performed to determine normalized flux during UF, which provided an estimation of membrane fouling during UF. Normalized flux ($J_P\ J_0^{-1}$) was calculated by dividing the permeate mass flux (J_P) of the peptide solution at a given time, t (m s^{-1}), by the initial permeate mass flux (J_0) of the peptide solution (m s^{-1}) in the same filtration.

Permeate flux (J_{Per}, m s^{-1}) and membrane fouling were described according to Darcy's law (equation 1):

$$J_{Per} = \frac{TMP}{\eta_{Per}\, R_{tot}} \quad (4)$$

where TMP is the transmembrane pressure (N m^{-2}), η is the dynamic viscosity of the permeating solution (kg m^{-1} s^{-1}), and R_{tot} is the total fouling resistance (m^{-1}). Water flux measurements, determined from the time taken to collect 10 g of permeate, were conducted in triplicates at a given TMP, for 5 different TMPs. Furthermore, water flux measurements were obtained before and after cleaning protocol for each UF experiment to determine the membrane resistance (R_m), fouling resistance (R_f), as well as cleaning efficiency. The cleaning protocol for the UF membrane, provided by the manufacturer, includes circulating millipore water at 60 ^oC, 0.2 % Tergazyme (Alconox Inc., White Plains, NY, USA), and 100 ppm NaClO through the UF system separately at a flow rate of 1.2 L min^{-1} and a TMP of 34.5 kPa. The efficiency of the cleaning protocol was verified by obtaining similar R_m, as estimated prior to the filtration (estimated R_m=4.73 x 10^{12} m^{-1}). UF retentate and permeate fractions were frozen at -20 ^oC. Feed,

retentate (*ret*) and permeate (*per*) fractions were analyzed for total solids, peptide concentration, and antioxidant capacity.

Total solids (TS) loss and total peptide loss during a filtration experiment was determined by equation 2 and 3, respectively.

$$\%\, TS\ loss = \left[\frac{TS_{feed} - (TS_{ret} + TS_{per})}{TS_{feed}}\right] \times 100 \qquad (5)$$

$$\%\, Peptide\ loss = \left[\frac{Peptide_{feed} - (Peptide_{ret} + Peptide_{per})}{Peptide_{feed}}\right] \times 100 \qquad (6)$$

TS loss refers to the quantity of TS initially present in the feed solution that was not recovered in permeate and retentate fractions. Total peptide loss refers to the peptide content in the feed solution that was not recovered in permeate and retentate fractions. TS and peptide losses occurred most likely due to membrane fouling.

3.4.2.2. Nanofiltration experiments

NF experiments were conducted in a cross-flow SEPA CF II cell (GE Osmonics, Minnetonka, MN, USA) equipped with G10 thin film composite membranes (2.5 kDa MWCO, active area of 1.4 x 10^{-2} m^2, Sterlitech Corporation (Kent, WA, USA)). The membranes are considered loose NF membranes. The G10 membrane has a contact angle of 50.3 ^{o} and a strong negative zeta potential (-67.9 mV at pH 4 and -72.4 mV at pH 8) [63]. The estimated R_m for the G10 membrane was 3.87 x 10^{14} m^{-1}.

Temperature of the NF feed solution was maintained at 22 ^{o}C with a refrigerated bath circulator (NESLAB RTE-111, Thermo Scientific, Asheville, NC, USA). A volumetric feed flow rate of 1.8 L min^{-1} and a TMP of 2 MPa were used. For each NF experiment, a new 0.12 m x 0.17 m cut off of the flat sheet G10 membrane was used, soaked overnight in millipore water, and subjected to compaction at 2 MPa for 30 min. Water flux measurements were performed before and after each NF experiment to determine R_m and R_f as per UF experiments.

The NF feeds were UF permeate fractions diluted with millipore water to a total solids content (TS) of 1.0 g L^{-1} and a feed volume of 2.0 L. For a given type of SPH, NF experiments were conducted in duplicate at a given pH. Two pH conditions, pH 4 and 8, were investigated. The pH of feed solutions was adjusted with either 1.0 M hydrochloric acid or 1.0 M sodium hydroxide. NF was conducted until 50 % of feed volume was collected in the permeate stream (volume concentration ratio=2). The mass of permeate

collected as a function of time was recorded using LabView 7.1 software (National Instruments, Austin, TX, USA), and permeate flux analyses were performed as for UF experiments.

NF retentate and permeate fractions were evaluated for total solids, peptide concentration and antioxidant activity. NF fractions were frozen at -20 ^{o}C.

3.4.3. Analytical methods

3.4.3.1. Total solids determination

A 2 mL sample was placed on an aluminum dish (VWR, Mississauga, ON, Canada), and incubated overnight in a conventional oven at 105 ^{o}C to evaporate the moisture in the sample. Dry mass in the dish provided a direct measure of TS. UF samples were weighed using a Satorius CPA2202S balance (readability=0.01 g; Data Weighing Systems, Inc., Elk Grove, IL, USA) and NF samples were weighed using a Satorius MSA124S balance (readability=0.1 mg; Data Weighing Systems, Inc., Elk Grove, IL, USA).

3.4.3.2. O'phthaldialdehyde (OPA) assay

OPA spectrophotometric assay was performed in triplicate to determine peptide concentration (estimated by equivalent phenyl-glycine concentration) for a given sample, as performed by Church et al. [76]. *L-(+)-α*-phenylglycine (2935-35-5, MP Biomedicals, Solon, OH, USA), 99.9 % sodium borate decahydrate (S9640-500G, Sigma-Aldrich, St. Louise, MO, USA), sodium dodecyl sulfate (L4509-250G, Sigma-Aldrich, St. Louise, MO, USA), phthaldialdehyde (P0657-5G, Sigma-Aldrich, St. Louise, MO, USA), and 99 % ethanol were used. OPA calibration curve consisted of a phenyl-glycine concentration range from 0-1.0 mmol L^{-1}.

3.4.3.3. Oxygen Radical Absorbance Capacity (ORAC) assay

The ORAC assay was performed according to the method of Ubeda et al. (2011) [77]. The following chemicals and reagents were employed: 0.5 M sodium dihydrogen orthophosphate monobasic solution (ACS 795, BDH Chemicals, Halifax, NS, Canada); 0.5 M sodium phosphate heptahydrate dibasic solution (BDH0296-500G, VWR, Mississauga, ON, Canada); 80 mM AAPH solution (2,2'-Azobis(2-dmethylpropionamidine) dihydrochloride) (440914-25G, Sigma-Aldrich, St. Louise, MO, USA); 5 mM Trolox

solution (6-hydroxy-2,5,7,8-tetramethylchroman-2-carboxylic acid) (238813-1G, Sigma-Aldrich, St. Louise, MO, USA); and 2.5 mM Fluorescein solution (065-00252, Wako Pure Chemical Industries, Osaka, Japan).

An ORAC calibration curve was prepared with Trolox concentration range from 0-100 μM. Phosphate buffer at pH 7.4 was prepared. Initial SPH, UF feed, UF retentate, and UF permeate fractions were diluted such that readings would fall within the linear range of the calibration curve.

A black 96-well plate was used to analyze all samples and standard solutions in triplicate. A volume of 100 μL of 2.5 nM fluorescein solution was added to each well, followed by 50 μL of sample or standard solution. The plate was covered with a plastic lid and incubated at 37 ^{o}C for 15 min, prior to the addition of 50 μL of AAPH solution to each well. The final volume of each well was 200 μL. A Synergy 4 microplate reader (BioTek, Winooski, VT, USA), was used for the analysis of fluorescein degradation. A temperature of 37 ^{o}C was maintained and with constant shaking to optimize peroxy radical formation by AAPH. Fluorescence excitation and emission wavelengths were 485 nm and 520 nm, respectively. Fluorescence measurements were collected every minute for 120 min.

3.4.3.4. Folin Ciocalteau Reagent (FCR) assay

The FCR assay was performed similarly to Zielinska et al. (2007) [78]. The following chemicals and reagents were used: Trolox; Folin and Ciocalteau Phenol Reagent 2 N (F9252, Sigma-Aldrich, St. Louise, MO, USA); and sodium carbonate (SX0400-1 500G, EMD Chemicals, Gibbstown, NJ, USA). The FCR calibration curve was prepared using a Trolox concentration range of 0-3 mM. Volumes of 20 μL of sample or Trolox standard solutions were added to 4 mL cuvettes. Each cuvette was incubated for 5 min at 22 ^{o}C after adding 150 μL of FCR reagent. Then, 600 μL of 15 % (w/v) sodium carbonate was added to each cuvette. A volume of 2230 μL of millipore water was added bringing the final volume to 3 mL. Cuvettes were shaken and incubated for 120 min at 22 ^{o}C. Absorbance measurements at 750 nm were obtained using the Spectronic Genesys 2 spectrophotometer (Milton Roy, Ivyland, PA, USA).

3.4.4. Statistical analysis

Paired comparison *t* test analyses were conducted to compare the significance between mean values of sets of samples. A 95 % confidence interval (α=0.05) for a two-sided *t* test was employed. Significance between means was declared when observed *t* values were greater than the critical *t* values.

3.5. Results and Discussion

3.5.1. Effect of temperature on peptide yield during enzymatic hydrolysis

SPI solutions were subjected to heat pre-treatment at 95 °C for 5 min to explore the possibility of attaining a higher peptide yield. Pepsin and pancreatin enzyme mixtures were employed for SPI hydrolysis in order to simulate the human digestion conditions for dietary proteins. Hence, resulting hydrolysates possessed free amino acids and small peptides that would likely be present in the lumen of the small intestine. The progress of the enzymatic hydrolysis with pepsin, followed by pancreatin, for SPI without (control SPH) and with (pre-heated SPH) heat pre-treatment at 95 °C during 5 minutes is presented in Figure 7.

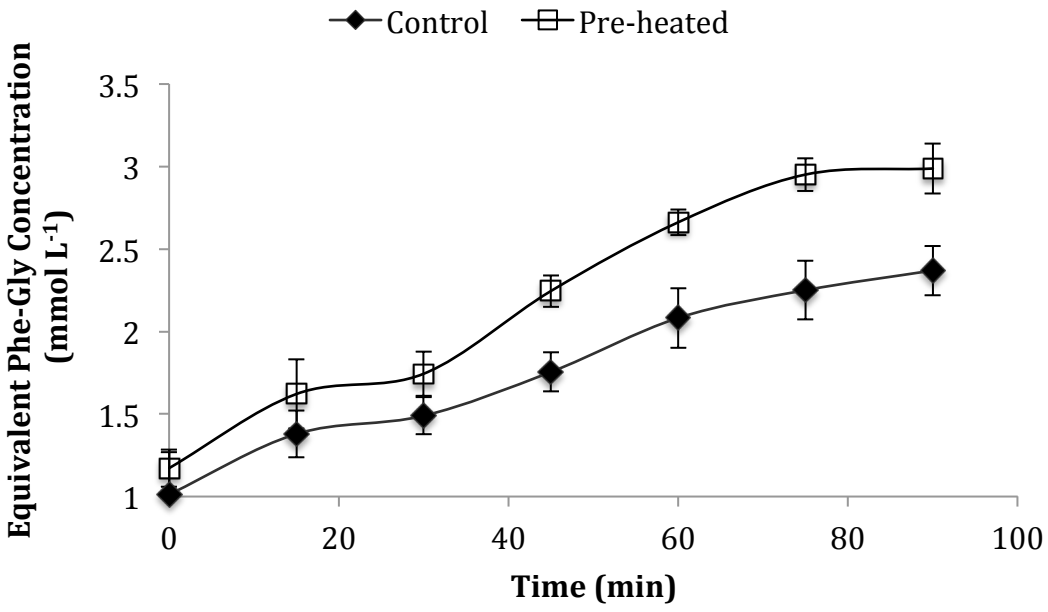

Figure 7: Progress of enzymatic hydrolysis of control and pre-heated soy protein hydrolysates assessed by OPA, providing peptide concentrations in terms of equivalent phenyl-glycine (Phe-Gly) concentrations (expressed as means with error bars representing standard deviations; n=3). Conditions: 3.12 % (w/v) SPI solution, 30 min pepsin digestion at pH 1.5 and 37 °C followed by 60 min pancreatin digestion at pH 7.8 and 40 °C.

The total peptide concentration for control and pre-heated SPH at the end of the first step of hydrolysis by pepsin (after 30 min) were not significantly different ($p=0.08$). However, the subsequent hydrolysis by pancreatin (after 90 min) resulted in a significantly higher peptide concentration for pre-heated SPH compared to control SPH ($p=0.015$). The denaturation temperatures of β-conglycinin and glycinin, the dominant proteins in SPI, are 71 °C and 92 °C, respectively [26]. Heating SPI to 95 °C ensured that the majority of the proteins in solution were denatured with the unfolding of polypeptide chains prior to enzymatic hydrolysis. This could facilitate the access by pancreatin to the peptide bonds in polypeptide chains, resulting in a higher degree of hydrolysis [79]. Achouri et al. (1998) found that heat pre-treatment of soy proteins isolate for 30 min at 80 °C decreased the required time to achieve a given degree of hydrolysis using microbial neutral proteinase A.S., compared to a non-heat pre-treated soy protein solution [79]. Since pepsin digestion was carried out at pH 1.5, protein unfolding should also have occurred due to the acidity [80]. A possible difference between the acidity and the heat pre-treatment could be the formation of linkages between polypeptide chains at high temperatures, such as disulfide bonds, affecting the structures and properties of peptides produced during the enzymatic hydrolysis of soy proteins [79].

3.5.2. Ultrafiltration of hydrolysates

3.5.2.1. Effect of SPI heat pre-treatment on total solids distribution

Significant amount of non-dissolved solids present in the hydrolysates were removed by ultracentrifugation prior to UF as a means to minimize fouling during UF. SPH after ultracentrifugation (UF feed) were subjected to a cross flow hollow fiber 10 kDa membrane MWCO step. The total solids content of the UF fractions are presented in Table 3.

Table 3: Total solids content of UF fractions for control and pre-heated soy protein hydrolysate (expressed as means ± standard deviations; n=2). UF conditions: 62 kPa TMP, 2.4 L min^{-1} feed flow rate, and 22 °C.

Sample	Total solids content (g L^{-1})	
	Control SPH	Pre-heated SPH
Feed	28.05 ± 0.01	28.36 ± 0.01
Retentate	26.14 ± 0.01	30.43 ± 0.00
Permeate	17.66 ± 0.01	20.15 ± 0.01

A significantly higher total solids content (TS) was observed in the UF retentate (26.14 g L^{-1}) compared to UF permeate (17.66 g L^{-1}) for control SPH ($p<0.01$). TS ratio of 1.06 (retentate: feed) and 0.72 (permeate: feed) were determined for control SPH. Similarly, a significantly higher TS was observed in the UF retentate (30.43 g L^{-1}) compared to UF permeate (20.15 g L^{-1}) for pre-heated SPH ($p<0.01$). TS ratios of 1.10 (retentate: feed) and 0.72 (permeate: feed) were determined for pre-heated SPH. Based on TS ratios, similar TS distributions were observed in UF for control and pre-heated SPH. TS loss due to UF for control and pre-heated SPH were 11.3 % and 8.6 %, respectively.

3.5.2.2. Effect of SPI heat pre-treatment on total peptide distribution

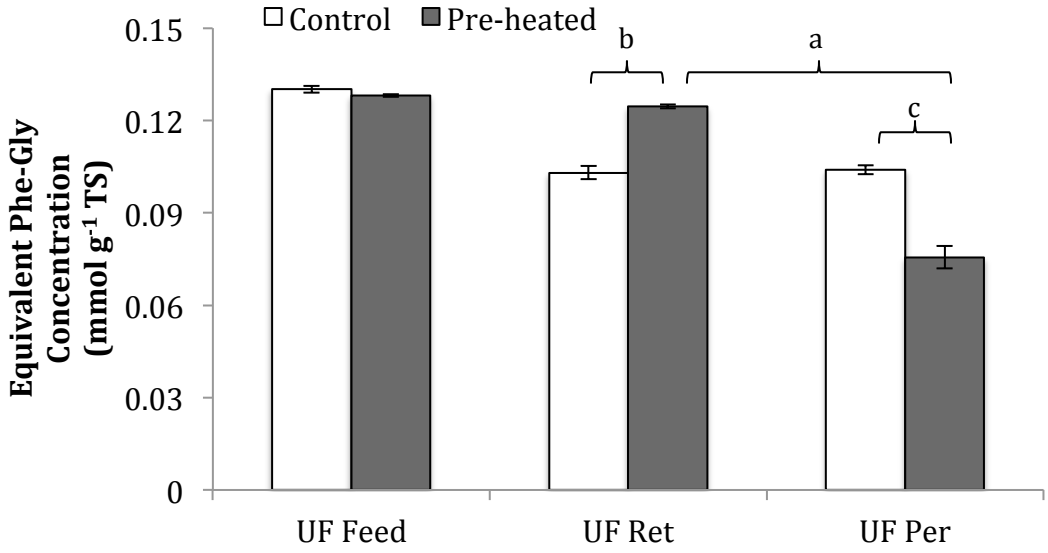

Figure 8: A comparison of peptide content of UF fractions from control and pre-heated soy protein hydrolysate, estimated by OPA as equivalent phenyl-glycine (Phe-Gly) concentrations (expressed as means with error bars representing standard deviations; n=3). OPA conditions: 0 – 1.0 mM Phe-Gly, absorbance at 340 nm. Significantly different fractions (a, b, and c) are identified by braces ($\alpha=0.05$).

No significant differences in peptide content between control and pre-heated SPH (Figure 8) were observed in the UF feed ($p=0.1$). No significant difference in peptide content between UF retentate (0.10 mmol g^{-1}) and permeate (0.12 mmol g^{-1}) was observed for control SPH ($p=0.56$). From the UF of control SPH, peptide content ratios of 0.79 (retentate: feed) and 0.80 (permeate: feed) were determined. In contrast, the UF retentate for pre-heated SPH (0.12 mmol g^{-1}) contained a significantly higher peptide content (a, $p<0.01$) than the UF permeate (0.08 mmol g^{-1}). Therefore, from the

UF of pre-heated SPH, peptide content ratios of 0.97 (retentate: feed) and 0.59 (permeate: feed) were determined. A significantly higher peptide content was present in the UF retentate from pre-heated SPH, compared to control SPH (b, $p<0.01$). The UF permeate from control SPH had a significantly higher peptide content compared to pre-heated SPH (c, $p<0.01$). Therefore, a higher content of peptides smaller than 10 kDa were present in control SPH compared to pre-heated SPH. Total peptide loss due to UF for control and pre-heated SPH were 32.4 % and 26.9 %, respectively.

Filtation performance was obtained by considering normalized flux. Normalized flux at the end of UF (SPH permeate flux at the end of UF normalized to initial flux of UF; $J_P\ J_0^{-1}$) for control and pre-heated SPH were 0.86 ± 0.08 and 0.88 ± 0.04, respectively, indicating limited fouling and no difference according to feed type.

3.5.2.3. Effect of ultrafiltration on antioxidant capacity

Antioxidant capacities determined by ORAC and FCR assays is presented in Figure 9 for the UF fractions for control and pre-heated SPH.

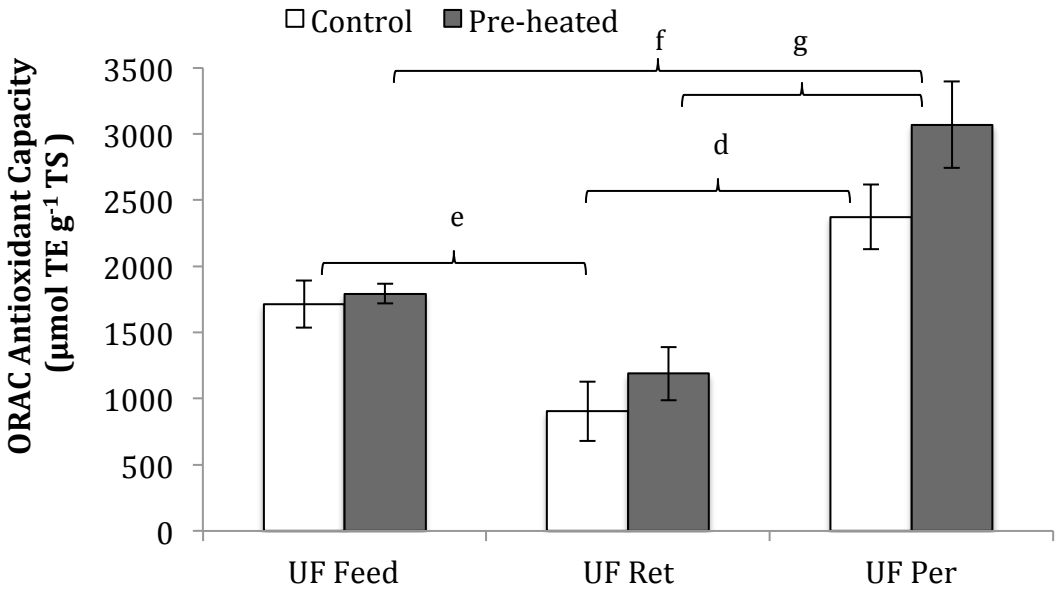

Figure 9: A comparison of the antioxidant capacity of UF fractions for control and pre-heated soy protein hydrolysate estimated by ORAC (expressed as means with error bars representing standard deviations; n=3). ORAC conditions: excitation at 485 nm, emission at 520 nm; constant shaking at 37 °C; Trolox 1-25 uM, Fluorescein 125 nM, AAPH 20 mM. Significantly different fractions (d, e, f and g) are identified by braces (α=0.05).

A significantly enhanced ORAC AC was observed for the UF permeate of control SPH (2372 µmol TE g^{-1}) compared to its retentate (d, $p=0.02$), but not for its feed

(p=0.06). The ORAC AC of UF retentate of control SPH (904 µmol TE g^{-1}) was significantly lower than its feed (1713 µmol TE g^{-1}; e, p=0.06). The ORAC AC observed for the UF permeate of pre-heated SPH (3069 µmol TE g^{-1}) was significantly higher than its feed (f, p<0.01) and retentate (g, p<0.01). In contrast to control SPH, no significant difference was observed in the ORAC AC between the UF retentate (1189 µmol TE g^{-1}) and feed (1793 µmol TE g^{-1}) of pre-heated SPH (p=0.05). This indicates the importance of molecular weight on ORAC AC as previously observed by Park et al. (2010) for the antioxidant capacity of SPH, produced by alcalase hydrolysis [9]. The SPI heat pre-treatment did not cause a significant increase in ORAC AC of UF fractions compared to control SPH (p>0.1).

Figure 10 compares the FCR antioxidant capacities (FCR AC) of the UF fractions for the two SPI treatments.

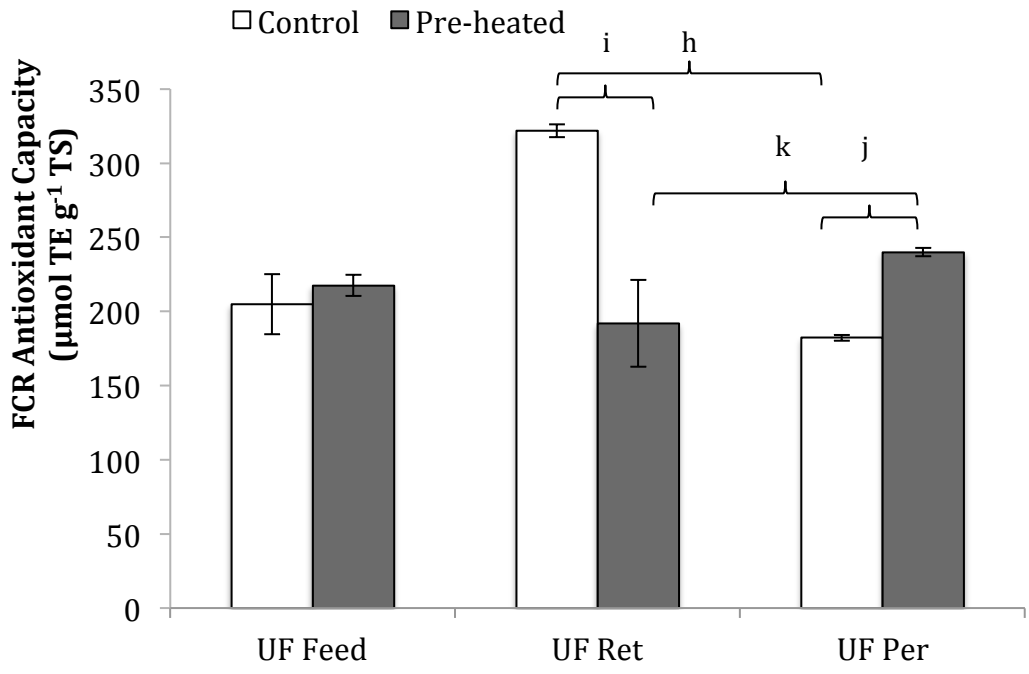

Figure 10: A comparison of the antioxidant capacity of UF fractions for control and pre-heated soy protein hydrolysate estimated by FCR (expressed as means with error bars representing standard deviation; n=3). FCR conditions: absorbance at 750 nm, 22 °C. Significantly different fractions (h, i, j and k) are identified by braces (α=0.05).

FCR AC of the UF fractions was significantly lower than the ORAC AC and its distribution among the UF fractions was generally different. UF retentate of control SPH (322 µmol TE g^{-1}) displayed a significantly higher FCR AC compared to its permeate (182 µmol TE g^{-1}; h), UF retentate of pre-heated SPH (192 µmol TE g^{-1}, i), and all other

UF fractions ($p<0.01$). The UF permeate fraction of pre-heated SPH (240 μmol TE g^{-1}) displayed a significantly higher FCR AC than the control SPH permeate (j, $p<0.01$) and pre-heated SPH retentate (k, $p=0.01$). Hence, the role of molecular weight of peptides on FCR antioxidant capacity was observed for the pre-heated SPH UF fractions, but not for the control SPH UF fractions. The observations of FCR AC for the pre-heated SPH UF fractions followed the same trend as their ORAC AC.

3.5.3. Nanofiltration of hydrolysates

3.5.3.1. Effect of SPI heat pre-treatment and pH on total solids distribution

The effects of SPI heat pre-treatment and pH during NF on TS distribution (Table 4) were assessed for similar TS feed (1 g L^{-1}).

No statistically significant difference was observed between the TS of NF permeate fractions at pH 4 and 8 for control SPH ($p>0.1$). This was also true for control SPH NF retentate fractions at pH 4 and 8. Similarly, no statistically significant difference was observed between the TS of NF permeate fractions at pH 4 and 8 for pre-heated SPH ($p>0.1$). This was also true for pre-heated SPH NF retentate fractions at pH 4 and 8. This suggested the lack of impact by pH on TS distribution in NF.

Table 4: Total solids content of NF fractions for control and pre-heated soy protein hydrolysate at pH 4 and 8 (expressed as means ± standard deviations; n=2). NF conditions: 1 g L^{-1} TS in feed, 2 MPa TMP, 1.8 L min^{-1} feed flow rate, and 22 ^{o}C.

NF fraction	Total solids content (g L^{-1})			
	Control SPH		Pre-heated SPH	
	pH 4	pH 8	pH 4	pH 8
Retentate	1.36 ± 0.16	1.24 ± 0.16	1.18 ± 0.07	1.34 ± 0.09
Permeate	0.54 ± 0.02	0.19 ± 0.12	0.35 ± 0.07	0.21 ± 0.09

No statistically significant difference was observed between NF permeate fractions of control and pre-heated SPH at both pH 4 and 8 ($p>0.1$), which suggested the lack of significant impact by heat pre-treatment on TS distribution in NF.

However, a higher TS loss at pH 4 for pre-heated SPH (24 %) was observed, as opposed to control SPH (5 %). The TS loss observed in NF at pH 8 was high but not affected by heat-pretreatment with 29 % for control SPH and 23 % for pre-heated SPH.

3.5.3.2. Effects of SPI heat pre-treatment and pH on total peptide distribution

Peptide content of the NF fractions for control and pre-heated SPH is provided in Figure 11. Due to size/charge interactions between the NF membrane and peptides in solution, differences in permeation of peptides were observed according to pH.

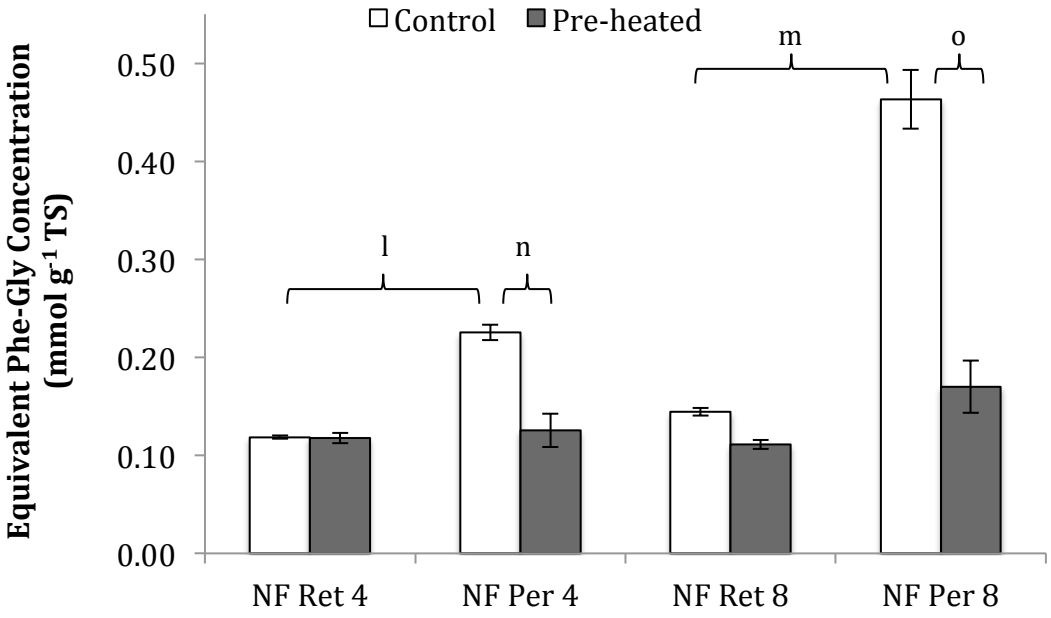

Figure 11: A comparison of peptide content of NF fractions from control and pre-heated soy protein hydrolysate at pH 4 and 8, estimated by OPA as equivalent phenyl-glycine (Phe-Gly) concentrations (expressed as means with error bars representing standard deviations; n=6). NF conditions: 1 g L^{-1} TS (NF feed), 2 Mpa TMP, 1.8 L min^{-1} feed flow rate, and 22 ^{o}C. Significantly different fractions (l, m, n and o) are identified by braces (α=0.05).

For control SPH at pH 4, the peptide content in the NF permeate (0.23 mmol g^{-1}) was significantly different than its retentate (0.12 mmol g^{-1}; l, $p<0.01$). Peptide content ratios of 1.14 (retentate: feed) and 2.17 (permeate: feed) were determined for NF fraction of control SPH. Similarly, NF permeate at pH 8 for control SPH (0.46 mmol g^{-1}) consisted of significantly higher peptide content than NF retentate (0.14 mmol g^{-1}; m, $p<0.01$); and resulting peptide content ratios were 1.39 (retentate: feed) and 4.46 (permeate: feed). In fact, the highest peptide content was obtained for the NF permeate at pH 8 and control SPH; hence was the most successful fractionation conditions with the G10 NF membrane.

Peptide contents in NF permeate (0.13 mmol g^{-1}) and retentate (0.12 mmol g^{-1}) of pre-heated SPH at pH 4 were not significantly different ($p=0.32$). This was further evidenced by their peptide content ratios (1.56 retentate: feed ratio; 1.66 permeate:

feed ratio). However, at pH 8, NF of pre-heated SPH resulted in a significantly higher peptide content in the permeate (0.17 mmol g^{-1}) compared to the retentate (0.11 mmol g^{-1}; $p<0.01$), which was also evidenced by their peptide ratios (1.47 retentate: feed; 2.25 permeate: feed).

The peptide content of the NF permeate fraction at pH 4 in the control (0.23 mmol g^{-1} TS) was statistically different (n, $p<0.01$) compared to the pre-heated SPH (0.13 mmol g^{-1} TS). Similarly, NF permeate at pH 8 for control SPH resulted in significantly higher peptide content (o, $p<0.01$) than pre-heated SPH.

At pH 4, the total peptide loss during NF of control SPH and HTSPHwere 10.9 % and 20.5 %, respectively. At pH 8, the total peptide loss during NF of control and pre-heated SPH were 4.2 % and 22.1 %, respectively. This reinforces the effects of SPI heat pre-treatment on structural changes in soy protein hydrolysates.

Statistically significantly higher peptide content ($p<0.01$) in the NF permeate was observed at pH 8 compared to pH 4 for both control and pre-heated SPH. This is in accordance with the concept of Donnan Potential and observations by Pouliot, et al. for the fractionation of whey protein hydrolysates by NF [12,13] where charge-based interactions between peptides and the NF membrane influenced peptide permeation during NF. The pI of soy proteins in SPI falls between pH 4-5 [25]. Proteins and peptides are subjected to protonation as pH decreases below their isoelectric point (pI), and to deprotonation as pH increases above their pI. By this phenomena, a majority of peptides in the NF feed solution were assumed to have a net positive charge at pH 4, while the NF membrane maintained a net negative surface charge (ζ=-67.9 mV), displaying counter-ion effects [63]. Due to attractions between opposite charges, the potential for membrane fouling increased. A majority of peptides in solution assumed a net negative charge at pH 8, similar to the NF membrane (ζ=-72.4 mV) [63]. Therefore, co-ion effects and electrostatic repulsions between the NF membrane and peptides were observed, resulting in decreased membrane fouling and absorption of peptides to the membrane. These phenomena were evidenced by a greater decline in normalized flux ($J_P J_0^{-1}$) during NF at pH 4 (0.72 ± 0.18) compared to pH 8 (0.84 ± 0.14) for control SPH; and at pH 4 (0.73 ± 0.08) compared to pH 8 (1.05 ± 0.13) for pre-heated SPH.

3.5.3.3. Effect of nanofiltration on antioxidant capacity

NF fractions were assessed for ORAC AC (Figure 12) and FCR AC (Figure 13). Relative to all NF fractions from control and pre-heated SPH (including the NF feeds), the NF permeates at pH 8 from control SPH (5562 µmol TE g^{-1}) and pre-heated SPH (5187 µmol TE g^{-1}) possessed significantly higher ORAC AC ($p<0.01$). These ORAC AC distributions indicated structural and compositional differences in peptides fractionated at pH 8 compared to pH 4. The trends in the ORAC AC of control and pre-heated SPH were similar, at both pH conditions, where NF permeate fractions displayed significantly higher ORAC ACs than their corresponding retentate fractions ($p<0.05$). This further illustrated the importance of molecular weight of peptides on ORAC AC, irrespective of peptide charge. As molecular weight of peptide fractions decreased, its ORAC AC increased. This is in agreement with the observations by Park et al. (2010) and Zhang et al. (2010) on soy protein hydrolysates [9,72]. No significant effects on ORAC AC of NF fractions were observed due to heat pre-treatment of SPI.

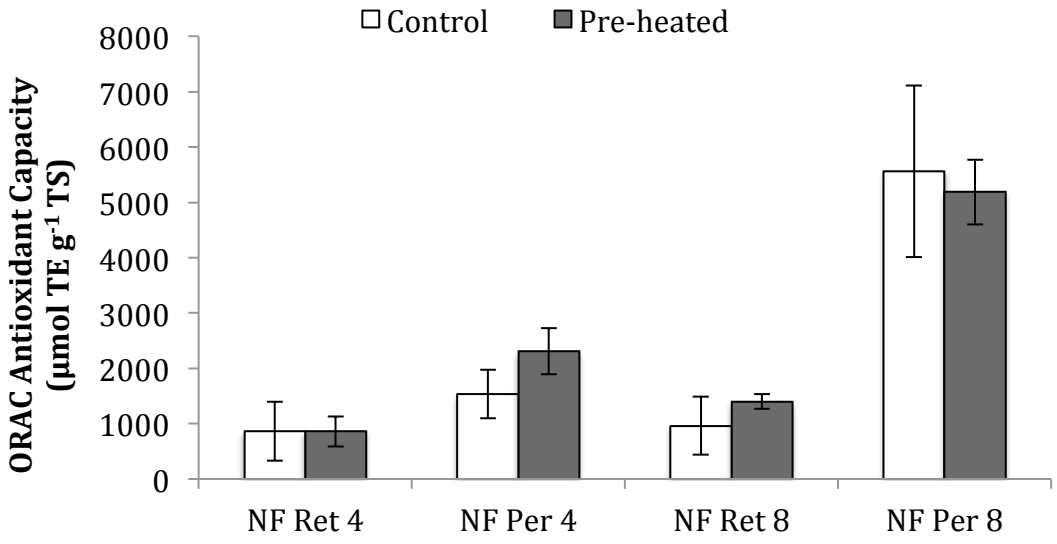

Figure 12: A comparison of the antioxidant capacity of NF fractions for control and pre-heated soy protein hydrolysate at pH 4 and 8, estimated by ORAC (expressed as means with error bars representing standard deviations; n=6). ORAC conditions: excitation 485 nm, emission 520 nm; constant shaking at 37°C; Trolox 1-25 uM, Fluorescein 125 nM, AAPH 20 mM.

The FCR AC of the NF fractions increased when compared to the NF feed (UF permeate), but was significantly lower than the ORAC AC. Contrary to the ORAC AC, the FCR AC of NF permeate at pH 8 for control SPH (576 µmol TE g^{-1}) was not significantly different ($p=0.32$) from pH 4 (405 µmol TE g^{-1}). However, FCR AC of the NF permeate at

pH 4 (804 µmol TE g^{-1}) was significantly lower than at pH 8 (1678 µmol TE g^{-1}) for pre-heated SPH (q, $p<0.01$). This effect was observed in the ORAC AC of pre-heated SPH NF fractions, as well. Significant increase in FCR AC due to heat pre-treatment was observed in two NF fractions: NF retentate at pH 4 (r, $p<0.01$), and NF permeate at pH 8 (s, $p<0.01$). At pH 4, NF retentate from pre-heated SPH (381 µmol TE g^{-1}) displayed a significantly higher FCR AC than control SPH (187 µmol TE g^{-1}). At pH 8, NF permeate from pre-heated SPH (1678 µmol TE g^{-1}) displayed a significantly higher FCR AC than control SPH.

Though SPI heat pre-treatment did not increase peptide content compared to the control, the NF permeate at pH 8 of pre-heated SPH represented the highest ORAC and FCR antioxidant capacity. Similarly, the NF permeate at pH 8 for the control SPH had a significantly higher ORAC AC than all NF fractions for this feed. The difference in ORAC AC and FCR AC of the NF permeate at pH 8 for control and pre-heated SPH were 6.7 % and 65.7 %, respectively.

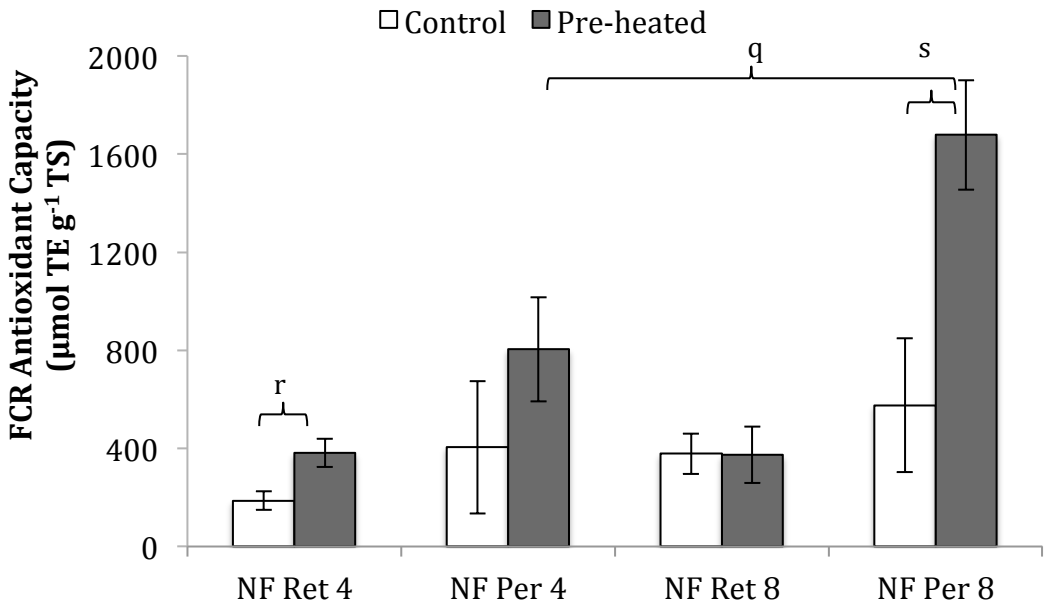

Figure 13: A comparison of the antioxidant capacity of NF fractions for control and pre-heated soy protein hydrolysate at pH 4 and 8, estimated by FCR (expressed as means with error bars representing standard deviations; n=3). FCR conditions: absorbance at 750 nm, 22 ^{o}C. Significantly different fractions (q, r, and s) are identified by braces (α=0.05).

3.5.4. Potential for SPI hydrolysates as a source of antioxidants

The ORAC antioxidant capacity, being the most common test used for *in vitro* antioxidant capacity of food products by food industries, and inspection/regulation

agencies, due to its biological relevance to *in vivo* antioxidant efficacy [81], provides an estimate of the potential of SPI hydrolysates as a source of antioxidants. The ORAC assay provides the degree of inhibition by an antioxidant molecule of peroxy radical-induced oxidation, and inhibition time [81].

The ORAC AC of the hydrolysate fractions generated during sequential UF NF fractionation in the current study is summarized in Table 5.

Table 5: A summary of ORAC antioxidant capacity of control and pre-heated soy protein hydrolysate fractions generated during enzymatic hydrolysis (n=3), UF (n=3), and NF at pH 8 (n=6). ORAC conditions: excitation 485 nm, emission 520 nm; constant shaking at 37 °C; Trolox 1-25 uM, Fluorescein 125 nM, AAPH 20 mM. Units of ORAC=µmol TE g^{-1} TS.

Process	Control SPH		Pre-heated SPH	
	ORAC AC	Compared to Initial SPI	ORAC AC	Compared to Initial SPI
Initial SPI (PRO-FAM 974)	403	1 x	403	1 x
Enzymatic Hydrolysis (UF Feed)	1713	4.3 x	1793	4.5 x
Ultrafiltration (Permeate)	2372	5.9 x	3069	7.6 x
Nanofiltration (Permeate pH 8)	5562	13.8 x	5187	12.9 x

The NF permeate at pH 8 for control SPH (5562 µmol TE g^{-1}) and pre-heated SPH (5187 µmol TE g^{-1}) were compared to naturally occurring antioxidant food components and ingredients, as shown in Table 6.

It is therefore apparent that membrane filtration by UF and NF of soy protein hydrolysates significantly improved the antioxidant capacity of the hydrolysates and allowed for optimization of fractions with superior functionalities.

Table 6: A comparison of the ORAC antioxidant capacities of select food items [81] to the control and pre-heated soy protein hydrolysate NF permeate fractions at pH 8.

Antioxidant description	ORAC AC (μmol TE g^{-1})	ORAC AC ratio NF permeate (pH 8): Antioxidant source	
		Control SPH	Pre-heated SPH
Raw bran	3124	1.8	1.7
Ground cloves	2903	1.9	1.8
Dried oregano	1763	3.2	2.9
Dried rosemary	1653	3.4	3.1
Ground cinnamon	1314	4.2	4.0
Dried vanilla beans	1224	4.5	4.2
Ground turmeric	1271	4.4	4.1
Acai fruit pulp	1027	5.4	5.1

3.6. Conclusion

Sequential membrane UF and NF of control and heat pre-treated soy protein hydrolysates improved the antioxidant functionality of peptides. The following were the key findings from this study:

1. Heat pre-treatment of SPI yielded a higher peptide concentration (per volume) in the hydrolysate solution compared to the control SPI. However, no significant difference in peptide content (per gram of solid) was observed in the hydrolysate solutions.
2. Control SPH had a significantly higher peptide content in the UF permeate than pre-heated SPH; and a significantly lower peptide content in the UF retentate than pre-heated SPH ($p<0.01$).
3. Control and pre-heated SPH UF permeate fractions (<10 kDa in MW) displayed higher ORAC AC compared to corresponding feed and retentate fractions, while retentate fractions (> 10 kDa in MW) displayed lower ORAC AC compared to the corresponding feed fractions. This suggested the importance of molecular weight of a peptide on antioxidant capacity.
4. Highest peptide content was observed in the NF permeate at pH 8 for control SPH (<2.5 kDa in MW). Co-ion membrane-peptide interactions (electrostatic repulsions between negatively charged peptides and the negatively charged membrane) at pH 8 yielded higher peptide contents and consequently displayed

higher ORAC antioxidant capacities relative to counter-ion interactions (pH 4) for a given SPH treatment. At pH 8, the NF permeate fractions for control SPH (5562 μmol TE g^{-1}) and pre-heated SPH (5187 μmol TE g^{-1}) displayed the highest ORAC AC, and were therefore the most promising antioxidant SPH fractions.

5. Compared to SPI PROFAM 974, sequential UF and NF at pH 8 steps have shown to increase the ORAC AC of SPH by over 13 fold for both control and pre-heated SPH, which are significant improvements to antioxidant capacity of peptides. Therefore, the potential for NF as a viable fractionation process for bioactive compounds was realized. The NF process can be improved from lab scale to a pilot scale study to assess its potential as an industrial fractionation process.

Peptide characterization will be performed in future work to identify the amino acid composition of the peptide fractions, and differences between peptides in control and pre-heated SPH fractions.

4. Assessment of the Contribution of Biological Species to Antioxidant Capacity of Ultrafiltration and Nanofiltration-derived Soy Protein Hydrolysate using Fluorescence Spectroscopy and Principal Component Analysis.

S. Ranamukhaarachchi, R. H. Peiris, C. Moresoli

Prepared for Biotechnology and Bioengineering

All experimental work and results presented in this manuscript were performed by Mr. Sahan Ranamukhaarachchi under the supervision of Dr. Christine Moresoli. Fluorescence and PCA analyses conducted in this study were guided by Dr. Ramila Peiris. Statistical analysis and data intepretation were performed by Mr. Sahan Ranamukhaarachchi and Dr. Ramila Peiris.

4.2. Abstract

The potential of intrinsic fluorescence and principal component analysis for its use as a rapid method for antioxidant capacity determination of protein hydrolysates during their fractionation by membrane operations has been evaluated. Soy protein hydrolysate fractions with different antioxidant capacity were produced by sequential ultrafiltration (UF) and nanofiltration (NF). Crude soy protein hydrolysates (SPH) were obtained by enzymatic hydrolysis (pepsin and pancreatin mixtures) of soy protein isolate thermally treated at 95 ^{o}C for 5 min, and subjected to sequential UF (10 kDa MWCO step) and NF (2.5 kDa MWCO step at pH 4 and 8). Collected UF and NF fractions were evaluated for antioxidant capacity with the Oxygen Radical Absorbance Capacity (ORAC) and Folin Ciocalteau Reagent (FCR) assays, and their fluorescence excitation-emission matrices (EEM) were obtained. Principal component analysis (PCA) of fluorescence EEM data for UF and NF fractions revealed two principal components (PC) that captured significant variance in the fluorescence spectra, and could be related to tryptophan (PC_1) and tyrosine (PC_2) amino acid residues based on their excitation and emission properties. Multi-linear regression models were developed to obtain relationships between the antioxidant capacity and the two PCs associated with the fluorescence EEM of the fractions. These models generated fluorescence and PCA-captured ORAC ($ORAC_{FPCA}$) and FCR (FCR_{FPCA}) estimates of UF and NF fractions. The $ORAC_{FPCA}$ and FCR_{FPCA} antioxidant capacities for NF samples displayed strong, linear relationships (R^2>0.99). A clustering effect that separated UF and NF peptide fractions with respect to $ORAC_{FPCA}$ and FCR_{FPCA} was observed, due to their differences in molecular weight, charge, and antioxidant capacities, indicating different roles of UF and NF membrane processes that were in play for improving the antioxidant capacities. The significance of this study hinges on the ability of fluorescence EEM and PCA to identify individual and combined contributions of tryptophan and tyrosine residues in SPH fractionated by sequential UF and NF to their antioxidant capacities that were not directly identified by ORAC and FCR assays. Therefore, the proposed method could be potentially developed as a rapid, non-destructive, online tool during membrane fractionation of protein hydrolysates with antioxidant capacity.

4.3. Introduction

An antioxidant is defined as a substance that can significantly decrease the unfavorable effects of reactive species, such as oxidative free radicals, on typical human physiological functions [53]. Numerous well-established assays for measuring the antioxidant capacity of a substance are available [6, 54]. These assays can be broadly categorized as hydrogen atom transfer (HAT)- and electron transfer (ET)-based assays. HAT-based assays, such as the oxygen radical absorbance capacity (ORAC), involve a complex scheme of reactions whereby an antioxidant and a substrate compete for peroxy radicals that are thermally generated by the breakdown of azo-compounds [6]. In the ORAC assay, fluorescence decay due to oxidative degeneration by peroxy radicals is monitored in the absence and presence of antioxidants. Fluorescence decay plots can be generated to obtain the net area under the curve (AUC), which gives a measure of the antioxidant capacity of a given species [6]. ET-based assays, such as the Folin Ciocalteau Reagent (FCR) and ferric reducing antioxidant power (FRAP) assays, employ simulated antioxidant actions where a redox-potential probe (i.e. fluorescent or colored probe) is used. Antioxidant capacity is thus measured by the reduction of an oxidant with a single electron transfer upon, which a color change in solution can be observed and spectrophotometrically quantified [6]. ET-based mechanisms employ non-physiological conditions (i.e. room temperature, irrelevant pH conditions to human physiology, etc.) and measure the reducing capacity of a molecule in the absence of reactive free radicals, whereas ORAC combines relative inhibition and time for inhibition of free radicals into one quantity [56,57].

Experimentally measuring ORAC and FCR antioxidant capacities are laborious methods, which involve toxic chemicals, multiple steps and prolonged analysis times. Given the importance of these assays and the challenges faced in conducting them, novel and rapid methods to capture relative antioxidant capacities of samples are of interest in food, nutrition and medicine. In this study, intrinsic fluorescence of soy protein hydrolysates (SPH) was assessed as a potential tool to capture relationships between antioxidant assays and antioxidant capacities.

Many proteins, such as soy proteins, contain the correct amino acid and peptide sequences for bioactive functions. However, these peptides are restricted from performing these functions within the sequence of their native protein by peptide bonds, which occupy the N- and C-termini of the individual amino acids, and by side

chain interactions between peptide chains. Upon liberation from their native protein sequence, certain peptides can fulfill antioxidant functions among other bioactive properties. A number of amino acid residues, including histidine, tyrosine, tryptophan, phenylalanine, proline, and leucine, have been identified as contributors to antioxidant capacity in peptides [2,41,59].

Intrinsic fluorescence refers to fluorescence that is caused by fluorophores, in the absence of scatterers and absorbers [66]. Intrinsic fluorescence spectroscopy, a non-destructive analytical tool, presents many advantages and applications in biological processes. It is a rapid technique with high sensitivity, specificity, and reproducibility. Many naturally occurring fluorophores are present in foods, which include tyrosine, tryptophan, phenylalanine, retinol, and riboflavin [65]. Thus, fluorescence analysis is employed: in quality assurance methodologies in the meat and fish industries (i.e. to measure collagen in connective tissues); to monitor the ripening of fruits and milk composition after pasteurization; and to investigate protein structures (based on the intrinsic fluorescence of aromatic amino acids) [65,67,68]. Applications of fluorescence in food analysis are explained [65]. Fluorophores have discrete spectral excitation-emission matrix (EEM) profiles describing their distinctive fluorescence properties. At a given excitation wavelength (Ex) fluorescence intensities of a sample can be collected at a range of emission wavelengths (Em). By collecting the fluorescence intensities at a range of Ex/Em, a fluorescence landscape or EEMs can be constructed. A fluorescence EEM may contain thousands of intensity points depending on the ranges of Ex/Em considered. Analysis of the fluorescence intensity data points captured within EEMs for the characterization of fluorophores and their contribution to food quality parameters like antioxidant capacities is challenging. Therefore, multivariate statistical methods can be used for extracting specific and sensitive information from the fluorescence EEM intensity data.

Multivariate statistical methods, such as principal component analysis (PCA), are often the methods of choice to capture variances and extract significant systematic trends in a sample data sets that contain large amounts of variables [65,69]. Detailed descriptions of PCA can be found in Eriksson et al. (2001) [70].

The objectives of this work were to assess the potential for fluorescence spectroscopy and PCA of fluorescence EEMs to monitor ORAC and FCR antioxidant

capacities during sequential UF and NF membrane fractionation of SPH. Potential relationships between ORAC and FCR antioxidant capacities were also examined.

4.4. Materials and Methods

4.4.1. Preparation of soy protein hydrolysates

Soy protein isolate (SPI) PRO-FAM 974 powder (Archer Daniels Midland Company, Decatur, IL, USA) was dissolved in Milli-Q (Millipore) water to obtain a 3.12 % (w/v) solution. The SPI solution was heated to 95 ^{o}C and held for 5 min. The control SPI solution was not subjected to heat pre-treatment.

4.4.1.1. Enzymatic hydrolysis of SPI solutions

Enzymatic hydrolysis procedure for SPI was developed from the work of Vilela, et al. (2006) [74]. Pepsin from porcine stomach mucosa and pancreatin mixture from porcine pancreas (Sigma-Aldrich, St. Louise, MO, USA) were employed for enzymatic hydrolysis of SPI solutions. Enzymatic hydrolysis using 0.5 % (w/v) pepsin was conducted at 37 ^{o}C and pH 1.5 during 30 min, followed by hydrolysis using 0.5 % (w/v) pancreatin mixture, which was conducted at 40 ^{o}C and pH 7.8 during 60 min. Heat pre-treatment and hydrolysis were performed in 500 mL batches, until 2000 mL of SPH were collected for each treatment. SPH were frozen at -20 ^{o}C until use.

4.4.2. Filtration experiments

4.4.2.1. Ultrafiltration experiments

Ultrafiltration experiments were performed with a hollow fibre polysulfone UF membrane module (UFP-10-E-4MA; 10 kDa MWCO, active area of 4.2 x 10^{-2} m^2; Amersham Biosciences, Westborough, MA, USA). UF was operated at a transmembrane pressure (TMP) of 62 kPa, feed flow rate of 2.4 L min^{-1}, and at room temperature (22 ^{o}C). Four UF experiments were performed (two per SPH), each had a feed volume of 1100 mL, and was run until 650 mL of permeate was collected. Frozen SPH samples were thawed overnight, and ultracentrifuged (Sorvall WX Ultra 100; Thermo Scientific, Asheville, NC, USA) with a A-621 rotor (31,901 G and 22 ^{o}C during 30 min) to remove non-dissolved solids. UF retentate and permeate fractions were sampled at the end of filtration and frozen at -20 ^{o}C. Feed, retentate and permeate fractions were evaluated

for total solids (TS) content, ORAC and FCR antioxidant capacities, and analyzed via fluorescence spectroscopy.

4.4.2.2. Nanofiltration experiments

Further fractionation of the UF permeates according to membrane molecular weight (MW) and charge was achieved by NF. The G10 NF thin film composite NF membrane was expected to retain peptides with MW larger than 2.5 kDa and with a negative charge. NF experiments were conducted in a cross-flow SEPA CF II cell (GE Osmonics, Minnetonka, MN, USA) equipped with G10 thin film composite membranes (2.5 kDa MWCO, active area of 1.4×10^{-2} m^2; Sterlitech Corporation, Kent, WA, USA). The membranes used are classified as loose NF membranes. The G10 membrane has a contact angle of 50.3 ^{o} and a strong negative zeta potential at pH 4 (-67.9 mV) and pH 8 (-72.4 mV) [63].

The feed volumetric flow rate was 1.8 L min^{-1}, the TMP was 2.0 MPa and the temperature was 22 ^{o}C. A new 0.12 m x 0.17 m piece of the flat sheet G10 membrane was used for each NF experiment.

The NF feeds were thawed UF permeate fractions diluted with Milli-Q (Millipore) water to a TS of 1.0 g L^{-1} and a final feed volume of 2.0 L. Initially, four NF experiments were performed for each SPH treatment: two at pH 4 and two at pH 8. The pH of NF feed solutions was adjusted using 1.0 M hydrochloric acid and 1.0 M sodium hydroxide. NF was conducted until 50 % of the feed volume was collected in the permeate stream (volume concentration ratio=2). NF permeates and retentates were sampled at the end of filtration and frozen at -20 ^{o}C. Accordingly, two additional NF experiments were performed using UF permeate for the heat pre-treated SPH at pH 4 and 8, during which permeate and retentate were sampled at a 5 min intervals during filtration providing 96 additional NF permeate and retentate samples.

Collected NF fractions were evaluated for TS, ORAC and FCR antioxidant capacities, and analyzed using fluorescence spectroscopy.

4.4.3. Analytical methods

4.4.3.1. Total solids (TS) determination

A known volume of a sample was placed on an aluminum dish (VWR, Mississauga, ON, Canada), and incubated overnight in a conventional oven at 105 ^{o}C to

evaporate the moisture. Dry mass in the dish was determined, which provided a direct measure of TS content of the sample.

4.4.3.2. O'phthaldialdehyde (OPA) assay

OPA spectrophotometric assay was performed to determine the peptide concentration (estimated by equivalent phenyl-glycine concentration). *L-(+)-α*-phenyl-glycine (2935-35-5, MP Biomedical, Solon, OH, USA), 99.9 % sodium borate decahydrate (S9640-500G, Sigma-Aldrich, St. Louise, MO, USA), sodium dodecyl sulfate (L4509-250G, Sigma-Aldrich, St. Louise, MO, USA), phthaldialdehyde (P0657-5G, Sigma-Aldrich, St. Louise, MO, USA), and 99 % ethanol were used. OPA calibration curve consisted of a phenyl-glycine concentration range from 0-1.0 mmol L^{-1}.

4.4.3.3. Oxygen Radical Absorbance Capacity (ORAC) assay

An ORAC calibration curve was prepared for a Trolox (6-hydroxy-2,5,7,8-tetramethylchroman-2-carboxylic acid; 238813-1G, Sigma-Aldrich, St. Louise, MO, USA) concentration range of 0-100 µM. A black 96-well plate was used to analyze all samples and standard solutions. A volume of 100 µL of a 2.5 nM Fluorescein (065-00252, Wako Pure Chemical Industries, Osaka, Japan) solution was added to each well followed by 50 µL of sample or standard solution. The plate was covered with a plastic 96-well plate lid and incubated at 37 ^{o}C for 15 min, prior to the addition of 50 µL of 2,2'-azobis-2-methyl-propanimidamide dihydrochloride (AAPH) solution to each well. A Synergy 4 microplate reader (BioTek, Winooski, VT, USA), was used for the analysis of Fluorescein degradation. A temperature of 37 ^{o}C was maintained with constant shaking to optimize peroxy radical formation by AAPH. Fluorescence Ex/Em was 485 nm/520 nm. Fluorescence measurements were collected every minute for 120 min.

4.4.3.4. Folin Ciocalteau Reagent (FCR) assay

An FCR calibration curve was prepared using a Trolox concentration range of 0-3 mM. Volumes of 20 µL of sample or trolox standard were added to 4.5 mL polymethylmethacrylate cuvettes (PMMA; UV-grade; VWR, Mississauga, ON, Canada). Each cuvette was incubated for 5 min at 22 ^{o}C after adding 150 µL of FCR reagent (F9252, Sigma-Aldrich, St. Louise, MO, USA). Then, 600 µL of 15 % (w/v) sodium carbonate (SX0400-1 500G, EMD Chemicals, Gibbstown, NJ, USA) was added to each cuvette followed by 2230 µL of Milli-Q (Millipore) water to achieve a final volume of the

cuvette to 3 mL. The cuvettes were shaken and incubated for 120 min at room temperature (22 ^{o}C). UV absorbance measurements at 750 nm were obtained using the Spectronic Genesys 2 spectrophotometer (Milton Roy, Ivyland, PA, USA).

4.4.4. Fluorescence analysis

Fluorescence analysis was adapted from Peiris et al. [69,71]. Varian Cary Eclipse Fluorescence Spectrofluorometer (Palo Alto, CA, USA) with a Peltier multicell holder was employed for intrinsic fluorescence measurements to produce EEMs. Fluorescence EEMs consisted of intensity reading captured within a range of Ex/Em of 250-340 nm and 300-600 nm respectively at 10 nm increments (3010 intensity values recorded per sample). In this range, protein substances, phenolic compounds, and colloidal particles can be detected [69]. PMMA cuvettes (UV-grade) with four optical windows were employed (VWR, Mississauga, ON, Canada). Emission spectra were obtained at a photomultiplier tube (PMT) voltage of 650 V, medium scanning rate, an excitation slit width of 5 nm, and an emission slit width of 5 nm. A spectrum for Milli-Q (Millipore) water was obtained under the same conditions to use as a baseline to minimize background noise and Raman scattering signals [69]. UF and NF samples, and Millipore water were maintained at pH ~7.0 and room temperature during analysis. Signal quenching effects were observed due to high concentrations of peptides in UF and NF samples at dilutions of up to 50-fold; therefore, to avoid quenching effects, 100-fold dilutions (40 µL of a sample in 3960 µL of Millipore water) were applied to all UF and NF samples prior to fluorescence analysis.

Data processing and the generation of EEM contour plots were obtained with Matlab 7.9.0 software (Mathworks, Inc., Natick, MA, USA).

4.4.4.1. Principal Component Analysis

The methodology for principal component analysis (PCA) was performed according to Peiris et al. (2010) [11]. Permeate and retentate fractions from two NF experiments for pre-heated SPH at pH 4 and 8 consisting of 96 samples (NF data set) were divided in two data matrices. The 47 fluorescence EEM of NF samples at pH 4 (X_{NF4}) was used in the PCA calibration (PCA_{NF}). The remaining 49 EEM of NF samples at pH 8 (X_{NF8}), were used in the validation of PCA_{NF} model. To verify the observations from PCA_{NF}, a second PCA calibration (PCA_{UF}) was completed with the EEM of UF samples (highly concentrated, larger peptides compared to NF fractions) and validated with the

EEM of NF fractions, including the 96 samples from the NF data set. The 8 EEM of the UF samples (Z_{UF}) was used for PCA_{UF}, followed by the validation of PCA_{UF} with the 112 EEM of NF samples (Z_{NF}). The combined data set of Z_{UF} and Z_{NF} was termed UF-NF data set.

PCA is a technique that extracts a smaller set of new variables, known as principal components (PCs) which are uncorrelated, mutually independent, and linearly related to the original variables in a data matrix [11]. PCs capture the proportion of systematic variance present in a data matrix, as explained by Eriksson et al. (2001) [70]. Hence, PCs can provide information on patterns and changes that occur in the original spectral data matrices (i.e. X_{NF4}, X_{NF8}, Z_{UF}, Z_{NF},). The process of data decomposition in a data matrix *X* by PCA can be explained by equation 7;

$$X = \sum_{i=1}^{n} t_i \cdot p_i + E \qquad (7)$$

where n represents the number of samples in the X data set, t_i represents scores, p_i represents loading values, and E is the residual matrix [71]. PCA projects fluorescence intensities to new planes with PCs, where the scores (t_i) are the new coordinates. PCs are related to the original data set (X matrix) by the loadings, which can be used to identify original spectral regions/variables in X that are correlated with specific fluorophores in the samples measured. Hence the scores of each PC correspond to specific fluorophore concentrations [11].

Pre-data processing, auto-scaling, was performed prior to PCA [70]. Random-subsets cross validation method was employed to determine the number of PCs that detect statistically significant trends in the data sets. PCA analyses, as well as data pre-treatments were performed using PLS Toolbox 3.5 (Eigenvector Research, Manson, WA, USA) in Matlab 7.9.0 (MathWorks Inc., Natick, MA, USA).

4.4.5. Multi-linear regression analysis

Multi-linear regression models (MLRMs) were developed (according to equation 8) for the NF data set (X_{NF}, n=96) by separately correlating measured ORAC and FCR values with the PCs that are significant and able to capture systematic changes in relevant species present in the NF samples. The fluorescence and PCA-captured ORAC ($ORAC_{FPCA}$) and FCR (FCR_{FPCA}) antioxidant capacities were estimated using these MLRMs based on their respective PC scores [82]. The same process was implemented on the UF-NF data set (n=120) to verify this procedure. The MLRMs serve to assess the

combined contribution of different peptide species on the antioxidant properties of the samples measured (as discussed later):

$$\hat{y} = \beta_0 + \beta_1 \cdot x_1 + \beta_2 \cdot x_2 + \ldots + \beta_n \cdot x_n \quad (8)$$

where $\hat{y}$ is the model-estimated ORAC or FCR antioxidant capacities, and β_n are model parameters (intercept and effects of x_n on $\hat{y}$). The x_i (i=1, 2, 3,...n) represents the PC score of i^{th} statistically significant PC that was able to capture systematic changes in the original fluorescence data and n is the number of statistically significant PCs derived in the PCA. Model parameters were evaluated by minimizing the sum of squared errors (SSE) for a given set of model fitted data. In multi-linear regression analysis of all the pre-heated SPH NF data at pH 4 and 8 (n=96), 47 samples (permeate samples from NF at pH 4 and 8) were used to build the MLRMs for $ORAC_{FPCA}$ and FCR_{FPCA}. The remaining 49 samples were used for validation of the MLRMs. In the combined UF-NF data set (n=120), 60 samples were randomly selected for model development, and the remaining 60 samples were used for model validation.

4.4.6. Statistical analysis

The R^2 values were determined for plots of MLRMs, as a measure of goodness-of-fit of linear regression [82].

4.5. Results and Discussion

4.5.1. Effects of UF and NF on peptide distribution and antioxidant capacity

The pre-heated and control SPH were subjected to UF (tangential flow hollow fiber 10 kDa membrane MWCO step) to remove large peptide fragments (> 10 kDa) and recover peptides smaller than 10 kDa. UF permeates collected for pre-heated and control SPH were then diluted to a TS content of 1 g L^{-1} and further fractionated by NF (tangential flow G10 flat sheet 2.5 kDa membrane MWCO) at pH 4 and 8. UF fractions possessed significantly higher peptide concentrations (1.52-3.65 mmol L^{-1}) and TS content (17.66-30.43 g L^{-1}) than NF fractions (0.026-0.295 mmol L^{-1} and 0.10-2.20 g L^{-1}, respectively).

The ORAC and FCR antioxidant capacities of the UF and NF samples collected during membrane filtration steps are presented in Figure 14 and Figure 15. Due to the fundamental differences between the two antioxidant assays employed in this study, a noticeable linear relationship between ORAC and FCR is absent (as discussed later).

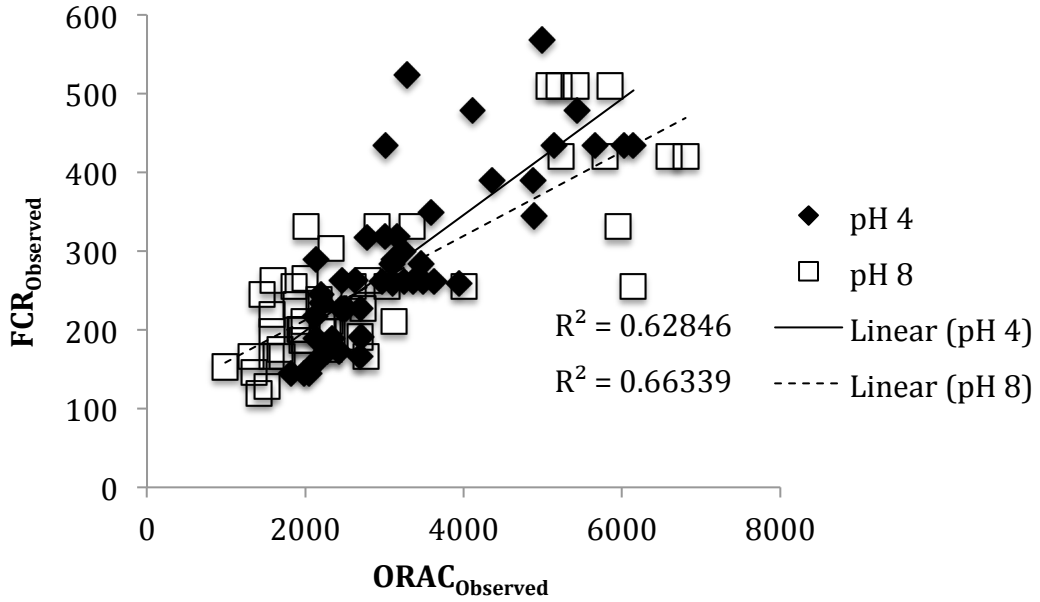

Figure 14: Plot of observed ORAC versus observed FCR antioxidant capacities for 96 NF samples for pre-heated soy protein hydrolysate at pH 4 and 8.

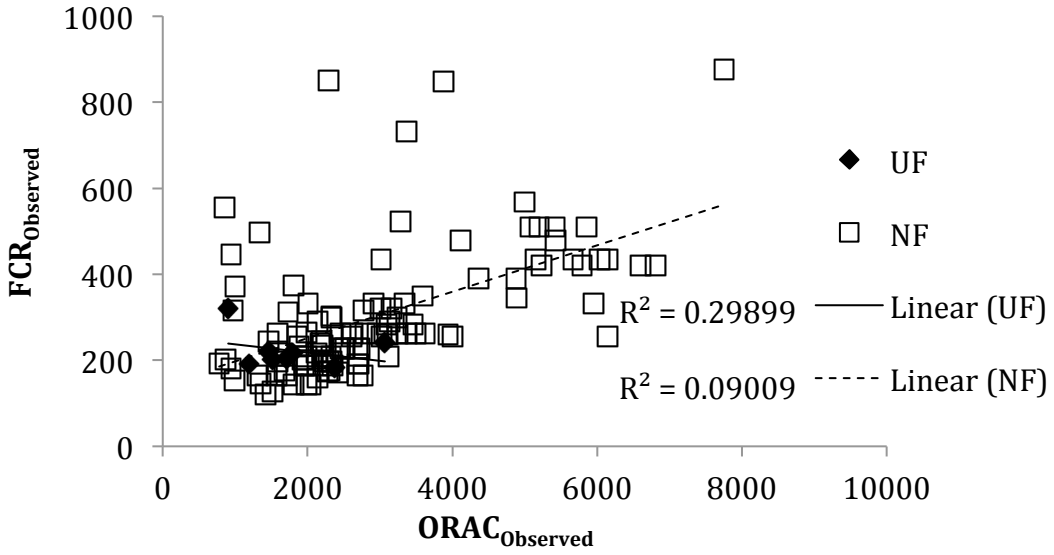

Figure 15: Plots of observed ORAC versus observed FCR antioxidant capacities for UF and NF samples.

4.5.2. Fluorescence EEMs for UF and NF peptide fractions

Typical fluorescence EEMs for UF and NF permeate fractions are provided in Figure 16. Two regions representing two types of proteinous substances (peak α and shoulder δ) and a region corresponding to Rayleigh light scattering (RS) were identified. Fluorescence regions identified by α and δ represent tryptophan and tyrosine, respectively [65,83]. Tryptophan fluoresces at Ex/Em ~275 nm/350 nm, and tyrosine

at Ex/Em ~275 nm/305 nm [83]. A region corresponding to RS that has been previously reported to provide information related to colloidal particles (γ) [11] in peptide solutions was also presented.

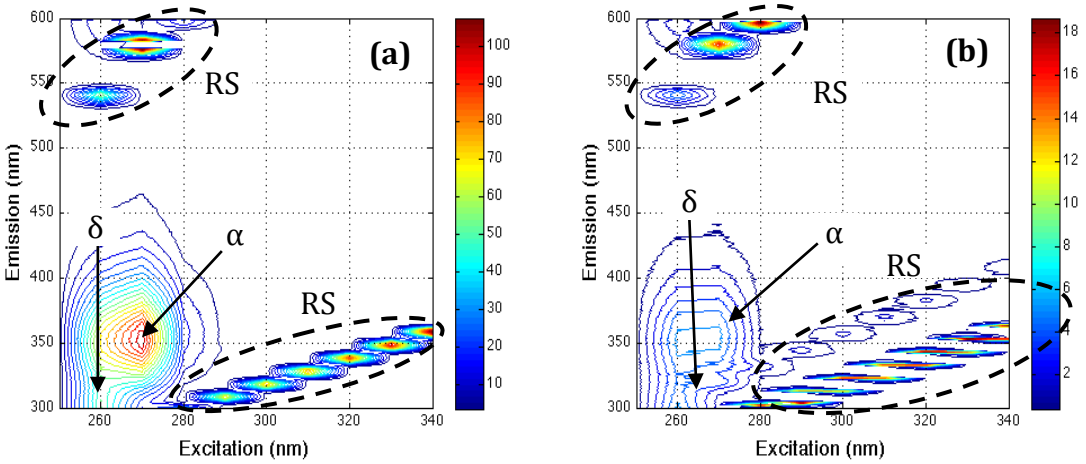

Figure 16: Fluorescence features observed in typical fluorescence EEMs for (a) UF permeate (peptide content of 0.076 mmol g^{-1}; TS of 20.2 g L^{-1}) and (b) NF permeate at pH 8 (peptide content of 0.125 mmol g^{-1}; TS of 0.4 g L^{-1}) for pre-heated soy protein hydrolysate. Rayleigh light scattering (RS) regions are indicated by the dashed lines.

4.5.3. Fluorescence loading plots for NF peptide fractions

PCA was performed separately on two sets of data: the NF data set for pre-heated SPH, and the UF-NF data set.

The NF data set (n=96) for pre-heated SPH consisted of fluorescence EEMs of permeate and retentate samples that were collected at 5 min intervals during NF for pre-heated SPH at pH 4 and 8. PCA generated PCs that explained systematic patterns present in the X_{NF4} matrix that were used for PCA_{NF} model development. Five statistically significant PCs were identified for X_{NF4} capturing a total variance of 72.8 % in NF permeate and retentate samples; however, only PC_1 (25 %) and PC_2 (18.5 %) identified significant features of NF samples (43.5 % of variance) while PC_3, PC_4, and PC_5 contained unidentifiable features, which cumulatively captured 29.3 % of variance. NF permeate and retentate samples were extremely dilute in nature and predominantly consisted of peptides (<2.5 kDa in MW). The remaining 27.2 % of variance not captured by these five PCs was due to instrument noise in fluorescence readings (~5 %) and other PCs that were found to be statistically insignificant.

PCA of X_{NF4} assigned a separate set of loading values for each PC (equation 7) such that for a given set of loading values that correspond to a given PC, there exist a

loading value for each spectral variable in the fluorescence data matrix (i.e. X_{NF4}). When these loading values were arranged according to the corresponding excitation and emission wavelength combinations in a data matrix (columns and rows representing excitation and emission wavelength ranges, respectively) a loading matrix could be generated [71]. Consequently, a loading plot, created by plotting loading values against their respective fluorescence Ex/Em wavelength coordinates, can be investigated to identify the spectral variable that a PC represents [84]. The loading plot for PC_1 (Figure 17a) displayed a predominant peak (α') at Ex/Em ~280 nm/400 nm, which was similar to the region where tryptophan (α peak in Figure 16) appeared; therefore, PC_1 scores can be directly correlated to the concentration of tryptophan containing peptides. Similarly, PC_2 (a dominant valley (δ') at Ex/Em ~275 nm/310 nm; Figure 17b) can be correlated to tyrosine-containing peptides; therefore PC_2 scores were inversely related to the concentration of tyrosine-containing peptides. Since these two statistically significant PCs were associated with antioxidant amino acids residues, they were used to estimate the $ORAC_{FPCA}$ antioxidant capacity (AC) and FCR_{FPCA} AC of SPH fractions.

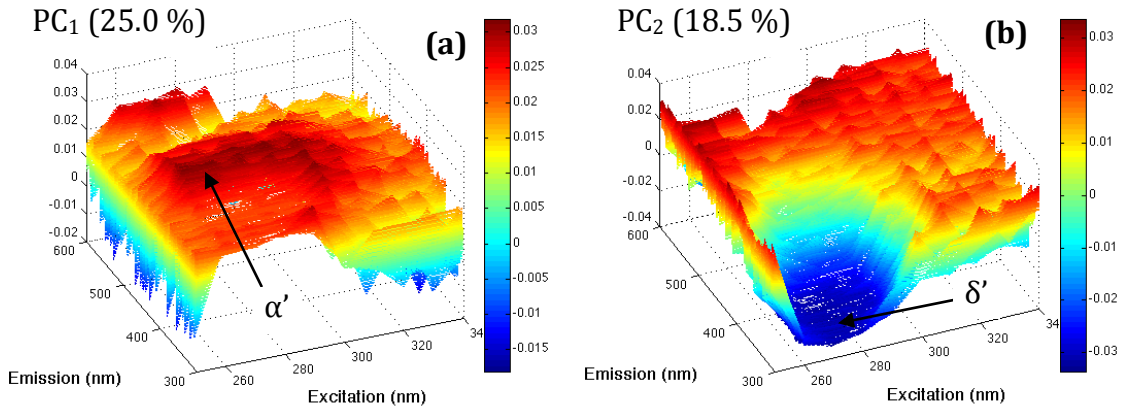

Figure 17: 3D illustrations of loading matrices obtained by PCA of NF spectral data (X_{NF4}) for (a) PC_1, and (b) PC_2. Variance captured by each PC is provided.

4.5.4. Fluorescence and PCA-captured relative ORAC and FCR antioxidant capacities during fractionation of SPH by NF

The measured ORAC and FCR ACs of the 96 NF fractions were then separately correlated with the tryptophan and tyrosine-containing peptide content, estimated in terms of PC_1 scores and PC_2 scores. This information was used to develop MLRMs that captured the relative combined contribution of tryptophan and tyrosine-containing peptides to ORAC and FCR ACs of SPH fractions (Equations 9 and 10). These relative combined contributions of tryptophan and tyrosine-containing peptides to ACs are

hereby named fluorescence and PCA-captured relative ORAC ($ORAC_{FPCA}$), and fluorescence and PCA-captured relative FCR (FCR_{FPCA}), respectively.

$$ORAC_{FPCA}=\beta_0 + \beta_1 \bullet PC_1 + \beta_2 \bullet PC_2 \quad (9)$$

$$FCR_{FPCA}=\alpha_0 + \alpha_1 \bullet PC_1 + \alpha_2 \bullet PC_2 \quad (10)$$

The β_0, β_1, and β_2 terms refer to the parameters that were estimated by minimizing the SSE between $ORAC_{FPCA}$ and measured ORAC values. The terms β_1 and β_2 can be considered as the individual contribution of tryptophan-containing peptides and tyrosine-containing peptides, respectively, to ORAC. Similarly α_0, α_1 and α_2 parameters were estimated by minimizing the SSE between FCR_{FPCA} and measured FCR values. Also, the terms α_1 and α_2 can be considered as the individual contribution of tryptophan- and tyrosine-containing peptides, respectively, to FCR. For the parameter estimation of equation 9 and equation 10 (i.e. calibration), PC scores of 47 NF permeate samples (pH 4 and 8) were used. Subsequently, another set of 49 NF samples (feed and retentate samples a pH 4 and 8) were used for the independent validation of these MLRMs.

The plot of FCR_{FPCA} vs. $ORAC_{FPCA}$ is shown in Figure 18. The $ORAC_{FPCA}$ and FCR_{FPCA} ACs for NF fractions at pH 4 and 8 displayed strong linear relationships (R^2>0.99; Figure 18). This linear relationship signifies that the combined role of tryptophan and tyrosine-containing peptides on the AC is a fundamental phenomenon that was captured in both ORAC and FCR measurements, which is consistent with previously published work [7,59]. The FCR assay is known to give a direct measure of the total phenolic content, which is due predominantly to the presence of aromatic amino acids (i.e. tyrosine and tryptophan) [7]. The significance of tyrosine and tryptophan in the ORAC AC of peptides has been shown by Nimalaratne et al. (2011) [59]. This phenomenon was however, not evident when the plot of measured FCR vs. measured ORAC (Figure 14) was considered (discussed below). Other researchers have proposed that these two methods could be used in combination due to the limitations and differences in the ORAC and FCR measurement protocols [7,85]. In this context, our proposed approach could be used to assess the common properties that are relevant to ACs from ORAC and FCR measurements. Thus, it can be viewed as a method for filtering information related to the combined contribution of tryptophan and tyrosine-containing peptides on the AC associated with ORAC and FCR measurements.

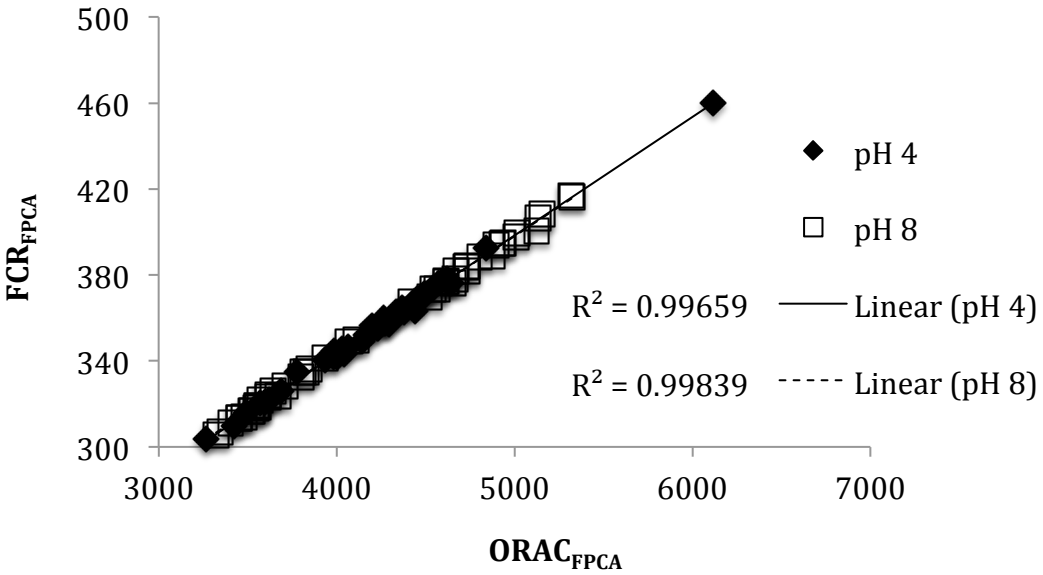

Figure 18: Plot of $ORAC_{FPCA}$ versus FCR_{FPCA} antioxidant capacity for 96 NF samples for pre-heated soy protein hydrolysate at pH 4 and 8.

In addition, the pH conditions employed during NF did not appear to affect the $ORAC_{FPCA}$ and FCR_{FPCA} ACs (Figure 18). This indicated that the combined contribution of tryptophan and tyrosine-containing peptides to ORAC and FCR ACs was pH and charge independent.

4.5.5. Correlation between FCR and ORAC measurements

The comparatively weaker correlation between the observed FCR and the observed ORAC for NF samples at pH 4 and 8 (R^2=0.62 and R^2=0.66, respectively) is shown in Figure 14.

The lower degree of goodness-of-fit could be attributed to the contributions to ORAC and FCR measurements by other species present in the NF samples that were not captured by the FCR_{FPCA} and $ORAC_{FPCA}$ estimates or that may not involve fluorescing components. In addition the fundamental differences in the underlying antioxidant mechanisms of the ORAC and FCR assays for a given sample (discussed before) may also contribute to these weak correlations [6,7,57]. The plots of observed ORAC vs. $ORAC_{FPCA}$ values, and observed FCR vs. FCR_{FPCA} values showed weak linear correlations (data not shown). This could be caused by the filtering effect that results in the calculation of $ORAC_{FPCA}$ and FCR_{FPCA} values.

4.5.6. Verification of results by PCA of UF samples

Since only NF samples were used to estimate $ORAC_{FPCA}$ and FCR_{FPCA} ACs, verification was necessary to determine if this trend would hold true for larger MW SPH fractions compared to NF fractions. Therefore, PCA_{UF} was conducted with UF fractions. UF-NF data set (combination of Z_{UF} and Z_{NF}; n=120) were analyzed with the same approach as the NF data set. The 96 samples analyzed in PCA_{NF} were included in this data set. The additional 24 samples (8 UF samples, 16 NF samples) served as independent data points for the verification of the proposed approach. Two statistically significant PCs were identified from PCA_{UF} of Z_{UF}, capturing a total variance of 89.4 % (55.2 % by PC_1 and 34.2 % by PC_2). PC_1 was identified as tryptophan-containing SPH, and PC_2 as tyrosine-containing SPH. Detailed evaluation of PCA_{UF} is provided in the appendix. The $ORAC_{FPCA}$ and FCR_{FPCA} ACs for these 120 samples were determined by MLRMs and the PC_1 and PC_2 for UF and NF samples.

Similar to the results presented in Figure 14, no relationship was identified between the measured ORAC and FCR ACs. A weak linear relationship for the UF samples (R^2=0.45; n=8), and a significantly improved linear relationship for the NF samples (R^2>0.99; n=112) was observed between the $ORAC_{FPCA}$ and FCR_{FPCA} values (Figure 19) confirming previous observations (Figure 18). This relationship was validated with the 16 independent NF samples.

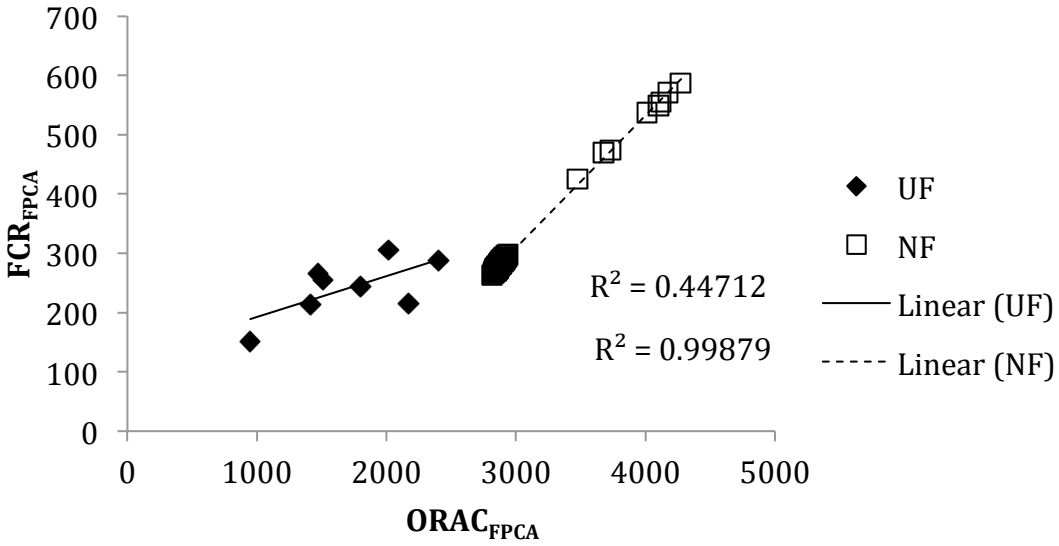

Figure 19: Plots of $ORAC_{FPCA}$ versus FCR_{FPCA} antioxidant capacities for the 96 NF samples and the additional 24 independent UF (n=8) and NF (n=16) samples.

The limited fit of the UF samples could be attributed to the limited number of UF samples employed in this study (n=8) or their variations with respect to heat pre-treatment, peptide concentrations (ranged from 1.52-3.65 mmol L^{-1}), and TS content (ranged from 17.66-30.43 g L^{-1}). The magnitude of the variations for the peptide concentrations (ranged from 0.026-0.295 mmol L^{-1}) and TS contents (0.10-2.20 g L^{-1}) of NF samples was extremely low compared to UF samples. Another cause for the limited fit could be the effect of the MW and charge of peptide fractions on AC, and on fluorescence intensity. Since the MW of the UF SPH fractions is significantly larger compared to NF fractions, their ACs is expected to be lower as a result of the confinement of antioxidative amino acid residues by peptide bonds and side chain interactions; and fluorescence intensities may have increased due to the presence of a higher concentration of fluorophores [9,65]. The contrasting effects of the broader MW distribution on AC and fluorescence emission intensity may have contributed to a larger variation in UF samples compared to NF samples consequently influencing their $ORAC_{FPCA}$ and FCR_{FPCA} values, and the limited fit (Figure 19).

Due to the differences in the peptides characteristics (MW distribution and lengths of peptide chains), peptide concentration, and TS content between UF and NF samples, a clustering effect that separated UF samples from NF was identified (Figure 19). The pre-heated SPH UF and NF peptide fractions could not be distinguished based on their FCR_{FPCA} values, but were clearly distinguished from their $ORAC_{FPCA}$ values. Though all 112 NF fractions followed the same trend, the effect of heat pre-treatment of SPI on the ACs of NF fractions could be identified by the positions of the two clusters within the NF samples with respect to both $ORAC_{FPCA}$ and FCR_{FPCA} (Figure 19).

A plot of observed ORAC vs. $ORAC_{FPCA}$ values provided a moderate linear fit for UF samples (R^2=0.66; data not shown), but there was no linear fit observed for NF samples. Observed FCR vs. FCR_{FPCA} values showed a weak relationship for UF and NF samples (Figure 15). These results are consistent with those presented in 4.5.4 and reinforce the principle of the filtering effect that was observed in the estimation of $ORAC_{FPCA}$ and FCR_{FPCA} values from fluorescence.

4.5.7. Potential for analysis of bioactive compounds and future applications

In this study, PCA of fluorescence EEMs for UF and NF peptide fractions, followed by multi-linear regression analysis, proved suitable to examine the underlying

relationship between the ORAC and FCR antioxidant assays, which are based on fundamentally different mechanisms for the characterization of antioxidant properties. The proposed approach developed in this study characterized the key features in peptides that contributed to their ACs. This method was able to evaluate the relative combined and individual contributions of tryptophan and tyrosine-containing peptides to the ACs of soy protein hydrolysates. Thus, this approach provides an avenue to assess the common features captured by ORAC and FCR antioxidant assays. The proposed method has potential applications in food and nutraceutical screening and quality control processes, where multiple biological components that impact the ACs in a sample can be identified, quantified, and evaluated along with their bioactive functionalities in one simple measurement. This method presents immense advantages for estimating the relative ACs of peptides, since determining absolute ACs experimentally using ORAC or FCR is inconvenient, time-consuming, and hazardous. The proposed method is rapid, sensitive, reproducible, non-destructive, and does not require hazardous chemicals. This approach may also be applicable in determining the contributions of biological species to other bioactive functionalities of peptides and macromolecules.

4.6. Conclusion

PCA of fluorescence excitation-emission matrix data for UF and NF peptide fractions, followed by multi-linear regression analysis, was used to capture specific species that contribute to the AC of SPH. Two statistically significant principal components (PCs) were found to be related to the tryptophan- and tyrosine-containing peptides content, estimated in terms of PC_1 and PC_2, respectively. MLRMs built using these PCs, for estimating $ORAC_{FPCA}$ and FCR_{FPCA} ACs of NF peptide fractions at pH 4 and 8, showed strong linear relationships (R^2>0.99). The following key conclusions were made:

1. A linear relationship observed between $ORAC_{FPCA}$ and FCR_{FPCA} for NF fractions signifies that the combined role of tryptophan and tyrosine-containing peptides on the AC is a fundamental phenomenon, which is captured in both ORAC and FCR measurements.

2. Using two different antioxidant assays (ORAC and FCR) in combination the proposed approach can assess common properties that are relevant to ACs from ORAC and FCR measurements.
3. Validation of the proposed approach with 24 independent UF and NF samples showed a significantly linear relationship for the NF samples (R^2>0.99; n=112) between the $ORAC_{FPCA}$ and FCR_{FPCA} values.
4. The weak linear relationship between $ORAC_{FPCA}$ and FCR_{FPCA} of the UF samples may be attributed to the limited number of UF samples (n=8), and their variations with respect to heat pre-treatment, significant range of peptide concentration and TS content.
5. A clustering effect distinguished pre-heated SPH UF and NF samples with respect to $ORAC_{FPCA}$; and control SPH NF samples from pre-heated SPH NF samples with respect to $ORAC_{FPCA}$ and FCR_{FPCA}.

Hence, the proposed approach provides an avenue to assess fundamental features of ACs captured by ORAC and FCR methods.

5. Amino Acid Analysis of Antioxidant Soy Protein Hydrolysate Fractions Separated by UF and NF

5.1. Introduction

A diverse number of peptides and free amino acids present bioactive functionalities, such as antioxidative properties. A common method of characterizing these bioactive peptide fractions is amino acid compositional analysis, which can be performed using techniques such as reverse phase HPLC (RPHPLC) and proton NMR spectroscopy. RPHPLC exploits the hydrophobicity and charge of peptides and amino acids [47]. Proton NMR spectroscopy measures proton signals emitted by molecules when subjected to a strong electromagnetic field, which causes them to excite and relax. These proton signals correspond to the relative number of protons in amino acids and peptides [50]. Detailed descriptions of these two methods are presented in 2.2.2.

Due to the degradation of amino acids in aqueous solutions at room temperature, pre- and post-column derivatization procedures have been implemented in amino acid analysis by RPHPLC [86]. Pre-column derivatization refers to the formation of amino acid derivatives prior to their separation. O'phthaldialdehyde (OPA)/β-mercaptoethanol (βME), ninhydrin, dimethylaminoazobenzene-4'-sulfonyl (DNS), and phenyl-isothiocyanate (PITC) are commonly employed as derivatizing agents in RPHPLC [86,87]. Pre-column derivatization provides many advantages to amino acid analysis, including rapid analysis, ease of use, high sensitivity, and greater separation efficiency [86]. In amino acid analysis, PITC derivatization is often preferred over DNS- and OPA/ βME-derivatization due to the higher stability of the derivatives, the ability to react with and detect primary and secondary amines, and the lack of interference from reagent peaks [86,87].

The objectives of this work were to estimate the amino acid composition in antioxidant peptide fractions isolated by membrane filtration of soy protein hydrolysates, and to determine the effects of NF on the fractionation of these antioxidant peptides using RPHPLC with pre-column PITC derivatization, and NMR spectroscopy. The potential for 1D-^{1}H NMR spectroscopy for amino acid analysis was also investigated.

5.2. Materials and Methods

5.2.1. Enzymatic hydrolysis of peptide fractions

Permeate fractions of soy protein hydrolysates, produced from soy protein isolate with no heat pre-treatment (control SPH) according to the method presented in section 3.4.1.2, were obtained by sequential UF and NF at pH 8 treatment. These two permeate fractions were subjected to complete enzymatic hydrolysis using pepsin from porcine stomach mucosa and pancreatin mixture from porcine pancreas (Sigma-Aldrich, St. Louise, MO, USA) to obtain the constituent amino acids of each peptide fractions.

Enzymatic hydrolysis was conducted by adding 750 µL of 0.5 % (w/v) pepsin to 15 mL of peptide sample at 37 ^{o}C and pH 1.5 over 30 min, followed by 3 mL of 0.5 % (w/v) pancreatin mixture to 15 mL of peptide sample at 40 ^{o}C and pH 7.8 over 60 min. The hydrolysates were placed in Amicon® Ultra-15 centrifuge tubes equipped with 3 kDa MWCO UF membranes (Millipore Corporation, Billerica, MA, USA) and centrifuged (4000 *G*, 85 mm rotor radius, 22 ^{o}C for 40 min) using a Damon IEC HN-S centrifuge (GMI Inc., Minneapolis, MN, USA) to separate the amino acids from the proteases. Complete hydrolysates of SPH fractions were frozen at -20 ^{o}C until use.

5.2.2. Analytical methods

5.2.2.1. Total solids determination

A 1.5 mL sample was placed on an aluminum dish (VWR, Mississauga, ON, Canada) and incubated overnight in a conventional oven at 105 ^{o}C to evaporate the moisture. Dry mass of the material in the dish provided a direct measure of TS.

5.2.2.2. Reverse-phase HPLC

Amino acid analyses of the complete hydrolysates of UF and NF permeate fractions were performed by RPHPLC adapted from Bidlingmeyer et al. (1984), Heinrikson and Meredith (1983), and Naderi (2010). The phenyl-isothiocyanate (PITC) pre-column derivatization technique was employed to form phenyl-thiocarbamyl (PTC) derivatives of amino acids being tested as follows. A 10 µL amino acid sample (obtained from the soy protein hydrolysate UF or NF permeate fractions) or amino acid standard (Sigma-Aldrich, St. Louise, MO, USA) was diluted to 2.5 mmol L^{-1}, and dried under vacuum. A 20 µL volume of 99 % ethanol:water:triethylamine (TEA; 121-44-8; Sigma-

Aldrich, St. Louise, MO, USA) solution in the volume ratio of 2:2:1 was added to the powder amino acid sample or standard, which was repeatedly subjected to vacuum drying (National Appliances Co. vacuum oven model 5831-7, Thermo Scientific, Asheville, NC, USA). The PITC (103-720; Sigma-Aldrich, St. Louise, MO, USA) derivatizing reagent (ethanol:TEA:water:PITC) was prepared in a volume ratio of 7:1:1:1, and 20 µL of the reagent was added to a powder sample in a sealed nitrogen environmental chamber to form PTC-amino acid derivatives. The samples were incubated in the sealed nitrogen environmental chamber for 20 min at 22 ^{o}C. The sample was subjected to vacuum drying to evaporate the residual reagent. Dried samples were then stored at room temperature.

The RPHPLC protocol required two solvents: solvent-A, a 50 mM sodium acetate (127-09-3; Sigma-Aldrich, St. Louise, MO, USA) solution containing 0.04 % (v/v) TEA and pH adjusted to 6.35 using glacial acetic acid; and solvent-B, 60 % (v/v) acetonitrile (75-05-8; EMD Chemicals, Billerica, MA, USA) in water. Each amino acid sample (10 µL) was dissolved in 500 µL of solvent-A. A Varian Pro-Star 210 HPLC (Varian Canada Inc., Mississauga, ON, Canada) equipped with an Agilent Eclipse Plus C_{18} column (150 x 4.6 mm ID, 5 µm pore size; Agilent Technologies Canada Inc., Mississauga, ON, Canada) was used. The mobile phase flow rate was 1 mL min^{-1}, the column temperature was 40 ^{0}C, and the UV-detector wavelength was 254 nm. A mobile phase gradient was used as follows: initially, 90 % of solvent-A and 10 % of solvent-B for 5 min, and increasing to 44 % solvent-A and 56 % solvent-B in a 20 min time period. The column was subsequently washed with 100 % solvent-B to elute any residual components from the column. Calibration curves were constructed for amino acid standards (alanine, arginine, aspartic acid, cysteine, glutamic acid, glycine, histidine, isoleucine, leucine, lysine, methionine, phenylalanine, proline, serine, threonine, tyrosine, and valine) at six dilutions (0.16-5.0 mmol L^{-1}), according to Bidlingmeyer (1984) [86]. The calibration curves and their linear regression models were used to determine sample amino acid concentrations.

5.2.2.3.^{1}H NMR Spectroscopy

Amino acid analyses of complete hydrolysates of UF and NF permeate fractions by proton NMR was performed by Eric Blondeel (Department of Chemical Engineering, University of Waterloo). The control SPH samples were diluted for NMR analysis by

adding 70 µL of Chenomx internal standard (Chenomx Inc., Edmonton, AB, Canada) to 630 µL of sample. The samples were subjected to a strong 600 MHz magnetic field pulse (600 MHz NMR spectrometer, Burker BioSpin Ltd., Milton, ON, Canada), and proton signals were recorded over a resonance frequency range of 0-10 Hz. The proton signals were collected and analyzed using the Chenomx NMR Suite 7.1 software developed and provided by David Chang (Chenomx Inc., Edmonton, AB, Canada).

5.3. Results and Discussion

Preliminary amino acid analysis was performed on the most promising antioxidant peptide fractions isolated by sequential membrane fractionation of soy protein hydrolysates, control SPH NF permeate fraction at pH 8 (5562 µmol TE g^{-1}). The UF permeate fraction for control SPH (2372 µmol TE g^{-1}), which was the feed solution for NF, was also analyzed to elucidate the effects of NF at pH 8 on the amino acid composition of peptides.

5.3.1. Amino acid analysis by reverse-phase HPLC

The RPHPLC chromatograms for amino acid standards (Figure 20), UF permeate (Figure 21a), and NF permeate at pH 8 (Figure 21b) are presented.

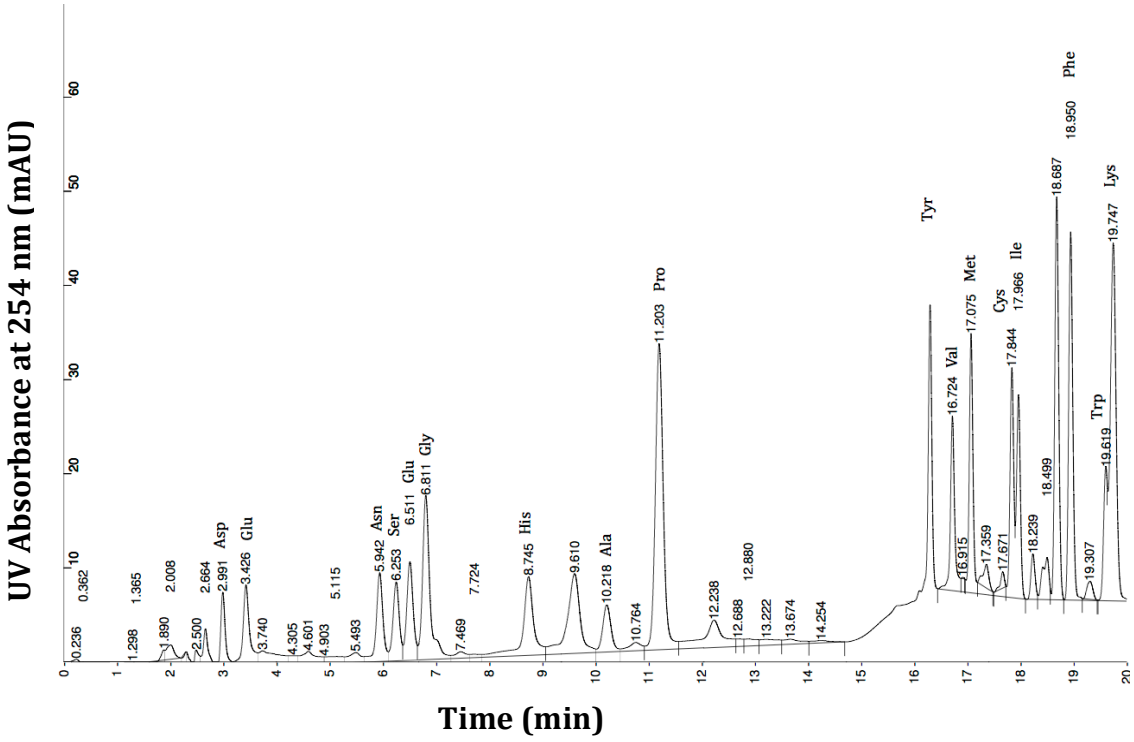

Figure 20: Elution profile for amino acid standards by reverse-phase HPLC. Conditions for HPLC: solvent A – 0.05 % (v/v) TEA in 50 mmol L^{-1} sodium acetate; solvent B – 60 % (v/v)

acetonitrile in water; flow rate 1.0 mL min^{-1}; gradient B from 10-56 % in 20 min; UV absorbance at 254 nm.

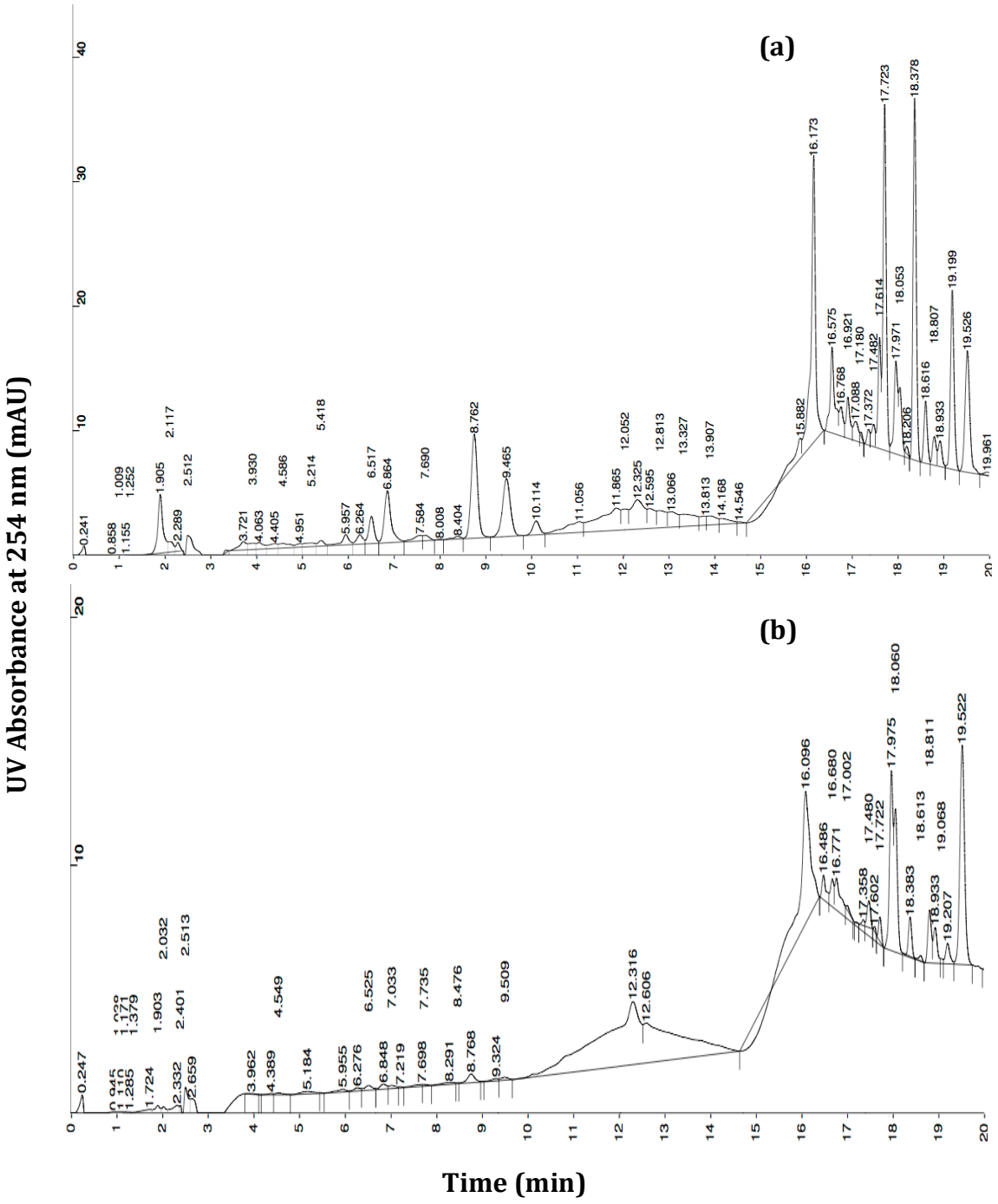

Figure 21: Elution profiles for amino acids in (a) UF permeate fraction and (b) NF permeate fraction at pH 8 for control soy protein hydrolysate separated by reverse phase HPLC. Conditions for HPLC: solvent A – 0.05 % (v/v) TEA in 50 mmol L^{-1} sodium acetate; solvent B – 60 % (v/v) acetonitrile in water; flow rate 1.0 mL min^{-1}; gradient B from 10-56 % in 20 min; UV absorbance at 254 nm.

The amino acid profile of the UF and NF permeate fractions are presented in Table 7. Since the total concentration of amino acids in the UF permeate fraction (15.80

mmol L^{-1}) was higher than the NF permeate fraction at pH 8 (4.88 mmol L^{-1}), amino acid concentrations did not allow for accurate comparisons between the two peptide fractions. Thus, using amino acid contents (amino acid concentration divided by total solids content of the overall sample) and molar compositions were found to be more appropriate.

Table 7: Amino acid composition of the UF permeate fraction (TS=13.125 g L^{-1}) and the NF permeate fraction at pH 8 (TS=0.161 g L^{-1}) for the control soy protein hydrolysate by reverse-phase HPLC with pre-column PITC derivatization. Amino acid concentrations (Conc.; mmol L^{-1}), content (mmol g^{-1}), and molar compositions (% content) are presented. Conditions for HPLC: eluent A – 0.05 % (v/v) TEA in 50 mmol L^{-1} sodium acetate; eluent B – 60 % (v/v) acetonitrile in water; flow rate 1.0 mL min^{-1}; gradient B from 10-56 % in 20 min; UV absorbance at 254 nm.

Amino acid	UF permeate fraction			NF Permeate fraction at pH 8		
	Conc. (mmol L^{-1})	Content (mmol g^{-1})	%	Conc. (mmol L^{-1})	Content (mmol g^{-1})	%
Alanine	0.73	2.76	4.59	0.02	7.72	0.50
Asparagine	0.30	1.16	1.92	0.06	18.90	1.23
Cysteine	1.59	6.04	10.04	0.03	8.62	0.56
Glutamine	0.59	2.25	3.74	0.07	20.25	1.32
Glycine	0.79	3.00	4.98	0.02	6.62	0.43
Histidine	2.04	7.76	12.89	0.27	83.92	5.48
Isoleucine	1.05	4.00	6.64	0.94	293.16	19.14
Leucine	0.36	1.35	2.25	0.17	53.14	3.47
Lysine	0.45	1.70	2.83	0.37	115.34	7.53
Methionine	0.30	1.13	1.88	0.00	0.00	0.00
Phenylalanine	0.24	0.93	1.55	0.14	42.51	2.77
Proline	0.17	0.65	1.08	1.09	337.60	22.04
Serine	0.31	1.19	1.97	0.08	24.05	1.57
Tryptophan	2.88	10.99	18.26	0.24	74.73	4.88
Tyrosine	2.87	10.94	18.19	1.33	413.22	26.97
Valine	1.14	4.33	7.20	0.10	32.22	2.10

Amino acid concentrations in the UF permeate were greater than the NF permeate at pH 8, with the exception of proline. Predominant amino acids in the UF permeate included histidine, tryptophan, and tyrosine; all are known contributors to antioxidant capacity (AC) of peptides [2,59]. The content of each amino acid per gram of total solid was higher in the NF permeate at pH 8 than for the UF permeate. Relatively high amino acid content of lysine (115.34 mmol g^{-1}), isoleucine (293.16 mmol g^{-1}),

histidine (83.92 mmol g^{-1}), leucine (53.14 mmol g^{-1}), proline (337.60 mmol g^{-1}), tryptophan (74.73 mmol g^{-1}), and tyrosine (413.22 mmol g^{-1}) were found in the NF permeate fraction a pH 8. The presence of these amino acids in higher contents in the NF permeate fraction at pH 8 was reflected in its ORAC (5562 µmol TE g^{-1}) AC.

A common characteristic of the amino acids present in high contents in the NF permeate at pH 8 is the hydrophobic nature with the exception of tyrosine (polar amino acid). Though the NF membrane surface elicited hydrophilic properties (contact angle of 50.3^{0}), over the course of NF, the membrane properties may have changed. This may suggest the influence of hydrophobicity on peptide fractionation by NF at pH 8 and on their ACs.

By comparing the relative amino acid compositions (%) in the UF permeate and NF permeate at pH 8, the selectivity of NF towards certain amino acids in peptides was evaluated. The relative content of isoleucine, leucine, lysine, phenylalanine, proline, and tyrosine increased due to NF at pH 8, compared to the UF permeate, most of which have been shown to contribute to the antioxidative functions of peptides [2,59].

Therefore, preliminary amino acid analysis by RPHPLC provided useful information regarding the amino acid profile of the NF permeate fraction at pH 8 and its significantly high AC in comparison to the feed (UF permeate fraction for control SPH).

5.3.2. Amino acid analysis by ^{1}H-NMR spectroscopy

The amino acid profiles analyzed by NMR are presented in Table 8 for control SPH UF permeate and NF permeate at pH 8. A detailed description of quantitative analysis of 1D-^{1}H NMR metabolics data is provided by Weljie et al. (2006) [88].

The amino acids detected and quantified by NMR appeared in higher contents in the NF permeate at pH 8 than the UF permeate with the exception of asparagine, glutamine and tryptophan. For example, the tyrosine content in the NF permeate at pH 8 was 0.637 mmol g^{-1}, compared to 0.083 mmol g^{-1} in the UF permeate. Leucine (0.61 mmol g^{-1}), phenylalanine (0.57 mmol g^{-1}), tyrosine (0.64 mmol g^{-1}), and valine (0.18 mmol g^{-1}) were present in higher contents in the NF permeate than the UF permeate and have been shown to contribute to the antioxidative functions of peptides [2,59]. These differences were consequently reflected on the ORAC ACs of the UF (2372 µmol TE g^{-1}) and NF permeate at pH 8 (5562 µmol TE g^{-1}) fractions.

The amino acid composition of the respective SPH fractions provided an indication of the selectivity of NF at pH 8. Threonine (4.44 %), leucine (18.07 %), lysine (13.0 %), and tyrosine (18.84 %) were present at a higher composition in the NF permeate at pH 8 than the UF permeate. The increase in composition of leucine, lysine, and tyrosine due to NF was observed by RPHPLC and NMR.

Table 8: Amino acid compositions of UF permeate (TS of 13.125 g L^{-1}) and NF permeate at pH 8 (TS of 0.161 g L^{-1}) for the control soy protein hydrolysate determined using NMR spectroscopy. Amino acid concentrations (Conc.; mmol L^{-1}), contents (mmol g^{-1}), and molar compositions (% content) are presented. Conditions for NMR: 1D-^{1}H NMR at 600 MHz pulse frequency.

Amino acid	UF Permeate			NF Permeate at pH 8		
	Conc. (mmol L^{-1})	Content (mmol g^{-1})	%	Conc. (mmol L^{-1})	Content (mmol g^{-1})	%
Alanine	0.285	0.022	3.66	0.031	0.193	5.71
Arginine	1.358	0.103	17.47	0.044	0.273	8.09
Asparagine	0.200	0.015	2.57	0.000	0.000	0.00
Glutamine	0.390	0.030	5.01	0.000	0.000	0.00
Isoleucine	0.433	0.033	5.57	0.033	0.206	6.10
Leucine	1.139	0.087	14.65	0.098	0.610	18.07
Lysine	0.483	0.037	6.21	0.071	0.439	13.00
Methionine	0.151	0.011	1.94	0.016	0.100	2.95
Phenylalanine	1.505	0.115	19.36	0.096	0.596	17.63
Threonine	0.135	0.010	1.74	0.024	0.150	4.44
Tryptophan	0.211	0.016	2.72	0.000	0.000	0.00
Tyrosine	1.094	0.083	14.07	0.102	0.637	18.84
Valine	0.392	0.030	5.05	0.028	0.175	5.18

5.3.3. Potential of reverse-phase HPLC and NMR for amino acid analysis of soy hydrolysate fractions

Alanine, glutamine, isoleucine, leucine, lysine, methionine, phenylalanine, tryptophan, tyrosine, and valine were quantified by both RPHPLC and ^{1}H-NMR techniques. Six amino acids, asparagine, cysteine, glycine, histidine, proline, and serine were identified and quantified by reverse-phase HLPC, but remained undetected by NMR. Similarly, NMR was able to detect and quantify arginine, aspartic acid, and threonine, which were not detected by RPHPLC in the UF and NF permeate samples.

These differences may be attributed to the fundamental differences in the detection, separation, and quantification of amino acids by these two techniques.

Figure 22 illustrates the differences in molar compositions of ten amino acids that were detected by both HPLC and NMR in the UF and NF permeate fractions.

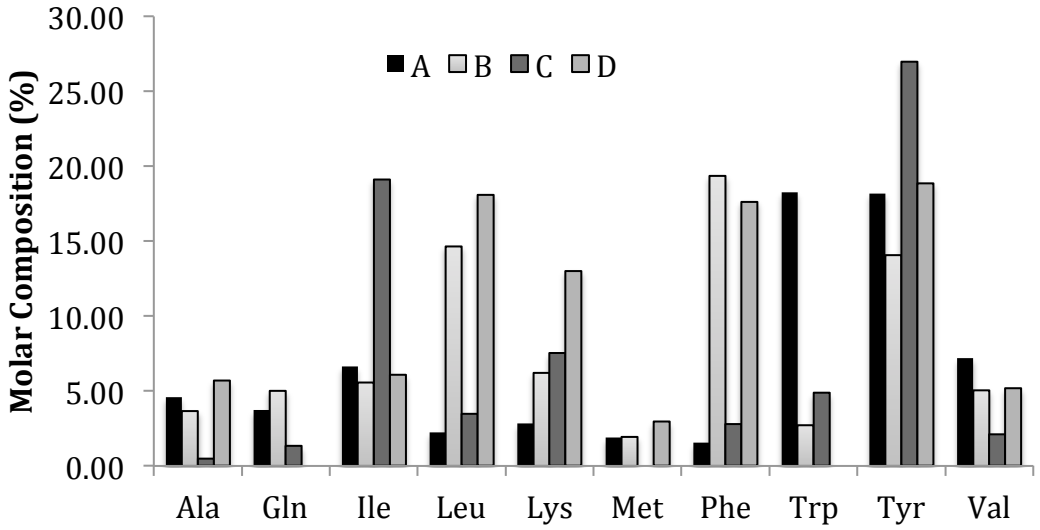

Figure 22: Molar compositions (% content) of amino acids quantified by reverse-phase HPLC and ^{1}H-NMR in the UF permeate fraction and NF permeate fraction at pH 8 for the control soy protein hydrolysate. A – HPLC results for UF permeate B – NMR results for UF permeate; C – HPLC results for NF permeate at pH 8; D – NMR results for NF permeate at pH 8. Conditions for HPLC: eluent A – 0.05 % (v/v) TEA in 50 mmol L^{-1} sodium acetate; eluent B – 60 % (v/v) acetonitrile in water; flow rate 1.0 mL min^{-1}; gradient B from 10-56 % in 20 min; UV absorbance at 254 nm. Conditions for NMR: 1D-^{1}H NMR at 600 MHz pulse frequency.

Relatively similar molar compositions were obtained for the UF permeate fraction by reverse phase HPLC and NMR for alanine (4.59 and 3.66 %, respectively), glutamine (3.74 and 5.01 %, respectively), isoleucine (6.64 and 5.57 %, respectively), methionine (1.88 and 1.94 %, respectively), tyrosine (18.19 and 14.07 %, respectively), and valine (7.20 and 5.05 %, respectively). This suggested that NMR represents an alternative analysis method to reverse phase HPLC for UF peptide fractions, which possessed higher peptide concentrations (1.52-3.65 mmol L^{-1}) than NF fractions (0.036-0.179 mmol L^{-1}). However, RPHPLC and NMR results were not in agreement for leucine and tryptophan, the cause of which was unknown.

In the NF permeate fraction at pH 8, only valine (2.10 and 5.18 %, respectively) was quantified similarly by RPHPLC and NMR. The reasons for the dissimilarities in the results from RPHPLC and NMR were unclear during this preliminary amino acid composition study.

5.3.4. Future work

Amino acid analysis of NF retentate fraction at pH 8 using RPHPLC and ^{1}H-NMR can provide estimates of the predominant amino acid residues that were rejected by the NF membrane. Similarly, the NF permeate and retentate fractions at pH 4 should be analyzed to identify the effects of pH during NF on amino acid composition of peptides. Finally, amino acid analysis of heat pre-treated SPH fractions from UF and NF should be analyzed and compared to the respective control SPH fractions to identify the key differences in peptide composition due to heat pre-treatment of SPI.

5.4. Conclusion

Amino acid analysis of UF and NF permeate fractions of control SPH by RPHPLC and NMR provided information on the amino acids profiles and its relationship to the high ORAC and FCR ACs of NF permeate fraction at pH 8. The amino acid compositions of the peptides that were purified by NF at pH 8 were also realized. Known contributors to ACs of peptides, tyrosine, proline, phenylalanine, histidine, tryptophan, and leucine were present in high contents in the NF permeate fraction at pH 8 compared to the NF feed, the UF permeate.

Through the preliminary amino acid analysis of the UF permeate fractions for control SPH, H-NMR spectroscopy represents a potential alternative to RPHPLC. However, for dilute samples with approximately 1 g L^{-1} of solids (i.e. NF peptide fractions), the use of NMR as an alternative method to RPHPLC for amino acid analysis may not be feasible.

6. Conclusions

In this study, sequential membrane UF and NF was investigated as a process alternative to fractionate and purify antioxidant peptides from SPH with superior antioxidant functionality; fluorescence spectroscopy in combination with PCA was also investigated for its potential to characterize the contributions of SPH to antioxidant capacity (AC). RPHPLC and ^{1}H NMR were assessed as tools to analyze the amino acid composition of antioxidant peptides.

An aqueous soy protein isolate (SPI) solution was subjected to heat treatment at 95 ^{o}C for 5 min prior to enzymatic hydrolysis. This heat pre-treatment (HT) increased the peptide concentration compared to the control SPI. However, no significant difference in peptide content was observed in the UF feed for control and pre-heated SPH.

SPH, after enzymatic hydrolysis and ultracentrifugation, was subjected to UF with a cross flow hollow fibre membrane module (10 kDa MWCO). Control SPH had significantly higher peptide content in the UF permeate than pre-heated SPH, and significantly lower peptide content in the UF retentate than pre-heated SPH ($p<0.01$). This may be attributed to structural modifications of peptides due to heat pre-treatment. The ACs of SPH fractions were determined using Oxygen Radical Absorbance Capacity (ORAC) and Folin Ciocalteau Reagent (FCR) assays. Control and pre-heated SPH UF permeate fractions (<10 kDa in MW) displayed higher ORAC ACs compared to corresponding feed and retentate fractions, while retentate fractions (> 10 kDa in MW) displayed lower ORAC ACs compared to the corresponding feed fractions. This suggests the importance of peptide molecular weight on AC.

The UF permeate fractions were diluted and subjected to NF with a cross flow flat sheet membrane (2.5 kDa MWCO) at pH 4 and pH 8 to further fractionate the SPH based on molecular weight and charge. The highest peptide content was observed in the NF permeate at pH 8 for control SPH (<2.5 kDa in MW, net negative charge). Co-ion membrane-peptide interactions (pH 8) yielded higher peptide contents and consequently displayed higher ACs relative to counter-ion interactions (pH 4) for control and pre-heated SPH. At pH 8, the NF permeate fractions for control SPH (5562

μmol TE g^{-1}) and pre-heated SPH (5187 μmol TE g^{-1}) displayed the highest ORAC ACs, and were therefore the most promising antioxidant SPH fractions collected.

Compared to SPI PROFAM 974 (the native soy protein isolate), sequential UF and NF at pH 8 steps have shown to increase the ORAC AC of peptides by thirteen-fold for both control and pre-heated SPH, which constitute significant improvements. Therefore, the potential for NF as a viable fractionation process for antioxidant peptides was demonstrated.

UF and NF samples (8 UF samples and 112 NF samples) were assessed for their ORAC and FCR ACs, and analyzed using fluorescence excitation-emission matrices (EEM). Weak linear correlations between observed FCR and observed ORAC values were identified for pre-heated SPH NF samples at pH 4 (R^2=0.63) and pH 8 (R^2=0.66). This was mainly due to fundamental differences between these two assays in measuring the AC.

PCA_{NF} of the fluorescence EEMs generated two significant PCs, which were identified to be tryptophan- (PC_1) and tyrosine- (PC_2) containing peptides. Using these two PCs, multiple linear regression models (MLRMs) were developed using NF permeate samples to estimate the $ORAC_{FPCA}$ and FCR_{FPCA} ACs and were independently validated with additional NF feed and retentate samples. Plots of FCR_{FPCA} vs. $ORAC_{FPCA}$ showed strong linear relationships for NF samples at pH 4 and 8 (R^2>0.99), indicating the similarities in relative combined contributions of tryptophan and tyrosine to ORAC and FCR ACs. A weak linear relationship was observed between the FCR_{FPCA} and $ORAC_{FPCA}$ values for the UF samples from PCA_{UF}. A strong linear relationship was observed between the NF samples where 16 independent NF samples followed the same trend as the 96 NF samples. This behavior can be viewed as a filtering effect from the experimentally measured ORAC and FCR values and expressed with the $ORAC_{FPCA}$ and FCR_{FPCA} ACs of peptides. The filtering achieved by PCA of the fluorescence signals could be caused by characteristics of the peptide samples that were not detected by fluorescence analysis and/or PCA, but were detected by experimental ORAC and FCR assays. Since these two antioxidant assays are used in combination, the proposed approach could be used to assess the commonalities that are relevant to ACs from ORAC and FCR measurements.

Preliminary amino acid analysis using RPHPLC and ^{1}H-NMR spectroscopy was conducted for control SPH NF permeate at pH 8 (the fraction with the highest ORAC AC; 5562 μmol TE g^{-1}) and UF permeate fractions. This analysis reveals that the amino acid content of known contributors to antioxidative functionalities of peptides (i.e. leucine, phenylalanine, tyrosine, and valine) has increased significantly for the NF permeate at pH 8 compared to the UF permeate (NF feed). These changes due to NF at pH 8 were reflected in the ORAC AC of permeate fractions from UF and NF at pH 8.

Based on the findings presented in this study, future work should include:

1. Peptide characterization using RPHPLC-mass spectrometry to determine the peptide sequences of highly antioxidant peptides. This will allow for identification of the differences between pre-heated and control SPH fractions.
2. Examination of the efficacy of prominent antioxidant peptide fractions using *in vivo* antioxidant studies, and in food systems.
3. Implementation of further UF experiments to test the fluorescence-PCA protocol to examine the relationship between FCR and ORAC assays.
4. Validation of the fluorescence-PCA protocol for other types of protein hydrolysates and other types of antioxidants.

7. References

[1] R. Marcuse. Antioxidative effect of amino-acids. Letters to Nature, 886.

[2] H. Chen, K. Muramoto, F. Yamauchi, K. Fujimoto, and K. Nokihara. Antioxidative properties of histidine-containing peptides designed from peptide fragments found in the digests of a soybean protein. Journal of Agriculture and Food Chemistry, 46 (1998) 49.

[3] H.M. Chen, K. Muramoto, and F. Yamauchi. Structural-analysis of antioxidative peptides from soybean beta-onglycinin. Journal of Agriculture and Food Chemistry, 43 (1995) 574.

[4] H.M. Chen, K. Muramoto, F. Yamauchi, and K. Nokihara. Antioxidant activity of designed peptides based on the antioxidative peptide isolated from digests of a soybean protein. Journal of Agriculture and Food Chemistry, 44 (1996) 2619.

[5] B.F. Gibbs, A. Zougman, R. Masse, and C. Mulligan. Production and characterization of bioactive peptides from soy hydrolysate and soy-fermented food. Food Research International, 37 (2004) 123.

[6] R. Apak, K. Güçlü, B. Demirata, M. Özyürek, S.E. Çelik, B. Bektasoglu. Comparative evaluation of various total antioxidant capacity assays applied to phenolic compounds with the CUPRAC assay. Molecules, 12 (2007) 1496.

[7] D. Huang, B. Ou, and R. Prior. The chemistry behind antioxidant capacity assays RID A-7439-2010. Journal of Agriculture and Food Chemistry, 53 (2005) 1841.

[8] A. Moure, H. Dominguez, and J.C. Parajo. Antioxidant properties of ultrafiltration-recovered soy protein fractions from industrial effluents and their hydrolysates. Process Biochemistry, 41 (2006) 447.

[9] S.Y. Park, J. Lee, H. Baek, and H.G. Lee. Purification and characterization of antioxidant peptides from soy protein hydrolysate. Journal of Food Biochemistry, 34 (2010) 120.

[10] I. Malcolm Pirnie, I. Separation Processes, and I. The Cadmus Group, Membrane filtration guidance manual, Uniited States Environmental Protection Agency, Cincinnati, Ohio, USA 2005.

[11] R.H. Peiris, C. Halle, H. Budman, C. Moresoli, S. Peldszus, P.M. Huck. Identifying fouling events in a membrane-based drinking water treatment process using principal component analysis of fluorescence excitation-emission matrices. Water Research, 44 (2010) 185.

[12] Y. Pouliot, M.C. Wijers, S.F. Gauthier, and L. Nadeau. Fractionation of whey protein hydrolysates using charged UF/NF membranes. Journal of Membrane Science, 158 (1998) 105.

[13] Y. Pouliot, S.F. Gauthier, and J. L'Heureux. Effect of peptide distribution on the fractionation of whey protein hydrolysates by nanofiltration membranes. Lait, 80 (2000) 113.

[14] S. Butylina, S. Luque, and M. Nystrom. Fractionation of whey-derived peptides using a combination of ultrafiltration and nanofiltration. Journal of Membrane Science, 280 (2006) 418.

[15] J.M.K. Timmer, M.P.J. Speelmans, and H.C. van der Horst. Separation of amino acids by nanofiltration and ultrafiltration membranes. Separation and Purification Technology, 14 (1998) 133.

[16] A. Moure, H. Dominguez, and J.C. Parajo. Fractionation and enzymatic hydrolysis of soluble protein present in waste liquors from soy processing. Journal of Agriculture and Food Chemistry, 53 (2005) 7600.

[17] North Caroline Soybean Producers Association, Inc., History of soybeans, 2012 (2011) 1.

[18] E. Dorff, The soybean, agriculture's jack-of-all-trades, is gaining ground across Canada, Statistics Canada, Ottawa, Ontario, Canada, 96-325-XIE-2007000, 2007 2009.

[19] K. Liu, Soybeans: Chemistry, technology and utilization, Gaithersburg, Maryland, USA, Aspen Publisher, Inc., 1999.

[20] E.W. Lusas, M.N. Riaz. Soy protein products: Processing and Use. Journal of Nutrition, 125 (1995) 573.

[21] M. Garcia, M. Torre, M. Marina, and F. Laborda. Composition and characterization of soyabean and related products. Critical Reviews in Food Science and Nutrition, 37 (1997) 361.

[22] J. Skorepova, Effect of electroacidification on ultrafiltration performance and physicochemical properties of soy protein extracts, University of Waterloo, Waterloo, Ontario, Canada 2007.

[23] V.R. Young, P.L. Pellett. Protein evaluation, amino acid scoring and the food and drug administration's proposed food labeling regulations. J. Nutr., 121 (1991) 145.

[24] K.S. Montgomery. Soy protein. Journal of Perinatal Education, 12 (2003) 42.

[25] D.P. Jaramillo, R.F. Roberts, and J.N. Coupland. Effect of pH on the properties of soy protein-pectin complexes. Food Research International, 44 (2011) 911.

[26] Z.S. Liua, S.K.C. Changa, T.L. Li, and E. Tatsumic. Effect of selective thermal denaturation of soybean proteins on soymilk viscosity and tofu's physical properties. Food Research International, 37: 8 (2004) 815.

[27] G. Walsh, Proteins-biochemistry and biotechnology, New York, USA, John Wiley & Sons, 2002.

[28] D.D. Miller, Food chemistry-a laboratory manual, New York, John Wiley & Sons, Ltd., 1998.

[29] G.C. Barrett, D.T. Elmore, Amino acids and peptides, Cambridge, UK, Cambridge University Press, 1998.

[30] J. Maldonado-Valderrama, A.P. Gunning, P.J. Wildea, and V.J. Morrisa. In vitro gastric digestion of interfacial protein structures: visualisation by AFM. Soft Matter, 6 (2010) 4908.

[31] D.W. Hill, F.H. Walters, T.D. Wilson, and J.D. Stewart. High performance liquid chromatographic determination of amino acids in the picomole range. Analytical Chemistry, 51 (1979) 1338.

[32] B. Ou, M. Hampsch-Woodill, and R.L. Prior. Development and validation of an improved oxygen radical absorbance capacity assay using fluorescein as the fluorescent probe. Journal of Agricultural and Food Chemistry, 49 (2001) 4619.

[33] R. Stevanato, S. Fabris, and F. Momo. New enzymatic method for the determination of total phenolic content in tea and wine. Journal of Agricultural and Food Chemistry, 52 (2004) 6287.

[34] H. Korhonen, A. Pihlanto. Bioactive peptides: production and functionality. International Dairy Journal, 16 (2006) 945.

[35] W. Chiang, C. Shih, and Y. Chu. Functional properties of soy protein hydrolysate produced from a continuous membrane reactor system. Food Chemistry, 65 (1999) 189.

[36] E. Monogioudi, G. Faccio, M. Lille, K. Poutanen, J. Buchert, and M. Mattinen. Effect of enzymatic cross-linking of b-casein on proteolysis by pepsin. Food Hydrocolloids, 25 (2010) 71.

[37] P.A. Frey, A.D. Hegeman, Enzymatic reaction mechanisms, New York, NY, Oxford University Press, 2007.

[38] N.J. Adamson, E.C. Reynolds. Characterization of casein phosphopeptides prepared using alcalase: Determination of enzyme specificity. Enzyme and Microbial Technology, 19 (1996) 202.

[39] S. Benjakul, W. Binsan, W. Visessanguan, K. Osako, and M. Tanaka. Effects of flavourzyme on yield and some biological activities of mungoong, an extract paste from the cephalothorax of white shrimp. Journal of Food Science, 74 (2009) 73.

[40] D.A. Clare, H.E. Swaisgood. Bioactive milk peptides: A prospectus. Journal of Dairy Science, 83 (2000) 1187.

[41] R. Hartmann, H. Meisel. Food-derived peptides with biological activity: from research to food applications. Current Opinion in Biotechnology, 18 (2007) 163.

[42] S. Maruyama, H. Mitachi, J. Awaya, M. Kurono, N. Tonizuka, and H. Suzuki. Angiotensin I-converting enzyme inhibitory activity of the C-terminal hexapeptide of αS1-casein. Agricultural and Biological Chemistry, 51 (1987) 2557.

[43] A.J. Kastin, Handbook of biologically active peptides, Burlington, MA, USA, Elsevier, 2006.

[44] S.F. Gauthier, Y. Pouliot, and D. Saint-Sauveur. Immunomudolatory peptides obtained by the enzymatic hydrolysis of whey proteins. International Dairy Journal, 16 (2006) 1315.

[45] M. Papagianni. Ribosomally synthesized peptides with antimicrobial properties: biosynthesis, structure, function, and applications. Biotechnology Advances, 21 (2003) 465.

[46] L.R. Snyder, J.J. Kirkland, and J.W. Dolan, Reverse phase chromatography, in anonymous, introduction to modern liquid chromatography, Third Edition, New Jersey, USA, John Wiley & Sons, Inc., 2010, pp. 20-357.

[47] T. Imoto, H.1. Yamada. Peptide separation by reversed-phase high performance liquid chromatography. Molecular and Cellular Biochemistry, 51 (1983) 111.

[48] J.C. Lindon, J.K. Nicholson, and J.R. Everett. NMR spectroscopy of biofluids. Annual Reports on NMR Spectroscopy, 38 (1999) 1.

[49] S. Margolis, B. Coxon. Amino-acid-analysis of angiotensin-i by proton nuclear magnetic-resonance spectroscopy. Analytical Biochemistry, 141 (1984) 355.

[50] E. Kellenbach, K. Sanders, and P.L.A. Overbeeke, The use of proton NMR as an alternative for the amino acid analysis as identity test for peptides, in U. Holzgrabe, I. Wawer and B. Diehl (Ed.), NMR spectroscopy in pharmaceutical analysis, Amsterdam, The Netherlands, Elsevier, 2008, pp. 429-430.

[51] N. Aranibar, M. Borys, N.A. Mackin, V. Ly, N. Abu-Absi, and S. Abu-Absi. NMR-based metabolomics of mammalian cell and tissue cultures. Journal of Biomolecular NMR, 49 (2011) 195.

[52] B. Diehl, U. Holzgrabe, and I. Wawer, NMR spectroscopy in pharmaceutical analysis, Amsterdam, The Netherlands, Elsevier, 2008.

[53] B. Halliwell, M.A. Murcia, S. Chirico, and O.I. Aruoma. Free radicals and antioxidants in food and in vivo: what they do and how they work. Critical Reviews in Food Science and Nutrition, 35 (1995) 7.

[54] A. Karadag, B. Ozcelik, and S. Saner. Review of methods to determine antioxidant capacities. Food Analytical Methods, 2 (2009) 41.

[55] D. Wang, L. Wang, F. Zhu, J. Zhu, X.D. Chen, and L. Zou. In vitro and in vivo studies on the antioxidant activities of the aqueous extracts of Douchi (a traditional Chinese salt-fermented soybean food). Journal of Food Chemistry, 107 (2007) 1421.

[56] V.R. Preedy, Beer in health and disease prevention, London, UK, Academic Press, 2008.

[57] G. Cao, R. Prior. Comparison of different analytical methods for assessing total antioxidant capacity of human serum. Clinical Chemistry, 44 (1998) 1309.

[58] G. Hori, M.F. Wang, Y.C. Chan, T. Komatsu, Y.C. Wong, and T.H. Chen. Soy protein hydrolyzate with bound phospholipids reduces serum cholesterol levels in hypercholesterolemic adult male volunteers. Bioscience, Biotechnology, and Biochemistry, 65 (2001) 72.

[59] C. Nimalaratne, D. Lopes-Lutz, A. Schieber, and J. Wu. Free aromatic amino acids in egg yolk show antioxidant properties. Food Chemistry, 129 (2011) 155.

[60] T. Thorsen, Fundamental studies on membrane filtration of coloured surface water, (1999).

[61] J.M.K. Trimmer, Properties of nanofiltration membranes; model development and industrial applications, Technische Universiteit Eindhoven, Eindhoven, Netherlands 2001.

[62] T. Tsuru, T. Shutou, S. Nakao, and S. Kimura. Peptide and Amino-Acid Separation with Nanofiltration Membranes. Separation Science and Technology, 29 (1994) 971.

[63] S. Bissegger, Development of a supplement for CHO cell culture serum-free media by the fractionation of peptide mixtures using nanofiltration, (2009).

[64] L. Meissner, Production, purification, and quantification of antioxidant peptides. Department of Chemical Engineering, University of Waterloo 2010.

[65] J. Christensen, L. Nørgaard, R. Bro, and S.B. Engelsen. Multivariate autofluorescence of intact food systems. Chemical Reviews, 106 (2006) 1979.

[66] Q. Zhang, M.G. Muller, J. Wu, and M.S. Feld. Turbidity-free fluorescence spectroscopy of biological tissue. Optics Letters, 25 (2000) 1451.

[67] E. Dufour, A. Riaublanc. Potentiality of spectroscopic methods for the characterisation of dairy products. I. Front-face fluorescence study of raw, heated and homogenised milks. Lait, 77 (1997) 657.

[68] I.U. Bron, R.V. Ribeiro, M. Azzolini, A.P. Jacomino, and E.C. Machado. Chlorophyll fluorescence as a tool to evaluate the ripening of 'Golden' papaya fruit. Postharvest Biology and Technology, 33 (2004) 163.

[69] R.H. Peiris, H. Budman, C. Moresoli, and R.L. Legge. Acquiring reproducible fluorescence spectra of dissolved organic matter at very low concentrations. Water Science and Technology, 60 (2009) 1385.

[70] L. Eriksson, E. Johansson, N. Kettaneh-Wold, and S. Wold, Multi- and megavariate data analysis, principles and applications, Umea, Sweden, Umetrics Academy, 2001.

[71] R.H. Peiris, H. Budman, C. Moresoli, and R.L. Legge. Understanding fouling behaviour of ultrafiltration membrane processes and natural water using principal component analysis of fluorescence excitation-emission matrices. Journal of Membrane Science, 357 (2010) 62.

[72] L. Zhang, J. Li, and K. Zhou. Chelating and radical scavenging activities of soy protein hydrolysates prepared from microbial proteases and their effect on meat lipid peroxidation. Bioresource Technology, 101 (2010) 2084.

[73] E.A. Pena-Ramos, Y.L. Xiong. Antioxidant activity of soy protein hydrolysates in a liposomal system. Journal of Food Science, 67 (2002) 2952.

[74] R.M. Vilela, L.C. Lands, H.M. Chan, B. Azadi, and S. Kubow. High hydrostatic pressure enhances whey protein digestibility to generate whey peptides that improve glutathione status in CFTR-deficient lung epithelial cells. Molecular Nutrition and Food Research, 50(11) (2006) 1013.

[75] Y. Ma, T. Wang. Deactivation of soybean agglutinin by enzymatic and other physical treatments. Journal of Agriculture and Food Chemistry, 58 (2010) 11413.

[76] F.C. Church, D.H. Porter, G.L. Catignani, and H.E. Swaisgood. An o-phthalaldehyde spectrophotometric assay for proteinases. Analytical Biochemistry, 146 (1985) 343.

[77] C. Ubeda, C. Hidalgo, M.J. Torija, A. Mas, A.M. Troncoso, and M.L. Morales. Evaluation of antioxidant activity and total phenols index in persimmon vinegars produced by different processes. LWT-Food Science and Technology, 44 (2011) 1591.

[78] D. Zielinska, D. Szawara-Nowak, and H. Zielinski. Comparison of spectrophotometric and electrochemical methods for the evaluation of the antioxidant capacity of buckwheat products after hydrothermal treatment. Journal of Agriculture and Food Chemistry, 55 (2007) 6124.

[79] A. Achouri, Z. Wang, and S.Y. Xu. Enzymatic hydrolysis of soy protein isolate and effect of succinylation on the functional properties of resulting protein hydrolysates. Food Research International, 31 (1998) 617.

[80] J. Jiang, Y.L. Xiong, and J. Chen. pH shifting alters solubility characteristics and thermal stability of soy protein isolate and Its globulin fractions in different pH, salt concentration, and temperature conditions. Journal of Agriculture and Food Chemistry, 58 (2010) 8035.

[81] D.B. Haytowitz, S. Bhagwat, USDA database for the oxygen radical absorbance capacity (ORAC) of selected foods, Release 2, 2011 (2010) 48.

[82] R.G. Steel, J.H. Torrie, Principles and procedures of statistics: a biometrical approach, New York, USA, McGraw-Hill, 1980.

[83] A. Baker. Fluorescence properties of some farm wastes: implications for water quality monitoring Water Research, 36 (2002) 189.

[84] T. Persson, M. Wedborg. Multivariate evaluation of the fluorescence of aquatic organic matter. Analytical Chimica Acta, 434 (2001) 179.

[85] E.N. Frankel, A.S. Meyer. The problems of using one-dimensional methods to evaluate multifunctional food and biological antioxidants. Journal of the Science of Food and Agriculture, 80 (2000) 1925.

[86] B. Bidlingmeyer, S. Cohen, and T. Tarvin. Rapid analysis of amino-acids using pre-column derivatization. Journal of Chromatography, 336 (1984) 93.

[87] R. Heinrikson, S. Meredith. Amino-acid-analysis by reverse-phase high-performance liquid-chromatography-precolumn derivatization with phenylisothiocyanate. Analytical Biochemistry, 136 (1984) 65.

[88] A.M. Weljie, J. Newton, P. Mercier, E. Carlson, and C.M. Slupsky. Targeted profiling: quantitative analysis of 1H NMR metabolics data. Analytical Chemistry, 78 (2006) 4430.

8. Appendix

8.1. Peptide Concentrations of UF and NF Samples

All UF and NF fractions collected were assessed for peptide concentration (as equivalent phenyl-glycine concentrations by the OPA assay.

Table 9: Peptide concentrations estimated by OPA as equivalent phenyl-glycine (Phe-Gly) concentrations (mmol L^{-1}) of UF and NF retentate and permeate fractions from control and pre-heated soy protein hydrolysate (expressed as mean with error bars representing standard deviations; n=3). The peptide concentrations of control and pre-heated SPH UF feeds were 3.649 ± 0.030 and 3.634 ± 0.013 mmol L^{-1}, respectively. OPA conditions: 0 – 1.0 mM Phe-Gly, absorbance at 340 nm.

Sample	Treatment	Sampling Time	Equivalent Phe-Gly Concentration (mmol L^{-1})	
			Retentate	Permeate
Control SPH	UF	End of filtration	2.694 ± 0.055	1.836 ± 0.025
	NF (pH 4)		0.162 ± 0.003	0.121 ± 0.004
	NF (pH 8)		0.179 ± 0.005	0.087 ± 0.006
Pre-heated SPH	UF	End of filtration	3.790 ± 0.018	1.524 ± 0.074
	NF (pH 4)		0.138 ± 0.006	0.044 ± 0.006
	NF (pH 8)		0.148 ± 0.006	0.036 ± 0.006
	NF (pH 4)	300 s	0.148 ± 0.008	0.104 ± 0.002
		600 s	0.198 ± 0.021	0.172 ± 0.018
		900 s	0.158 ± 0.002	0.190 ± 0.038
		1200 s	0.162 ± 0.005	0.148 ± 0.027
		3600 s	0.166 ± 0.016	0.153 ± 0.007
		6600 s	0.175 ± 0.003	0.138 ± 0.010
	NF (pH 8)	300 s	0.184 ± 0.007	0.050 ± 0.001
		600 s	0.208 ± 0.010	0.064 ± 0.023
		900 s	0.200 ± 0.002	0.071 ± 0.000
		1200 s	0.200 ± 0.006	0.082 ± 0.007
		3600 s	0.234 ± 0.004	0.026 ± 0.087
		7200 s	0.295 ± 0.033	0.101 ± 0.005

8.2. Total Material Balances for UF and NF Experiments

The following tables (Table 10, Table 11, Table 12, Table 15) provide total solids and total peptide balances during UF and NF for control and pre-heated SPH.

Table 10: Total solids content (TS) balance for control soy protein hydrolysate

Sample	TS (g L^{-1})	Volume (L)	Mass of TS (g)	% TS Loss
Digest	28.00	2.00	56.00	
UF Feed	24.69	2.00	49.38	
UC Solids Removed			6.62	11.82
UF Permeate	17.66	1.00	17.66	
UF Retentate	26.14	1.00	26.14	
UF Solids loss			5.58	11.30
NF Feed	1.00	2.00	2.00	
NF pH 4 P1	0.53	1.00	0.53	
NF pH 4 R1	1.48	1.00	1.48	
pH 4 NF 1 Solids loss			0.00	0.00
NF pH 4 P2	0.55	1.00	0.55	
NF pH 4 R2	1.25	1.00	1.25	
pH 4 NF 2 Solids loss			0.20	10.00
NF pH 8 P1	0.10	1.00	0.10	
NF pH 8 R1	1.35	1.00	1.35	
pH 8 NF 1 Solids loss			0.55	27.50
NF pH 8 P2	0.28	1.00	0.28	
NF pH 8 R2	1.13	1.00	1.13	
pH 8 NF 2 Solids loss			0.60	30.00

Table 11: Total solids content (TS) balance for pre-heat treated soy protein hydrolysate

Sample	TS (g L^{-1})	Volume (L)	Mass of TS (g)	% TS Loss
Digest	30.15	2.00	60.30	
UF Feed	27.66	2.00	55.32	
UC Solids Removed			4.98	8.26
UF Permeate	20.15	1.00	20.15	
UF Retentate	30.43	1.00	30.43	
UF Solids loss			4.74	8.57
NF Feed	1.00	2.00	2.00	
NF pH 4 P1	0.30	1.00	0.30	
NF pH 4 R1	1.23	1.00	1.23	
pH 4 NF 1 Solids loss			0.48	23.75
NF pH 4 P2	0.40	1.00	0.40	
NF pH 4 R2	1.13	1.00	1.13	
pH 4 NF 2 Solids loss			0.48	23.75
NF pH 8 P1	0.15	1.00	0.15	22.50

NF pH 8 R1	1.40	1.00	1.40	
pH 8 NF 1 Solids loss			0.45	
NF pH 8 P2	0.28	1.00	0.28	
NF pH 8 R2	1.28	1.00	1.28	
pH 8 NF 2 Solids loss			0.45	22.50

Table 12: Comparison of total solids loss of control and pre-heated soy protein hydrolysates

Process	% TS Loss	
	Control SPH	Pre-heated SPH
Ultracentrifugation	11.82	8.26
Ultrafiltration	11.30	8.57
Nanofiltration pH 4	5.00 ± 7.1	23.75 ± 0
Nanofiltration pH 8	28.75 ± 1.8	22.50 ± 0

Table 13: Total peptide content balance for control soy protein hydrolysate

Sample	Peptide content (µmol)	% Loss
Digest	$3.50x10^{-2}$	3.11
UF Feed	$3.39x10^{-2}$	
UC Solids Removed	$1.09x10^{-3}$	
UF Permeate	$2.24x10^{-2}$	-35.24
UF Retentate	$2.34x10^{-2}$	
UF Solids loss	$-1.20x10^{-2}$	
NF Feed	$1.27x10^{-4}$	-137.32
NF pH 4 P1	$1.21x10^{-4}$	
NF pH 4 R1	$1.80x10^{-4}$	
pH 4 NF 1 Solids loss	$-1.74x10^{-4}$	
NF pH 4 P2	$1.21x10^{-4}$	-108.56
NF pH 4 R2	$1.43x10^{-4}$	
pH 4 NF 2 Solids loss	$-1.38x10^{-4}$	
NF pH 8 P1	$6.80x10^{-5}$	-115.15
NF pH 8 R1	$2.05x10^{-4}$	
pH 8 NF 1 Solids loss	$-1.46x10^{-4}$	
NF pH 8 P2	$1.06x10^{-4}$	-103.71
NF pH 8 R2	$1.53x10^{-4}$	
pH 8 NF 2 Solids loss	$-1.32x10^{-4}$	

Table 14: Total peptide content balance for pre-heated soy protein hydrolysate

Sample	Peptide content (µmol)	% Loss
Digest	$3.67x10^{-2}$	1.03
UF Feed	$3.63x10^{-2}$	
UC Solids Removed	$3.78x10^{-4}$	
UF Permeate	$1.52x10^{-2}$	-46.23
UF Retentate	$3.79x10^{-2}$	
UF Solids loss	$-1.68x10^{-2}$	
NF Feed	$7.54x10^{-5}$	-175.98
NF pH 4 P1	$5.16x10^{-5}$	
NF pH 4 R1	$1.57x10^{-4}$	
pH 4 NF 1 Solids loss	$-1.33x10^{-4}$	
NF pH 4 P2	$3.61x10^{-5}$	-106.69
NF pH 4 R2	$1.20x10^{-4}$	
pH 4 NF 2 Solids loss	$-8.05x10^{-5}$	
NF pH 8 P1	$2.72x10^{-5}$	-94.15
NF pH 8 R1	$1.19x10^{-4}$	
pH 8 NF 1 Solids loss	$-7.10x10^{-5}$	
NF pH 8 P2	$4.51x10^{-5}$	-195.12
NF pH 8 R2	$1.78x10^{-4}$	
pH 8 NF 2 Solids loss	$-1.47x10^{-4}$	

Table 15: Comparison of total peptide content of control and pre-heat treated soy protein hydrolysates.

Process	% Loss of Total Peptides	
	Control SPH	Pre-heated SPH
Ultracentrifugation	3.11	1.03
Ultrafiltration	32.38	26.89
Nanofiltration pH 4	-10.89 ± 10.1	-20.45 ± 24.5
Nanofiltration pH 8	-4.16 ± 4.0	-22.10 ± 35.6

8.3. Permeate Flux Analysis

Mass of permeate collected over the course of each filtration process was recorded. From these data, permeate flux analyses were conducted. Instantaneous permeate mass flux as a function of time were calculated. A ratio of permeate mass flux at time *t* to flux at the beginning of the filtration is determined, known as the normalized flux. A plot of normalized flux as a function of time during a filtration can provide information on membrane fouling, and can be used for filtration diagnostics. Plots of normalized flux as a function of time during the UF (Figure 23) and NF (Figure 24 and Figure 25) are provided for control and pre-heated SPH. Table 16 provides additional information on UF and NF experiments that were performed.

Table 16: Water flux (WF) and permeate flux (PF) analyses for UF and NF experiments. Initial and final measurements are expressed with subscripts of i and f, respectively. Conditions for UF: TMP of 62kPa, volumetric flow rate of 2.4 L min^{-1}, and 22 ^{o}C. Conditions for NF: TMP of 2 MPa, volumetric flow rate of 1.8 L min^{-1}, and 22 ^{o}C. R_m refers to membrane resistance (estimated by WF before filtration), and R_f refers to fouling resistance ($R_{total,\ f} - R_{total,\ i}$). Units:WF (kg m^{-2} s^{-1} Pa^{-1}), PF (m^{-2} s^{-1}), and R_m and R_f (m^{-1}).

Filtration of SPH		pH	WF_i	WF_f	PF_i	PF_f	R_m	R_m+R_f	R_f
UF	Control	7.8	14.83	13.59	0.37	0.30	$4.68x10^{12}$	$5.11x10^{12}$	$4.29x10^{11}$
			13.59	13.35	0.41	0.38	$5.11x10^{12}$	$5.20x10^{12}$	$9.10x10^{10}$
	Heat		15.38	10.92	0.45	0.39	$4.52x10^{12}$	$6.36x10^{12}$	$1.85x10^{12}$
			15.14	12.16	0.62	0.56	$4.59x10^{12}$	$5.71x10^{12}$	$1.13x10^{12}$
NF	Control	4	11.64	6.00	0.62	0.53	$2.09x10^{14}$	$4.38x10^{14}$	$2.29x10^{14}$
			4.59	3.69	1.22	1.01	$6.34x10^{14}$	$7.70x10^{14}$	$1.37x10^{14}$
		8	8.87	5.75	0.85	0.73	$2.63x10^{14}$	$4.66x10^{14}$	$2.03x10^{14}$
			12.03	6.33	1.09	0.81	$2.78x10^{14}$	$4.08x10^{14}$	$1.30x10^{14}$
	Heat	4	5.95	3.83	0.83	0.65	$4.71x10^{14}$	$6.64x10^{14}$	$1.93x10^{14}$
			6.52	3.65	0.86	0.59	$4.23x10^{14}$	$7.23x10^{14}$	$3.00x10^{14}$
		8	4.79	3.37	1.10	0.85	$5.65x10^{14}$	$8.15x10^{14}$	$2.51x10^{14}$
			11.41	9.17	0.95	0.85	$2.56x10^{14}$	$2.67x10^{14}$	$1.19x10^{13}$

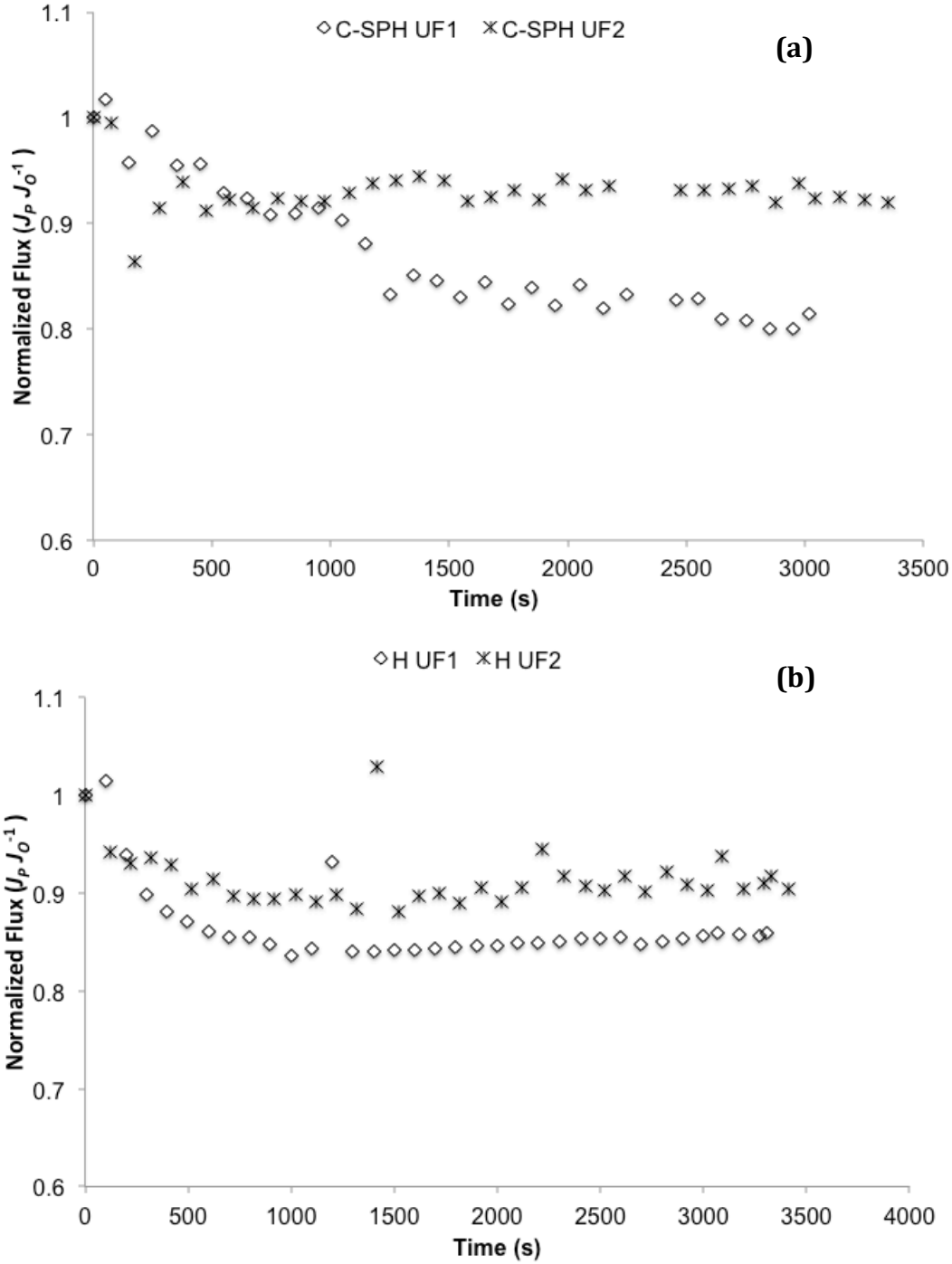

Figure 23: Normalized flux as a function of time in (a) UF of control, and (b) pre-heated soy protein hydrolysate. Conditions for UF: TMP of 62kPa, volumetric flow rate of 2.4 L min^{-1}, and 22 ^{o}C.

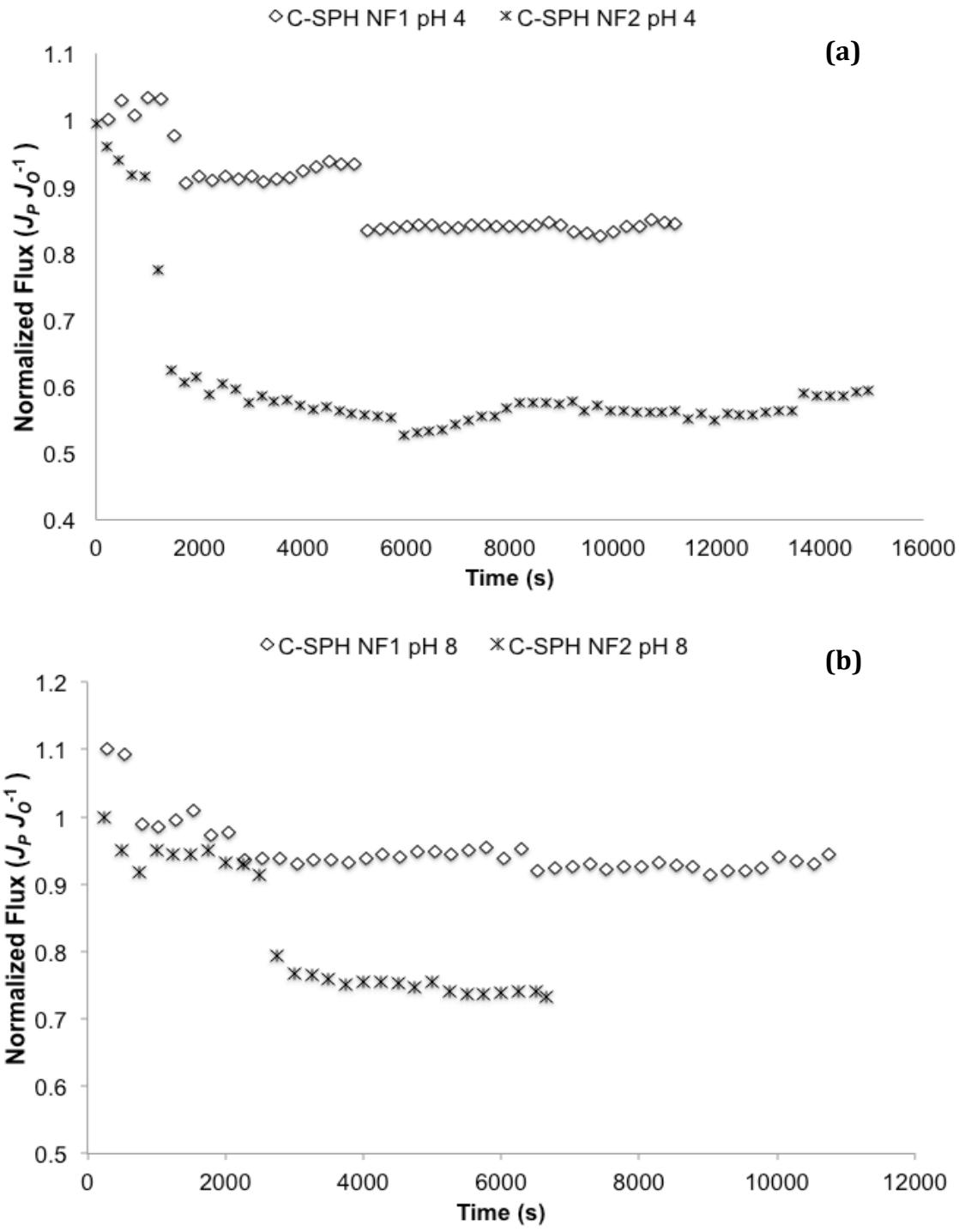

Figure 24: Normalized flux as a function of time during NF for control soy protein hydrolysate at (a) pH 4 and (b) pH 8. Conditions for NF: TMP of 2 MPa, volumetric flow rate of 1.8 L min^{-1}, and 22 ^{o}C.

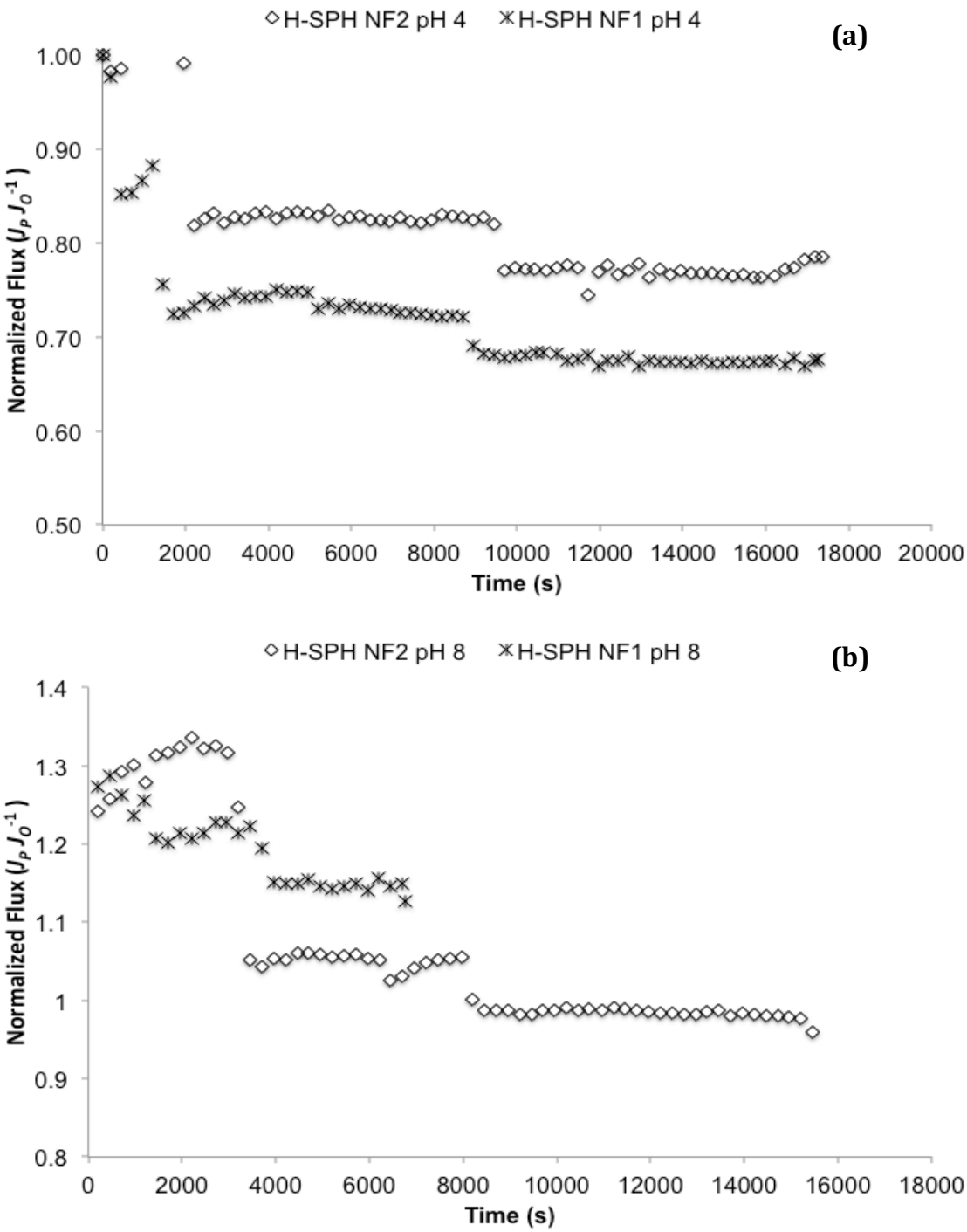

Figure 25: Normalized flux as a function of time during NF for pre-heated soy protein hydrolysate at (a) pH 4 and (b) pH 8. Conditions for NF: TMP of 2 MPa, volumetric flow rate of 1.8 L min^{-1}, and 22 ^{o}C.

8.3.1. Sample Calculations:

8.3.1.1. Normalized flux estimation:

Normalized flux for NF 2 at pH 4 for control SPH was determined between 260 s and 262 s. The following steps were taken.

From the data collected during NF (mass of permeate as a function of time), instantaneous mass flux can be determined at a given time interval by equation 11, where M represents mass (g), t time (s), and A area of the membrane (0.014 m^2).

$$J_P = \frac{d(M)}{dt} \times \frac{1}{A} = \frac{(M_2 - M_1)}{(t_2 - t_1)(A)} \qquad (11)$$

The initial permeate mass flux (J_0) was determined as the average instantaneous permeate mass fluxes during the first two minutes of filtration, and was found to be 2.44 g m^{-2} s^{-1}.

At t_1=260 s, M_1=9.37 g; at t_2=262 s, M_2=9.43 g. Therefore:

$$J_P = \left(\frac{9.43\ \text{g} - 9.37\ \text{g}}{262\ \text{s} - 260\ \text{s}}\right) \times \left(\frac{1}{0.014\ \text{m}^2}\right) = 2.14\ \text{g m}^{-2}\ \text{s}^{-1}$$

Normalized flux at this time interval can then be estimated by:

$$\frac{J_P}{J_0} = \frac{2.14\ \text{g m}^{-2}\ \text{s}^{-1}}{2.44\ \text{g m}^{-2}\ \text{s}^{-1}} = 0.88$$

8.3.1.2. Total resistance (R_{tot}) estimation:

WF measurements were obtained by determining in triplicates the time taken to collect 10 g of permeate, at five TMPs. Equation 12 was obtained by plotting WF as a function of TMP. The change in WF as a function of TMP was 5.37 x 10^{-9} kg m^{-2} s^{-1} Pa^{-1} prior to NF 2 at pH4 for control SPH. Before a filtration, R_{tot} is determined as R_m using WF measurements, using equation 13. After a filtration, R_{tot} is determined as the sum of R_m and R_f, again using WF measurements.

$$\text{WF} = \left((5.37\times10^{-9})(\text{TMP}) + (9.05\times10^{-4})\right)\times1000 \qquad (12)$$

$$R_{tot} = \left(\frac{\rho_{Water}}{\eta_{Water}}\right) \times \left(\frac{\Delta\ \text{TMP}}{\Delta\ Permeate\ Flux}\right) \qquad (13)$$

The density (ρ) and viscosity (η) of water at 25 °C is 997.13 kg m^{-3} and 8.91 x 10^{-4} Pa s, respectively. Therefore, the R_{tot} (R_m) prior to NF at pH 4 for control SPH was found to be:

$$R_{tot} = \left(\frac{1\times10^{-3}}{998.29}\right) \times (5.37\times10^{-9}) = 2.07\times10^{14}\ \mathrm{m}^{-1}$$

For the UF experiments, the relative ratio of the membrane resistance due to fouling (R_f) measured at the end of the filtration to the clean membrane resistance (R_m) are expressed as a percentage, and increased by approximately 5 % for control SPH and 33 % for pre-heated SPH. Similarly, during NF total membrane resistance due to fouling (ratio of R_f to R_m expressed as a percentage, as per UF experiments) increased by 66 % at pH 4 compared to 62 % at pH 8 for control SPH; and by 56 % at pH 4 as opposed to 25 % at pH 8 for pre-heated SPH.

8.4. Fluorescence analysis and PCA

8.4.1. Flow chart of process

Figure 26 below provides a flow chart of the procedures implemented in this research.

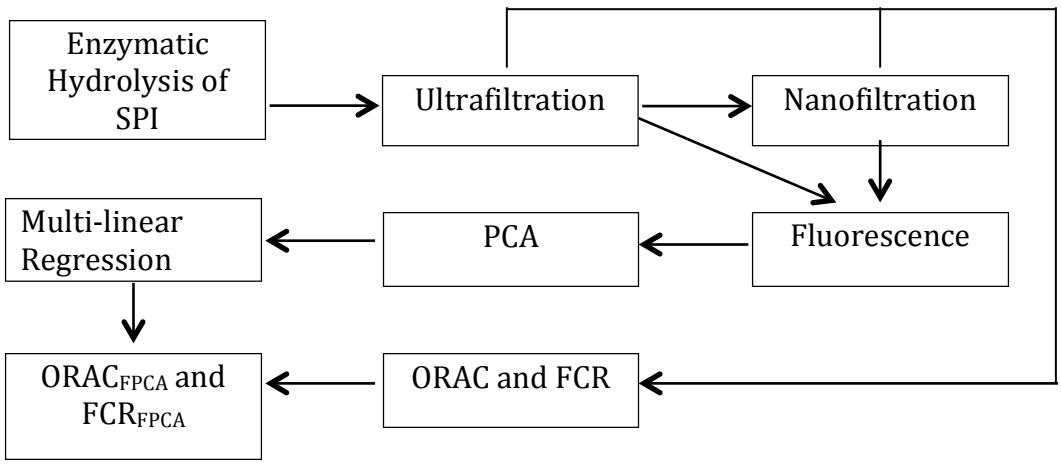

Figure 26: Flow chart of the methodologies implemented

8.4.2. Enhancement of antioxidant capacity during peptide fractionation

In 3.5, fractionation of UF permeates for control and pre-heated SPH showed to improve the antioxidant capacities of peptides, especially at pH 8. The additional NF experiments performed for pre-heated SPH at pH 4 and 8 provided the opportunity to monitor the improvement of antioxidant capacity of peptides as a function of filtration time (Figure 27).

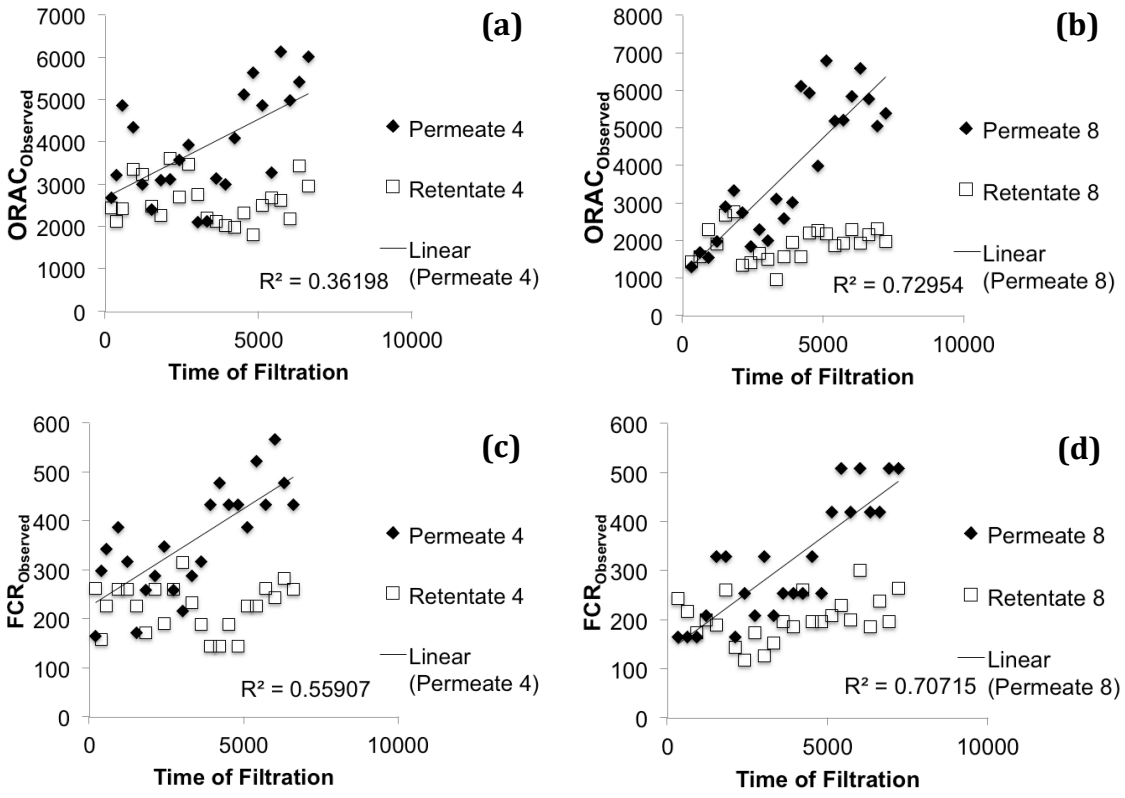

Figure 27: Measured ORAC antioxidant capacity of permeate and retentate fractions as a function of time during NF for heat pre-treated soy protein hydrolysates at (a) pH 4, and (b) pH 8; and measured FCR antioxidant capacity of NF permeate and retentate fractions as a function of time during NF at (c) pH 4, and (d) pH 8.

8.4.3. PCA of NF and UF data sets

Table 17 provides statistically significant PCs and the variances captured by them for the NF and UF data (X_{NF4} and Z_{UF}).

Table 17: Principal components and captured variances by PCA for NF (X_{NF4}) and UF (Z_{UF}) spectral data.

Principal Component	NF Spectral Data (X_{NF4})		UF Spectral Data (Z_{UF})	
	Variance Captured (%)	Cumulative Variance (%)	Variance Captured (%)	Cumulative Variance (%)
1	25.0	25.0	55.2	55.2
2	18.5	43.5	34.2	89.4

The UF-NF data set consisted of a large variety of samples from the pre-heated and control SPH fractionation streams. These fractionation streams included UF permeate and retentate fractions, and NF permeate and retentate fractions at pH 4 and 8 collected for each SPH treatment.

PCA generated a number of new variables (PCs) that explained any systematic patterns present in X_{UF} used for PCA_{UF} model development. Two statistically significant PCs were identified for Z_{UF}, capturing a total variance of 89.4 %. The 10.6 % of variance that had not been captured by these two PCs was due to instrument noise in fluorescence readings (~5 %) [71], and other statistically insignificant PCs generated by PCA (<4 % variance captured by each PC).

Loading plots for PC_1 and PC_2 are presented in Figure 28. The loading plot for PC_1 (Figure 28a) displayed a predominant peak (α'') at Ex/Em ~280 nm/350 nm. The location of the α'' peak corresponded to the location of peaks α and α' (due to intrinsic fluorescence of tryptophan) in Figure 16 and Figure 17a. Therefore, PC_1 was largely conformed to tryptophan-containing peptides present in samples. The loading plot for PC_2 (Figure 28b) displayed a dominant valley (δ'') rather than a peak at Ex/Em ~275 nm/310 nm, which corresponded to the location of δ and δ' peaks in Figure 16 and Figure 17b (due to intrinsic fluorescence of tyrosine) [83]. Therefore, PC_2 was correlated with tyrosine-containing peptides.

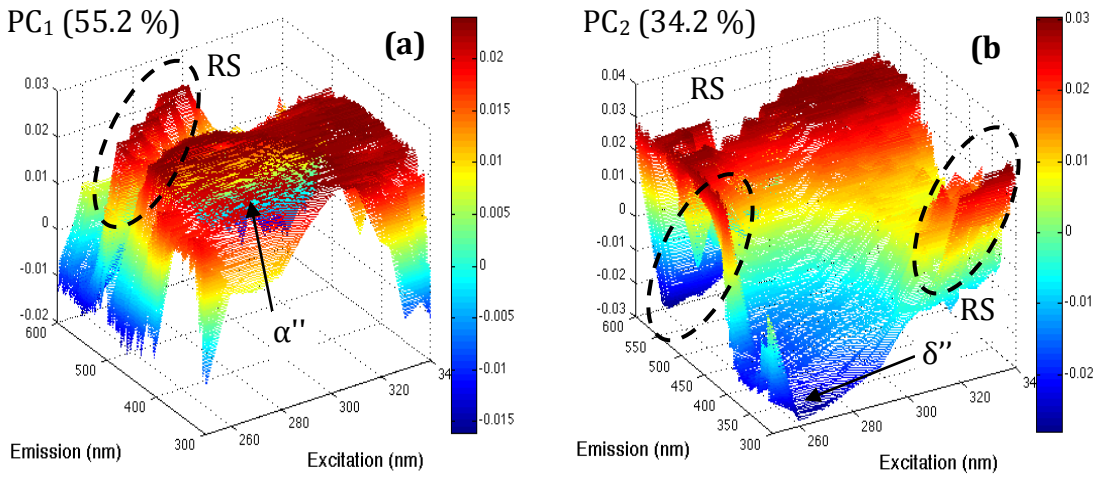

Figure 28: 3D illustrations of loading matrices obtained by PCA of UF spectral data for (a) PC_1 and (b) PC_2. Rayleigh light scattering (RS) regions are indicated by the dashed lines. Variance captured by each PC is indicated.

8.4.4. Linear regression models

The MLRMs built using NF samples (from PCA_{NF}) for heat pre-treated SPH are provided in equations 14 and 15:

$$ORAC_{FPCA}=4270.81 + 14.36\ (PC_1) - 11.10\ (PC_2) \quad (14)$$

$$FCR_{FPCA}=358.11 + 0.82\ (PC_1) - 0.56\ (PC_2) \quad (15)$$

Two MLRMs more were built by minimizing the SSE of 60 randomly selected UF and NF samples (from PCA_{UF}), and the models was validated using the remaining 60 samples. The MLRMs are represented by equations 16 and 17 (below).

$$ORAC_{FPCA}=1716.83 - 7.49\,(PC_1) + 11.56\,(PC_2) + 0.08\,(PC_1 \bullet PC_2) \quad (16)$$

$$FCR_{FPCA}=241.96 + 0.16\,(PC_1) + 1.54\,(PC_2) + 0.01\,(PC_1 \bullet PC_2) \quad (17)$$

Residual plots were used to ensure that trends in sample errors are not present. The interaction terms in equations 16 and 17 were found to be significant. From the UF-NF data set, ~17 samples were found to contain high errors (%) for $ORAC_{FPCA}$ and FCR_{FPCA} values. The root means squared errors (RMSE) for these samples were determined with and without the interaction term in equations 16 and 17. It was determined that by adding the interaction term, the RMSE of the 17 samples for ORAC and FCR models decreased by ~50 %. Observed ORAC and FCR values were plotted against each other (Figure 15).

Estimating the absolute ORAC and FCR antioxidant capacities of peptides using the proposed method did not provide accurate outcomes. The comparisons between experimentally measured, and fluorescence and PCA-captured antioxidant values from PCA_{NF} and PCA_{UF} are presented in Figure 29.

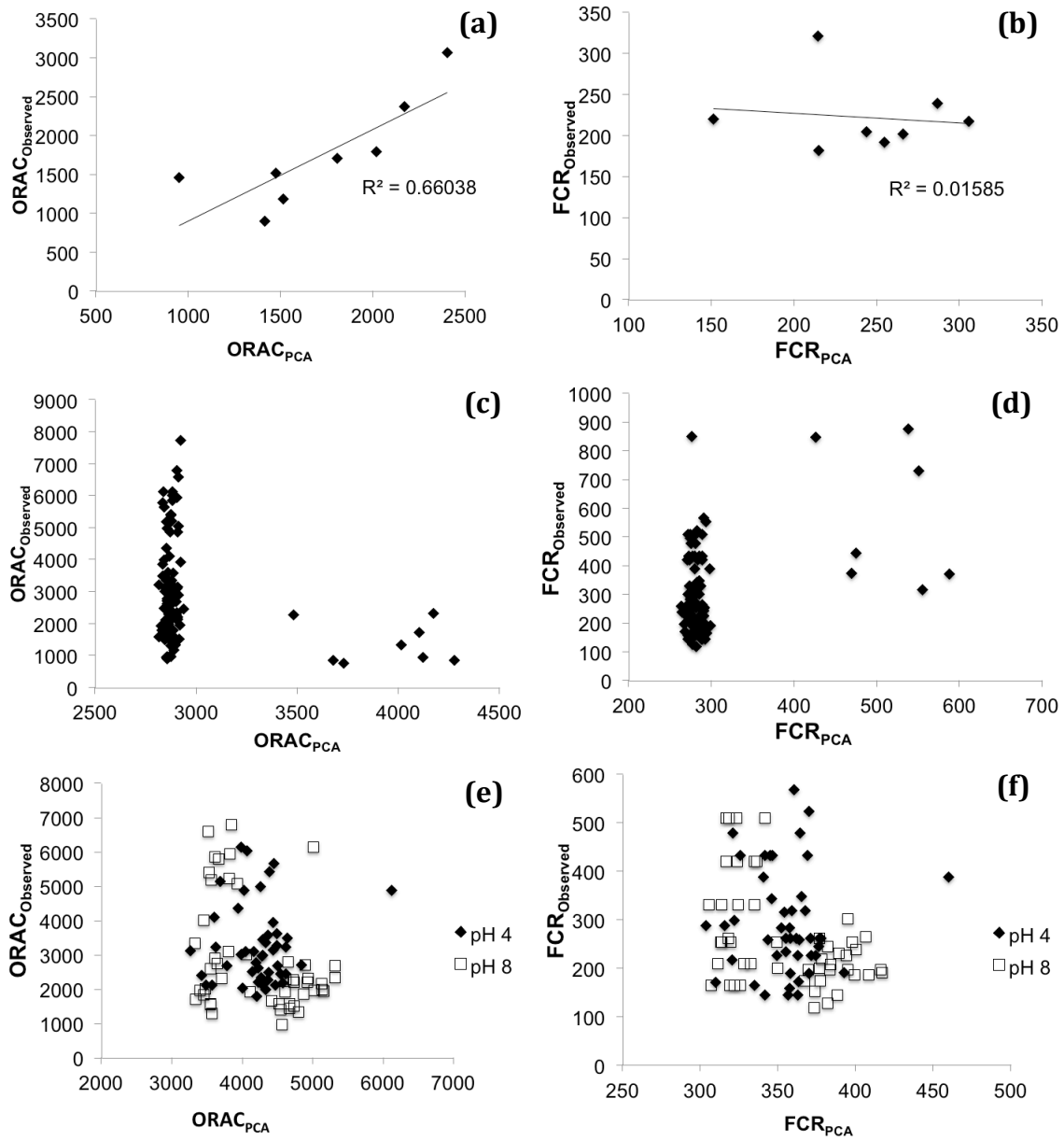

Figure 29: Comparisons of experimentally measured antioxidant capacities to PCA-captured antioxidant capacities for (a, b) UF samples and (c, d) NF samples from $PCA_{UF;}$ and for (e, f) NF samples at pH 4 and 8 from PCA_{NF}. The UF and NF samples in figures a-d consisted of heat pre-treated and control soy protein hydrolysates, while in figures e-f consisted of solely heat pre-treated soy protein hydrolysates.

8.4.5. Residual Plots

Residual plots were produced to validate the linear regression models and observe any trends in the variance captured by the models. The presence of any noticeable trends in the errors captured by the model, plotted against model predicted values suggested the lack of fit of the model. Figure 30 presents the residual plots for the linear regression models represented by equations 14-17 for $ORAC_{FPCA}$ and FCR_{FPCA} values.

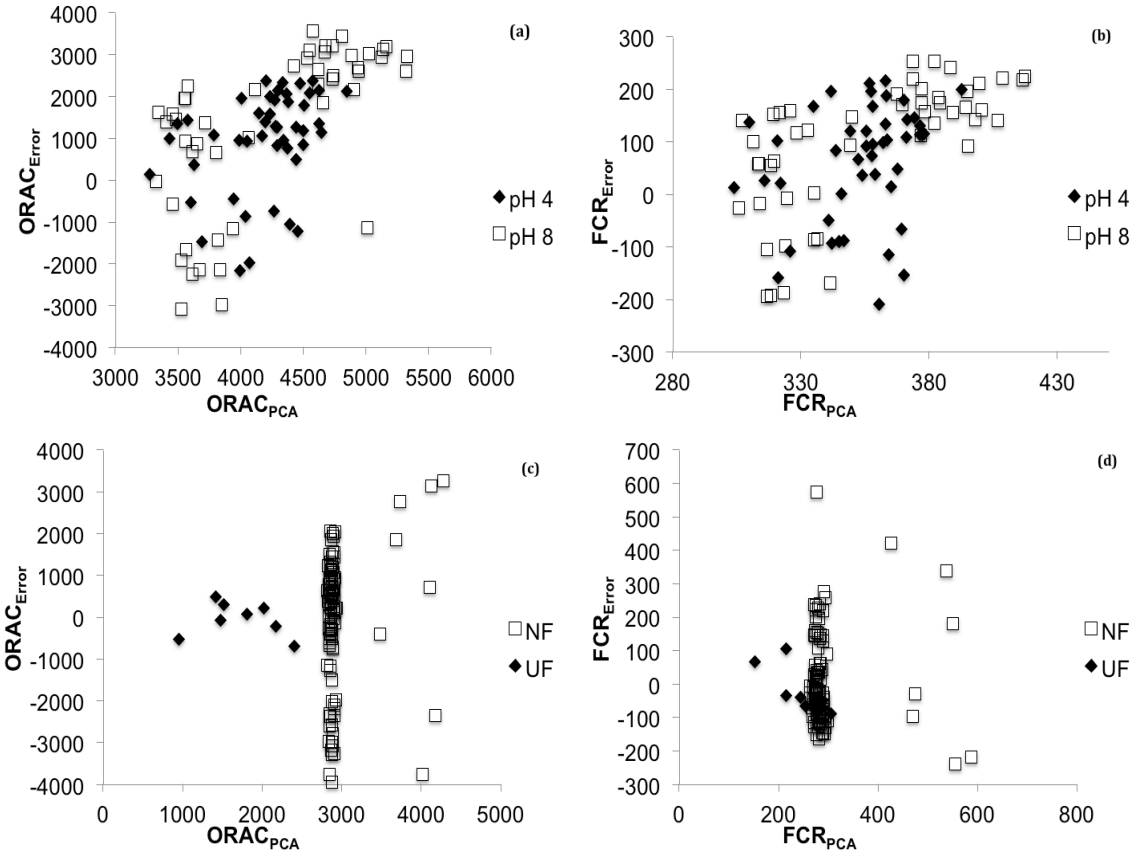

Figure 30: Residual plots for linear regression models for (a) $ORAC_{FPCA}$ values (equation 14), and (b) FCR_{FPCA} values (equation 15) based on PCA_{NF} (n=96) for the NF of heat pre-treated soy protein hydrolysates at pH 4 and 8; and (c) $ORAC_{FPCA}$ values (equation 16), and (d) FCR_{FPCA} values (equation 17) based on PCA_{UF} (n=120) for the UF and NF of control and heat pre-treated soy protein hydrolysate.